Universidade de Lisboa

Faculdade de Medicina de Lisboa

ISQUÉMIA CEREBRAL AGUDA E MODELAÇÃO PELO SULFETO DE HIDROGÉNEO

Maria Isabel Santos Lestro Henriques

DOUTORAMENTO EM MEDICINA

NEUROLOGIA

2014

Universidade de Lisboa

Faculdade de Medicina de Lisboa

ISQUÉMIA CEREBRAL AGUDA E MODELAÇÃO PELO SULFETO DE HIDROGÉNEO

Maria Isabel Santos Lestro Henriques

Orientador: Professor Doutor José Manuel Morão Cabral Ferro

Co-Orientador: Professor Doutor Exupério Díez-Tejedor

MEDICINA

NEUROLOGIA

A impressão desta dissertação foi aprovada pelo Conselho Científico da Faculdade de Medicina de Lisboa em reunião de 24 de Março de 2015

This research was supported by the International Neuroscience Doctoral Programme (sponsored by the Champalimaud Foundation, Calouste Gulbenkian Foundation, and Fundação para a Ciência e Tecnologia), Lisbon, Portugal, and by the INVICTUS (Spanish Neurovascular Network) research grant (RD 12/0014/0006) from Research Institute Carlos III, Ministry Science and Innovation, Madrid, Spain.

To my parents, for their example and their intellectual stimulus.

ACKNOWLEDGEMENTS

Many people were involved in the development and concretization of this work.

I started this project, as a member of the first International Neuroscience Doctoral Program of the Fundação Champalimaud, from which I was selected together with a heterogeneous group of nine fellow students, with whom I have the benefit of spending the first year in the Gulbenkian Institute for Science in Oeiras where this project was planned and got under way.

I thank Professor José Ferro for accepting to guide me in this scientific journey as he did already in 2000, during my Master in Neurosciences at the University of Coimbra. He has been an inspiring teacher since I know him, and I feel honored that he shared his knowledge, experience, and time.

In the person of Professor Exuperio Diez-Tejedor I had the luck to meet someone who would, right from the beginning, not only agree to support the project but also made it possible for me to accomplish my project in his Neuroscience and Cerebrovascular Laboratory, in IdiPAZ, Madrid. I am deeply grateful for his support throughout all stages of the project, in the good and in the difficult moments. It was a great honor and pleasure to work in his group during these last years.

I affectionately thank the lab team in Madrid, who not only adopted me as friend and co-worker but also taught me almost everything I know about lab work, its pitfalls and tricks, as well as resistance to failure and despair. They are not only a team of very well prepared neuroscientists, but also very good "labmates". I thank Maria who is our leader and a never ending source of energy and enthusiasm, trendy Berta always so kind and attentive, and a master in lab job, Jaime, the *vanguardist*, always with a soluction for all kind of problems, and smooth Laura, yet always assertive. I will always remember our colleague Julia who passed away in 2012, and who taught me a lot more than just how to operate rats, and Mercedes who left the lab in the meantime. Thanks also to the collaboration of SIERMAC, in the person of Professor Sebastian

Cerdain and of the patient Teresa from whom I learnt what I know about MRI in rodents.

I would also like to thank the selection team from the Champalimaud Neuroscience Program, my fellow colleagues in the programme, and my mentors at Champalimaud, Professor Domingos Henrique and Professora Suzana Lima, for being always available for counseling and advice, as well as the Administration and Clinical Board of Centro Hospitalar de Lisboa Zona Central, namely Dra. Teresa Sustelo, and the Director of the Department of Neurology, Dr. Pedrosa, for their consent and support in carrying out this project.

Finally yet notably, I thank my husband Hans Christian Eickhoff and my children Miguel and Madalena for all their tolerance and loyalty, as well as their comprehension with my long stays in Madrid and weekends dedicated to my thesis instead of fully enjoying their company. Thank you Hans, for your encouragement right from the beginning, for your critical suggestions and counseling, and for reviewing the manuscript.

INDEX

ACKNOWLEDGMENTS 9

INDEX 11

ABBREVIATIONS 15

LIST OF FIGURES 19

SUMMARY 23

RESUMO 27

INTRODUCTION 37

1. CEREBROVASCULAR DISEASE

1.1. STROKE BURDEN 37

1.2. BOTTLE-NECKS IN ISCHEMIC STROKE RESEARCH 38

2. PATHOPHISIOLOGY OF ISCHEMIC STROKE AND CELL DEATH

2.1 RISK FACTORS AND REGULATION OF CEREBRAL BLOOD FLOW 39

2.2. THE ISCHEMIC CASCADE 40

3. ACUTE TREATMENT: NEUROPROTECTION AND THE NEED FOR THERAPEUTIC WINDOW ENLARGEMENT

3.1. TIME IS BRAIN 43

3.2. NEUROPROTECTION VS. BRAIN PROTECTION 44

4. PENUMBRA AND CORE

4.1. THE PENUMBRA CONCEPT 46

4.2. ISCHEMIA IS ABOUT CELL DEATH 48

4.3. "MICRO CORES AND MICRO PENUMBRAS" 51

5. ISCHEMIC TOLERANCE: HYPOTHERMIA AND HIBERNATION

5.1 LACK OF CEREBRAL BLOOD FLOW WITHOUT PERMANENT NEUROLOGICAL DEFICIT 52

5.1.1. HYPOTHERMIA 52

5.1.2. DORMANCY AND HIBERNATION 54

5.2 NITRIC OXIDE, CARBON MONOXIDE, AND HYDROGEN SULFIDE 55

5.3. PREVIOUS WORKS WITH H_2S AFTER EXPERIMENTAL STROKE 57

6. REFERENCES 59

AIMS AND SCOPE OF INVESTIGATION 71

SECTION 1: ACUTE BRAIN ISCHEMIA, HYPOTHERMIA AND HIBERNATION: THE ROLE OF OXIDATIVE PHOSPHORYLATION INHIBITORS

INTRODUCTION 77

HYPOTHERMIA 78

NITRIC OXIDE, CARBON MONOXIDE AND HYDROGEN SULFIDE 79

OXIDATIVE PHOSPHORYLATION INHIBITORS AND HIBERNATION 80

CONCLUSION 82

REFERENCES 83

SECTION 2: EXPOSURE TO HYDROGEN SULFIDE DIMINISHES INFARCT SIZE AND ENHANCES RECOVERY: EXPERIMENTAL DATA IN A MCAO MODEL IN RODENTS

INTRODUCTION 89

MATERIAL AND METHODS 90

RESULTS 95

DISCUSSION 96

CONCLUSIONS 99

FIGURES 2.1, 2.2, 2.3 101

REFERENCES 104

SECTION 3: HYDROGEN SULPHIDE PROTECTION AFTER ACUTE ISCHEMIC STROKE INCLUDES REACTIVE OXYGEN SPECIES (ROS) MODULATION WITH DECREASED EXPRESSION OF NOX-4

INTRODUCTION 111

MATERIAL AND METHODS 112

RESULTS 118

DISCUSSION 119

CONCLUSIONS 121

FIGURES 3.1, 3.2, 3.3 122

REFERENCES 126

SECTION 4: INTRALESIONAL PATTERN OF MRI ADC MAPS PREDICT OUTCOME IN EXPERIMENTAL STROKE

INTRODUCTION 133

MATERIAL AND METHODS 133

RESULTS 141

DISCUSSION 144

STUDY LIMITATION AND POTENCIAL BIAS 148

CONCLUSIONS 149

FIGURES 4.1, 4.2, 4.3 150

REFERENCES 156

DISCUSSION 161

STUDY LIMITATIONS 166

IMPLICATIONS AND FUTURE RESEARCH 167

REFERENCES 168

CONCLUSION 173

ABBREVIATIONS

ADC: apparent diffusion coefficient (MRI)

ADL: activities of daily living

AMPA: α-amino-3-hydroxy-5-methyl-4-isoxazolepropionic acid

ATP: adenosine triphosphate

CBF: cerebral blood flow

CBS: cystathionine beta-synthase

CBV: cerebral blood volume

CSE: cystathionine gamma-lyase

cm: centimeter

CNS: central nervous system

CO: carbon monoxide

CO_2: carbon dioxide

CVA: cerebrovascular accident

ºC : degree centigrade

d: day/ days

DAPI: 4', 6-Diamidino-2-Phenylindole

DSC MRI: Dynamic susceptibility contrast – Magnetic Resonance Imaging

DNA: Deoxyribonucleic acid

DWI: Diffusion-weighted imaging (MRI)

EU: European Union

EPI: echo planar imaging

Fe-Cu: Iron-Cupper redox center (in cytochrome oxidase)

FMUL: Faculdade de Medicina da Universidade de Lisboa

G : giga

Gd: gadolinium

GFAP: glial fibrillary acid protein

h: hour

^1H: chemical compound with one hydrogen atom

HSP-27: heat shock protein 27

H_2S: hydrogen sulfide

HO_1: heme oxygenase-1

H&E: hematoxylin and eosin stain

.JPG/JPEG: Joint Photographic Experts Group

K (ATP) channel: ATP-sensitive potassium channel

LTP: long term potentiation

MCA: middle cerebral artery

MCAO: middle cerebral artery occlusion

microM: micro molar (μM)

min: minutes

ml: milliliter

MMP: matrix metalloproteinase

MRI: magnetic resonance imaging

MTT: mean transient time

mv: millivolt

n: number

NADPH: nicotinamide adenine dinucleotide phosphate

NeuN: neuronal nuclei

NIH: National Institutes of Health

NINDS: National Institute of Neurological Diseases and Stroke

NMDA: N-methyl D-aspartate

NO: nitric oxide

NOS: nitric oxide synthetase

NOX-4: NADPH oxidase 4

$O_{2.}$ Oxygen

PET: positron emission tomography

pMCAO: permanent middle cerebral artery occlusion

ppm: parts per million

rADC: relative apparent diffusion coefficient

RARE: rapid acquisition with relaxation enhancement sequence

rCBF: relative CBF

ROI: region of interest

ROS: reactive oxygen species

rpm: revolutions per minute

s: second

SD: standard deviation

SEM: standard error of the mean

SOD-2: superoxide dismutase 2

SPECT: single photon emission computed tomography

rtPA: recombinant tissue plasminogen activator

T2 : T2-weighted image sequence (MRI)

TUNEL: Terminal deoxynucleotidyl transferase dUTP nick end labeling

US: United States

UAM: Universidad Autónoma de Madrid

6-0: size of suture material

Δ CBF: differential CBF between ipsilateral and contralateral side

LIST OF FIGURES

***FIGURE 1** . ISCHEMIC CASCADE*

***FIGURE 2.1**. RATS EXPOSED TO H_2S SHOW BETTER FUNCTIONAL OUTCOME AND SMALLER LESION SIZE*

***FIGURE 2.2**. RATS EXPOSED TO H_2S SHOW BETTER INTRALESIONAL CBF AT 24H*

***FIGURE 2.3**. BODY TEMPERATURE DURING EXPERIMENTS IN RATS EXPOSED TO H_2S AND CONTROLS*

***FIGURE 3.1** RATS EXPOSED TO H_2S AFTER pMCAO SHOWED LOWER EXPRESSION OF CELL DEATH, NOX-4 AND HSP27 AT 24H*

***FIGURE 3.2** DECREASED EXPRESSION OF CELL DEATH AND ROS GENERATING ENZYME NOX-4 AT 14D IN RATS EXPOSED TO H_2S*

***FIGURE 3.3.** BODY TEMPERATURE DURING EXPERIMENTS IN RATS EXPOSED TO H_2S AND CONTROLS*

***FIGURE 4.1** . LESION SIZE AND FUNCTIONAL OUTCOME OF TWO DIFFERENT INTRALESIONAL PATTERNS OF MRI ADC MAPS: HOMOGENEOUS AND HETEROGENEOUS*

***FIGURE 4.2**. EXPRESSION OF CELL DEATH AND IMMUNOHISTOCHEMICAL MARKERS AT 24H AFTER pMCAO IN TWO DIFFERENT INTRALESIONAL ADC PATTERNS: HOMOGENEOUS AND HETEROGENEOUS.*

***FIGURE 4.3**. DWI AND PWI MRI OF HOMOGENEOUS AND HETEROGENEOUS PATTERN.*

SUMMARY

SUMMARY

In the present study, we explored the effect of short-term exposure to hydrogen sulfide (H_2S) after acute ischemia in an animal model of pMCAO. We hypothesized that H_2S exposure after acute ischemic stroke modulates ischemic lesion either by an early protective effect or by promoting post-ischemic repair. To address our hypothesis we exposed rats to H_2S after pMCAO and measured functional outcome and infarct size *in vivo* and *post-mortem*. We identified underlying markers of cytoprotection and repair. Finally, we compared brain imaging with immunohistochemical data to look for early imaging features of ischemic tissue damage that may relate to functional outcome.

H_2S exposure after pMCAO improved functional outcome and decreased infarct size and the expression of cell death. H_2S may act very early in the ischemic process, since there were lower levels of acute injury-related markers at 24h without enhancement of repair-associated markers for vasculogenesis, angiogenesis or synaptogenesis at day 14. Significant benefit is likely to occur before major tissue damage develop and includes modulation of NOX-4, a major enzyme generator of reactive oxygen species (ROS) and endothelial dysfunction, as well as by vasomodulation of intralesional microcirculation, since intralesional CBF assessed by PWI MRI improved in rats exposed to H_2S. Given that H_2S limits brain damage after experimental ischemic stroke, hydrogen sulfide donors may play a role as new drugs in the context of acute ischemic stroke.

RESUMO

RESUMO

1. INTRODUÇÃO E CONTEXTO

Nas últimas décadas obtiveram-se resultados promissores com várias substâncias neuroprotectoras, em estudos pré-clínicos em modelos de isquémia cerebral. No entanto nenhuma comprovou eficácia e segurança em contexto de ensaio clínico em doentes com acidente vascular cerebral (AVC) isquémico agudo. Entre os factores que contribuíram para as dificuldades na extrapolação dos resultados, realça-se a ausência de homogeneidade nos instrumentos de medida funcional e no modo de aquisição dos exames de imagem, nomeadamente quanto à definição de penumbra. Existe evidência de que, na ausência de reperfusão, a área de penumbra isquémica se transforma de modo célere em área de necrose, aumentando assim o volume da lesão e agravando o prognóstico funcional.

A hibernação e a hipotermia grave são duas situações metabólicas extremas onde, apesar da ausência ou de diminuto fluxo sanguíneo cerebral (CBF), é possível não ocorrer isquémia cerebral nem defeito neurológico permanente. O conhecimento dos processos através dos quais estes estados de hipometabolismo protegem no contexto de oligemia e isquémia, pode contribuir para a compreensão da complexa fisiopatologia da isquémia aguda cerebral. A possibilidade de induzir um estado de hipometabolismo onde as necessidades energéticas estejam mais adequadas à oferta energética, após isquémia aguda, diminuindo o consumo de oxigénio, pode contribuir para alargar a janela de oportunidade terapêutica para trombólise.

Foi possível induzir um estado semelhante à hibernação em mamíferos que não hibernam, pela inalação de uma mistura do gaz sulfeto de hidrogénio (H_2S) com atmosfera. Durante o período de inalação, observou-se significativa diminuição das suas taxas metabólicas (nomeadamente do consumo de O_2 e da eliminação de CO_2) e da sua temperatura corporal. Após 6 h, e ao serem de novo colocados a respirar atmosfera voltavam, de modo espontâneo, às suas taxas metabólicas e temperatura basais, sem interferência no seu estado de saúde a curto ou longo prazo.

Os efeitos biológicos do H_2S parecem depender, em particular, da sua capacidade de inibição da fosforilação oxidativa mitocondrial, competindo com o O_2 na ligação à enzima citocromo C oxidase, a nível da cadeia de transporte de eletrões mitocondrial. No entanto, os efeitos biológicos do H_2S dependem entre outros fatores da dose de exposição e da sua duração. Em concentrações da ordem dos microMolar, o H_2S parece ter um efeito neuroprotector no *stress* oxidativo, e modelador da morte celular, interferindo nas vias das capases e kinases. No contexto da isquémia aguda cerebral, o papel do H_2S parece relacionar-se ainda com o seu papel de sensor de oxigénio, de regulador da comunicação glial e neuronal e do controlo do tónus vascular local, e não apenas da sua capacidade em induzir hipotermia. Neste contexto, a hipotermia pode ser consequência e não causa do hipometabolismo induzido. As propriedades de sensor de O_2 permitem a monitorização do O_2 do meio, contribuindo assim para uma libertação adequada de O_2 aos tecidos, tanto em contexto de isquémia como em basal.

Os dados existentes sobre o uso de H_2S em contexto de isquémia cerebral eram escassos e discordantes, quando desenhamos este projeto. O primeiro trabalho de exposição ao H_2S após isquémia cerebral focal permanente não demonstrou benefício funcional. Os trabalhos seguintes, que incluíram animais mais idosos, modelos de reperfusão e tempos de exposição prolongados, demonstraram benefício funcional e uma diminuição do volume da lesão final após isquémia do território da artéria cerebral média (ACM). Estes resultados estão de acordo com a literatura existente relativamente a isquémia noutros órgãos como o rim ou coração onde a exposição ao H_2S ou a dadores de H_2S também melhora a função e diminui o volume final da lesão isquémica. Deste modo, o potencial benefício da exposição a H_2S ou dadores de H_2S no contexto de isquémia aguda cerebral pode ser uma área de interesse translacional.

2. HIPÓTESE

Neste estudo avaliámos a hipótese de que após isquémia aguda cerebral, o H_2S actue como protector cerebral por modular o *stress* oxidativo pós isquémico e a expressão de espécies reactivas de oxigénio, ou por promover a reparação tecidular ulterior.

Para analisar esta hipótese estudámos os efeitos da exposição ao H_2S num modelo animal de oclusão permanente da artéria cerebral média (pMCAO) em ratazana Sprague-Dawley, medindo o resultado funcional, o tamanho do enfarte *in vivo* e *post-mortem*, analisando ainda marcadores de protecção celular, morte celular e reparação celular após pMCAO, e comparando os dados de imagem *in vivo* com os de imunohistoquímica.

3. MÉTODOS

Comparámos 3 grupos de ratos macho adulto Sprague-Dawley,randomizados: *Sham* (n= 14), pMCAO (n=22) e pMCAO seguido de exposição durante 24 min a atmosfera com 40ppm de H_2S em caixa acrílica fechada, 3h após a indução da isquémia (n= 23). A amostra foi sacrificada às 24h e ao 14º dia. Usamos codificação para manter a alocação ao grupo sempre cega ao observador, excepto durante o procedimento cirúgico. Medimos o tamanho do enfarte com a sequência T_2 de ressonância magnética nuclear (MRI) e com hematoxilina/eosina (H&E). Avaliamos a funcionalidade antes dos procedimentos, às 24h e aos 14 dias com a escala de Rogers modificada e o teste de Rotarod. Avaliámos a morte celular usando a técnica TUNEL. Para o estudo de protecção e reparação celular, utilizámos marcadores da oxidase do NADPH 4 (NOX-4), de proteína acídica fibrilhar glial (GFAP), de fator de crescimento endotelial vascular (VEGF), de sinaptofisina, de superóxido dismutase 2 (SOD2) e de proteína de choque térmico 27 (HSP-27). Usamos beta-actina como controlo de carga (1:400, Sigma-Aldrich™). Para a técnica de Western-Blot fizeram-se 3 réplicas experimentais de cada experiência (n= 4 animais por grupo). Uma vez que os dados não seguiam uma distribuição normal, o teste de Mann-Whitney foi usado para comparar 2 amostras e o teste de Kruskal-Wallis para comparar mais de 2 amostras do mesmo grupo ou mais de 2 grupos.

4. RESULTADOS

A temperatura corporal foi significativamente mais baixa após indução da anestesia em todos os grupos. Após exposição ao H_2S durante 24 minutos, a temperatura corporal diminuiu 1,85ºC (média), começando a normalizar logo que os animais reiniciavam a respiração com atmosfera normal. Duas horas após a exposição, nenhuma alteração na temperatura corporal basal era mensurável.

Observámos um melhor resultado funcional às 24h após pMCAO nos animais expostos ao H_2S quando comparado com o grupo controlo tanto com a escala modificada de Rogers como com o teste de Rotarod. Esse benefício manteve-se até ao 14º dia, data de sacrifício desse grupo. Relativamente às dimensões do enfarte, aos 14 dias tanto na sequência T2 de MRI como em *post-mortem* com H&E, os animais expostos ao H_2S apresentavam enfartes de menores dimensões comparativamente aos do grupo controlo. Às 24h após pMCAO não encontrámos diferenças significativas nas dimensões dos enfartes medidos com a sequência T2 MRI entre os animais tratados (expostos ao H_2S) e os controlos. O grupo tratado apresentava, no entanto, nas sequências de difusão (DWI) nos mapas de Coeficiente de difusão aparente (ADC) um padrão de heterogeneidade intralesional. Esta heterogeneidade dentro da área isquémica inclui áreas centrais e periféricas da lesão, existindo áreas centrais com coeficientes de difusão superiores a áreas periféricas da lesão. Quando avaliamos a perfusão cerebral na área de isquémia com MRI de perfusão, verificamos que a diferença entre o fluxo sanguíneo cerebral no lado contralateral e o isquémico era menor nos animais expostos ao H_2S, que tinham assim melhor perfusão relativa na área de isquémia.

Relativamente à expressão de morte celular, os animais tratados apresentaram significativamente menor expressão de células TUNEL positivo, tanto às 24h como aos 14d. Ao 14º dia, não se verificou diferença nos níveis de expressão dos marcadores VEGF ou sinaptofisina entre tratados e controlos. Os níveis de expressão de GFAP estavam diminuídos aos 14d em animais tratados. Os níveis de SOD-2 aos 14 dias estavam diminuídos relativamente ao grupo controlo, mas não às 24h. Os níveis de expressão de NOX-4 eram significativamente menores em animais expostos ao H_2S,

tanto às 24h como no 14ºdia. A expressão do marcador HSP-27 foi significativamente menor em animais tratados às 24h mas não ao 14ºdia.

5. DISCUSSÃO

Os nossos resultados demonstram que a exposição a H_2S após isquémia cerebral aguda em modelo animal de pMCAO melhora o resultado funcional e diminui a dimensão do enfarte cerebral aos 14 dias. A melhoria no resultado funcional foi observada nos dois instrumentos de medida e manteve-se até ao dia de sacrifício.

A sequência T2 de MRI às 24h não demonstrou diferença significativa no tamanho do enfarte, para o que pode contribuir a presença de edema cerebral com consequente aumento de volume. No entanto aos 14 dias e na avaliação post-mortem usando a coloração H&E às 24h, os animais tratados apresentavam lesões de menor dimensão. Curiosamente, os animais expostos ao H_2S apresentavam ainda nos mapas de ADC áreas de heterogeneidade intralesional que correspondiam a coeficientes de ADC mais elevados e mais diversos, tanto em áreas centrais como periféricas da lesão isquémica. Este facto pode contribuir para explicar a discrepância entre a dimensão da lesão *in vivo* e a melhoria funcional às 24h. No entanto, o tamanho da lesão parece ser insuficiente como medida isolada de evidência de efeito protector.

Estudos de genómica demonstraram evidência da expressão de genes associados ao desenvolvimento do SNC e a factores tróficos na área central da lesão isquémica. Às 24h, os mapas de ADC do grupo tratado mostraram coeficientes de ADC heterogéneos dentro da lesão isquémica que corresponderão a áreas de diferente difusão de água e portanto de integridade tissular diversa, dentro da área de isquémia. Estas heterogeneidades podem representar o que foi previamente descrito como "*mini cores*" e "*mini penumbras*".

Quando comparamos com estudos de perfusão o CBF em ambos os hemisférios nos grupos expostos a H_2S e em controlos, verificamos menor diferença nos animais expostos ao H_2S. Para esta melhor perfusão da lesão isquémica em animais expostos

ao H_2S após pMCAO, podem contribuir mecanismos de microvasoregulação, uma característica da acção biológica do H_2S. No presente estudo, a presença de heterogeneidades dentro da lesão isquémica corresponde a um melhor prognóstico funcional, a uma menor dimensão do enfarte e a uma melhor preservação do tecido cerebral em risco de isquémia definitiva.

A hipotermia, quando não induzida por factores externos, pode ser consequência de hipometabolismo e não a causa das alterações metabólicas. A modelação pelo H_2S, no contexto de isquémia aguda cerebral, tem sido associada à indução de hipotermia especialmente em protocolos que incluem tempos de exposição prolongados ao H_2S. No presente estudo, após exposição durante apenas 24 min, observamos uma diminuição de 1.85ºC que os animais recuperam em menos de 2 horas. Assim, a hipotermia parece ser um efeito fugaz do hipometabolismo induzido pelo H_2S, e outros mecanismos parecem estar envolvidos, pois o seu efeito protector se mantem pelo menos até ao 14ºdia. Será ainda de realçar que, contrariamente aos protocolos prévios com tempos de exposição muito prolongados, a exposição durante 24 min foi igualmente eficaz. A pequena diminuição de temperatura observada com a exposição breve ao H_2S permitirá, em contexto translacional, antever a ausência de necessidade de internamento em unidades de cuidados intensivos, que os riscos da hipotermia moderada a grave não permitem dispensar. As limitações do presente estudo incluem o uso de apenas uma dose de H_2S, pois doses diferentes poderão ter efeitos distintos no resultado final. Devido a limitações orçamentais e à característica exploratória da investigação, não incluímos animais idosos, fêmeas ou animais com co-morbilidades associadas a doença cerebrovascular. Também, apenas avaliámos o resultado clínico funcional com testes de funções motoras. No entanto, em todos os casos a MRI permitiu excluir os animais em que por falha cirúrgica, o território da MCA não se encontrava enfartado. Os efeitos a longo prazo da exposição ao H_2S, após oclusão permanente da MCA não foram investigados, pois o estudo incluía comparação de dados imagiológicos e *post-mortem* às 24h e aos 14 dias.

6. CONCLUSÕES

No presente estudo, a exposição precoce ao H_2S após pMCAO melhora o prognóstico funcional e diminui a dimensão da lesão isquémica final. A perfusão cerebral foi superior nas lesões isquémicas dos animais expostos ao H_2S e os estudos de difusão revelaram um padrão de heterogeneidade nos coeficientes de ADC de áreas centrais e periféricas da lesão. A heterogeneidade intralesional, observada como um padrão mosqueado nos mapas de ADC em animais expostos ao H_2S, corresponde a animais com melhores resultados funcionais e menor dimensão final da lesão isquémica e com melhor preservação tecidular nos animais tratados. Assim, este padrão poderá revelar-se de interesse do ponto de vista translacional, visto que as decisões de reperfusão dependem também da imagem cerebral, onde o padrão de heterogeneidade nos mapas de ADC parece distinguir e prever um melhor prognóstico funcional tanto em ratos tratados como em ratos não tratados.

O H_2S poderá actuar muito precocemente no processo isquémico pois encontramos uma expressão diminuída de marcadores de lesão aguda às 24h, sem aumento da expressão de marcadores de reparação de vasculogénese, angiogénese ou sinaptogénese ao 14º dia. O benefício mais marcante parece ocorrer antes que o tecido se deteriore, e inclui a modelação de NOX-4, uma enzima geradora de espécies reactivas de oxigénio, e mediadora de disfunção endotelial.

INTRODUCTION

INTRODUCTION

1. CEREBROVASCULAR DISEASE

Stroke is a rapidly developing focal brain dysfunction of vascular origin lasting more than 24h, including ischemic stroke, intracerebral hemorrhage, subarachnoid hemorrhage and cerebral venous thrombosis (WHO MONICA Project Principal Investigators, 1988).

Ischemic stroke occurs after a sudden interruption of a brain artery by thrombosis or embolism and is the most common type of stroke, representing more than three quarters of all strokes (Feigin et al., 2003). Once considered a disease of the artery itself, current data support a broader view, including a model where all brain cells and structures participate in the mechanisms of both tissue damage and repair. Structures involved include glia, neurons, matrix components, and vascular cells that act together in specialized frameworks like the neurovascular unit.

In the last decades, stroke research was centered on the neuron itself, trying to achieve "neuroprotection" or avoid neuronal death. Lately, attention focused on death or recovery of all cells or groups of cells involved , as well as their matrix structure, and ischemic stroke is no more just considered a matter of neuronal death (Caplan et al., 2011; Moskowitz et al., 2010).

1.1. STROKE BURDEN

Stroke is a devastating disease and the second leading cause of death worldwide (Moskowitz et al., 2010). The burden of stroke estimated from stroke incidence and prevalence studies in Europe showed regional differences, although variations in methodology should also be taken into account when interpreting the numbers. A recent review including 44 incidence and 12 prevalence studies emphasized that in Western Europe incidence will rise from 1.1 million per year in 2000 to as much as 1.5 million per year in 2025, merely because of expected changes in demographic factors and ageing of populations (Truelsen et al., 2006). In Europe, projections consider an increase in the ratio of people aged over 65, at highest risk for acute stroke, from 20%

in 2000 of the total population to 35% in 2015. In Portugal, epidemiological data showed an estimated incidence of 187/100 000 inhabitants, being the first cause of dependency and death after the age of 65 (Correia et al., 2013, 2004).

However, stroke mortality in Europe shows significant differences between Western and Eastern European countries. While Western European countries have lower and declining stroke mortality rates, in Eastern Europe, mortality rates are not only higher but also increasing if compared using age-standardized mortality rates from death certificates (Sarti et al., 2000).

1.2. BOTTLE-NECKS IN ISCHEMIC STROKE RESEARCH

In the clinical setting, we witnessed relevant changes in the attention paid to the disease. Diagnosis and treatment sustained a remarkable advance, including new and better imaging methods and a redesigned organization of stroke care. The advent of acute stroke units and publication of guidelines for stroke management and for the prevention of major complications, alongside with the generalization of pharmacologic reperfusion with recombinant tissue plasminogen activator (rtPA) improved patient care and outcome after an acute event. Nevertheless, there are still several bottlenecks not yet resolved in both primary and secondary prevention, as well as in acute stroke care. Obstacles include the lack of a biological marker of ischemia in the acute clinical setting that would allow confirming ischemia, even when clinical signs had already faded. Additionally, there is no approved alternative for reperfusion therapy in the majority of patients with ischemic stroke that are not eligible for rtPA treatment.

In the large group of patients that do not qualify for reperfusion after acute ischemic stroke, many present with an unknown interval since onset of symptoms. However, this interval is crucial for the decision to start reperfusion therapy since it has been shown that there is a threshold after which reperfusion is futile and even potentially harmful (Ferro, 1997; Hacke et al., 2008; Hussein et al., 2010; Lees et al., 2010). Consequently, reperfusion should not be used if cell death in ischemic areas has

already occurred due to higher risk of hemorrhagic transformation. Yet, a therapeutic window might still exist in patients whose brain tissue in the infarct area is still potentially salvable in MRI image signaling (Cheng et al., 2013). Since time is a major variable of tissue integrity and potential reversibility of ischemic lesions, image markers for ischemia time that correlate with histological status are considered a highly desirable target for investigation.

Unfortunately, in the field of pharmacological neuroprotection, no drug investigated to date showed both clinical benefit and an adequate safety profile despite several new therapeutic approaches that were tested in stroke models and clinical trials during decades of both basic and clinical research (Dirnagl, 2006). Therefore, new pharmacological targets have still to be established in order to improve treatment of acute ischemic stroke and ultimately diminish individual and global burden of stroke.

2. PATHOPHISIOLOGY OF ISCHEMIC STROKE AND CELL DEATH

2.1. RISK FACTORS AND REGULATION OF CEREBRAL BLOOD FLOW

Major cerebrovascular risk factors cannot be modified like age, male sex, Afro-American or Hispanic origin (in the US population), or family history of cerebrovascular disease. Other risk factors like hypertension, diabetes, smoking habits, dyslipidemia, or cardiac embolism due to atrial fibrillation can be controlled by lifestyle modifications or medical interventions, reducing significantly the chance of ischemic stroke.

Risk factors for stroke act by damaging physiological adaptive mechanisms that guarantee an adequate brain perfusion under different circumstances. They promote a change of both structure and function of the arterial wall, including the interface with the circulating blood, through pathophysiological mechanisms like atherosclerosis with subsequent narrowing and stiffness of the arteries, arterioles, and capillaries. This process is associated with loss of regulation of local cerebral blood flow (CBF). At the microvascular level, adaptative mechanisms of the endothelium are no longer perfect, leading to an inadequate oxygen and energy supply with loss of adaptive increase in

blood flow usually evoked by neuronal activity (Arrick et al., 2007; Iadecola and Davisson, 2008). Additionally, the impairment of cerebrovascular autoregulation that keeps CBF stable during variations in systemic blood pressure, compromises the development of collateral circulation and increases the probability of ischemia (Moskowitz et al., 2010).

The presence of risk factors also promotes changes in cerebral arteries by mechanisms that include production of reactive oxygen species (ROS). Major vascular sources of ROS are superoxide-producing enzyme nicotinamide adenine dinucleotide phosphate (NADPH) oxidase, mitochondrial enzymes, uncoupling of nitric oxide synthetase (NOS), and xanthine oxidase. Under physiological circumstances, ROS participate in regulation of cellular metabolism. However, when ROS increase to toxic levels mainly by excessive production or insufficient neutralization by antioxidant enzymes, cell injury occurs through mechanisms that include lipid peroxidation, protein oxidation and DNA damage (Olmez and Ozyurt, 2012). Endothelial dysfunction involves increased levels of ROS and decreased levels of nitric oxide (NO). Major vascular damage due to oxidative stress is related to the inactivation of NO by free superoxide radicals, reducing the availability of NO and consequently its protective role (Pacher et al., 2007). Thus, the regulation of microvascular flow is affected by the loss of the regulatory effect of endothelial NO, leading to vasoconstriction and inadequate NO-related vascular responses (Schulz et al., 2008).

2.2 THE ISCHEMIC CASCADE

When a cerebral artery is obstructed and no adequate blood supply is provided despite response from collateral circulation and microcirculation, brain cells start a process that will end up in cell death either by apoptosis or necrosis (Kulik et al., 2008; Shuaib et al., 2011). The ischemic cascade begins with an inadequate production of energy resources, mainly adenosine triphosphate (ATP). The resulting anaerobic metabolism that develops in the ischemic lesion unbalances the normal acid-base homeostasis. ATP-dependent ion pump transport fails and causes depolarization of cell membranes, thus leading to imbalanced ion flux including enlarged calcium influx and potassium

efflux. High intracellular calcium levels trigger the release of excitatory amino acids (mainly glutamate) that stimulate calcium-permeable-N-methyl D-aspartate (NMDA) and α-amino-3-hydroxy-5-methyl-4-isoxazolepropionic acid (AMPA) receptors, leading to even more calcium influx. Subsequently, cells become overexcited by excessive calcium levels triggering an activation of proteases, lipases, and reactive oxygen species (ROS). This pathophysiological process, also referred to as excitotoxicity, represents a series of events that ultimately leads to cell death during the ischemic cascade.

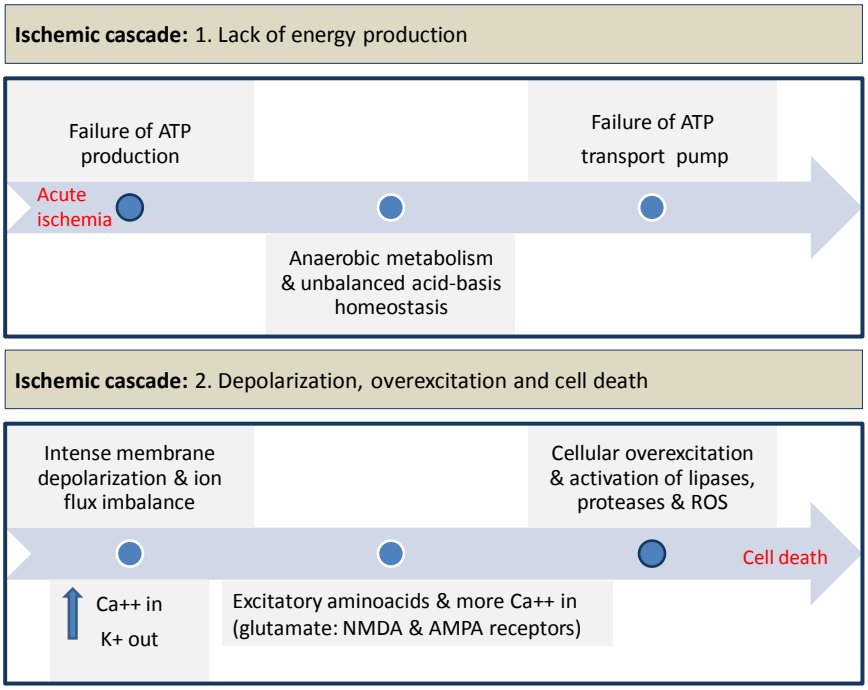

Figure 1. Ischemic cascade

When the cell membrane integrity is lost, mainly due to the intervention of phospholipases, the control of ion influx or efflux becomes impossible. As a result, mitochondrial integrity can no longer be maintained and apoptotic factors and toxins are liberated promoting cell death through mechanisms that include apoptosis and necrosis. As cells die through necrotic processes, they further liberate glutamate and

other cytotoxic products that provoke severe damage in the cells of the peri-infarct zone. Finally, vascular integrity is lost leading to the disruption of the protective blood-brain barrier. In consequence, brain edema is intensified and triggers further secondary brain injury.

Cell death is a particular aspect of cerebral ischemia, not only referring to neuronal death but also to other cell types and components of the blood-brain barrier. The twilight zone between cell death and recovery to normal homeostasis through reperfusion is the focus of current research in acute stroke.

3. ACUTE TREATMENT: NEUROPROTECTORS AND THE NEED FOR THERAPEUTIC WINDOW ENLARGEMENT

In the recent past, the development of new and better brain imaging techniques and the progress in the knowledge of stroke pathophysiology due to biomolecular research contributed to an increased interest in cerebrovascular diseases. Since the 1990's, treatment options for acute ischemic stroke include arterial reperfusion using thrombolytic agents. However, functional benefit from reperfusion could only be shown if used during a short time window after stroke (Bluhmki et al., 2009). Initial clinical studies demonstrated that vessel recanalization was effective in selected patients if intravenous thrombolysis with recombinant tissue plasminogen activator was used within 3h after onset of acute symptoms (Hacke et al., 1995; "Tissue plasminogen activator for acute ischemic stroke. The National Institute of Neurological Disorders and Stroke rt-PA Stroke Study Group.," 1995). As the reduced time window excluded the majority of stroke patients, new trials were carried out to investigate the safety and effectiveness of an enlarged time window that would permit to extend the established time frame for reperfusion treatment up to 4.5h after symptom onset in clinical protocols in Europe (Bluhmki et al., 2009). Yet, the small time window contributes to the fact that less than 15% of the patients with acute ischemic stroke are eligible for thrombolysis. In consequence, research on factors that would permit an enlargement of the time window is highly desirable and may focus on modulation of the ischemic cascade to delay apoptotic processes and cell death. In this context,

neuroprotectors can be useful in pre-hospital acute stroke medication, wake-up stroke, and patients excluded from thrombolysis including delayed arrival. Moreover, neuroprotective treatment may be beneficial in a synergic approach in addition to thrombolysis and may enlarge the therapeutic window.

3.1. TIME IS BRAIN

The concept of "time is brain", emerging from the need to start thrombolysis as early as possible after ischemic stroke, has contributed to the development of updated organizational models in acute stroke care, regarding the structure and procedures of emergency medical services. The need to understand the reasons for delay that ultimately excludes patients from access to thrombolysis has led research on pre-hospital and in-hospital therapeutic delay (Gomez et al., 1994). Despite different methodologies, overall results showed that in-hospital times from hospital door to acute image interpretation and clinical evaluation by a neurologist were too long. However, pre-hospital delay accounted for the largest contribution if considering the total interval from symptom onset to thrombolysis (Díez-Tejedor and Fuentes, 2012; Evenson et al., 2001; Hill et al., 2000).

Furthermore, studies that attempted to obtain a quantitative estimate of the pace of neural circuitry loss during ischemic stroke highlighted the urgency of acute stroke care. In untreated patients, the approximate rate of neuron loss reached up to 1.9 million neurons per minute, alongside with destruction of synapses and myelinated fibers (Saver, 2006). More recently, evaluation of the benefit of early thrombolytic treatment in the United States showed that intervention was associated with reduced mortality and better functional outcome at discharge. These findings support efforts to improve emergency management of stroke patients, but also highlight the need for a better pharmacological management of pre-hospital acute stroke care. In the context of brain ischemia, it would be desirable to find the equivalent of nitrates for acute coronary disease that delay irreversible ischemia and save many cardiac patients before reaching the hospital.

In the light of above-mentioned evidence, strategies that include public campaigns on the recognition of common stroke symptoms and reinforcement of the importance of early admission after symptom onset were widely employed in order to promote early arrival after symptom onset at hospital emergency rooms. Yet, the best strategy to maintain population awareness after media campaigns has still to be established. Isolated interventions resorting on popular mass media like TV are unlikely to guarantee extended effects on population behavior and lack a positive cost-benefit analysis (Goldstein, 2003; Silver et al., 2003; Tadros et al., 2009). However, the attitude towards the problem has shifted and health care workers and the public in general nowadays look at acute stroke as a clinical emergency, requiring specific care as promptly as possible.

Advances in the treatment of acute ischemic stroke and the advent of thrombolysis led to the development and implementation of dedicated wards and specific care for this group of patients. In so-called "stroke units", teams with special training in cerebrovascular disease began to attend acute stroke patients. This new type of organization of acute stroke care in specialized units proved to provide benefit in the short and long-term follow-up. Mortality decreased and patient functional independency improved, with a higher chance of returning to live at home, one year after the acute event (“Organised inpatient (stroke unit) care for stroke.,” 2013). The improvement in functional outcome could still be observed at 5 and 10 years of follow-up, when compared to patients treated in non-dedicated wards (Alberts et al., 2005; Drummond et al., 2005; Indredavik et al., 1999; Langhorne and Dennis, 2004).

3.2. NEUROPROTECTION *VS.* BRAIN PROTECTION

Since the majority of patients do not meet criteria for thrombolysis, neuroprotective strategies are needed to prevent definitive ischemia and cell death after stroke. However, and despite a huge amount of research, none of the more than 1000 neuroprotective drugs proposed in the setting of acute stroke that were promising in pre-clinical research proved to have clinical benefit (Ferro and Dávalos, 2006; Radermacher et al., 2012). Reasons for translation failure of experimental data into

clinical context include pleomorphic ischemic pathophysiology, double-sword effect of drugs and confounding immunobiochemical markers in different times after ischemia. Furthermore, publication bias leads under-reported negative results and inadequate replication of primary results. Other quality issues in basic research include outdated estimations of sample size, lack of randomization, failure in validation of scales, lack of control for relevant physiological parameters, and missing representation of female and older animals as well as models that include animals with common associated risk factors for stroke. Thus, most experimental models fail to express the multifaceted features of stroke patients and suffer from methodological issues. Additionally, as stroke does not comprise just a single mechanism, focusing on a unique pharmacological target is probably inadequate (Dirnagl, 2006). Furthermore, acute stroke involves all brain cells and structures. Consequently, strategies must not only target the protection of neuronal cells ("neuroprotection") but also other cells and structures (Endres and Dirnagl, 2002; Fukuda and del Zoppo, 2003; Gutiérrez et al., 2013; Liang et al., 2004; Mergenthaler et al., 2004; Traystman, 2003).

In response to the failure to tackle the step from bench to bedside, researchers tried to establish criteria and guidelines for quality control in preclinical stroke research (Lapchak et al., 2013; Saver et al., 2009). Some topics were already dealt with in the Stroke Therapy Academic Industry Roundtable (STAIR) that tried to understand the lack of success of translational research in stroke and edited recommendations for standards in preclinical neuroprotective and restorative drug development (“Recommendations for standards regarding preclinical neuroprotective and restorative drug development.,” 1999), as well as for clinical trials evaluating acute stroke therapies (“Recommendations for clinical trial evaluation of acute stroke therapies.,” 2001).

An additional critical issue is the interpretation of experimental data given that many stroke targets and markers can be biphasic and act differently in the ischemic sequence of events (Caplan et al., 2011).

Nonetheless, complete understanding of cell death after brain ischemia is missing so far, with consequences concerning new acute treatment strategies. Research on

protection of all brain cells (and not only the neuron "neuroprotection") after focal brain ischemia is needed, in order to develop new therapeutic targets. The ideal protector would include the possibility of being given blindly after symptom onset, in order to avoid brain tissue deterioration and ultimately cell death. Additionally, it would be safe enough not to harm patients that eventually suffer from other types of stroke.

On the other hand, besides rushing after symptoms onset, another possibility could include the reduction of metabolic needs in order to improve the balance between energy needs and production inside the ischemic tissue. In nature, this equilibrium is sometimes obtained in conditions like extreme external cold or hibernation, where despite lack of total or severely reduced cerebral blood flow, reversibility to normal homeostasis is possible without permanent ischemic damage.

4. PENUMBRA AND CORE

4.1. THE PENUMBRA CONCEPT

After acute stroke, the ischemic injury shows areas with a different potential for recovery, depending mainly on residual perfusion threshold, collateral circulation and capacity of microcirculation response. The classical description of penumbra after focal brain ischemia in primates (Astrup et al., 1981) includes the demonstration through measurements of electrical activity that inside the ischemic injury subsist regions that are dysfunctional but not yet dead. Neurons would not fire action potentials but could still sustain their resting membrane potentials (-70 mV), and, provided that blood flow was improved, these areas recovered with restoration of action potentials. However, if ischemia was prolonged, neurons died after anoxic depolarization, as described before (Astrup et al., 1977).

Consequently, the destiny of cells and matrix after acute stroke depends on the area where they are located inside the ischemic region: the region with a lower degree of hypoperfusion where no reversibility could be expected, the so called "ischemic core",

or the remaining hypoperfusion region, not to be recruited directly into ischemic tissue, the "penumbra", where potentially salvageable tissue depends on the access to reperfusion (Baron, 2001). As such, the penumbra represents the part of ischemic brain tissue that is damaged but not yet dead and whose recovery ability decreases over time.

From the perspective of therapeutic rescue of ischemic tissue, the "ischemic core" represents an area beyond possible rescue, electrically silent and irreversibly damaged, with energy and ion homeostasis failure. From the hemodynamic point of view, the ischemic core is perfused below the threshold of brain tissue survival (5-8 ml/100g/min in the first hours after ischemic onset) (Baron, 1999). Penumbra can also be defined as hypoperfused tissue at risk of infarction that contributes to clinical deficit and whose early reperfusion permits a better functional outcome (Lo, 2008; Moustafa and Baron, 2008).

Research on penumbra focused initial into ischemic regulation of electrophysiology, cerebral blood flow, and metabolism. Lately, on molecular mechanisms mediating cell death in the penumbral spot and imaging tools that allow to differentiate brain tissue compromise after acute ischemia (Lo, 2008). The possibility to "visualize" the penumbra both in MRI and in PET studies is considered of high translational interest since it permits individualized information regarding the existence and size of penumbra regions in each patient and the evaluation of the potential interest of reperfusion, avoiding futile reperfusion in cases where the brain tissue is irreversibly damaged.

Interestingly, the progression from injury to infarct in the penumbra metabolism may not be linear. Some penumbra areas that seem to be dying can also be, at the same time, starting endogenous repair and remodeling. Since the observation that some "dreadful" mediators linked with cell death pathways are upregulated in the acute phase of stroke and may actually promote repair, many mediators started to be seen as having a "double-edged sword" behavior, modulating both injury and repair. Furthermore, some molecular targets are thought of as having a biphasic role, mediating injury during acute phase, but contributing to remodeling and repair in the

recovery phase. Examples of this "double behavior" include NMDA antagonists or extracellular proteases of matrix metalloproteinase (MMP) that were promising in experimental research but of no proven clinical benefit after clinical trials. This double behavior, dependent on the interval after the onset of the acute event, contributed to the comprehension of how and why some neuroprotective drugs failed in the clinical context (Caplan et al., 2011).

Future research on penumbra should focus on further clarifying not only how but when and where normal brain tissue switches to a deleterious sequence of events and then back from damage to repair (Lo, 2008).

4.2. ISCHEMIA IS ABOUT CELL DEATH

All brain cell types and structures are potentially involved in the pathophysiology of ischemic stroke, and ischemia is about death of different cell types at different time points in different regions of the ischemic lesion. Lesion progression to cell death include other factors than lack of blood supply, such as inflammation. However, defining correctly the moment of irreversible cell death can be difficult and depends on the techniques employed (Zille et al., 2012).

Mechanisms involved in cell death after a sudden lack of arterial blood flow, include necrosis with disintegration of the cell membrane and release of cell content, and apoptosis with nuclear dissolution and chromatin condensation without loss of membrane integrity. Other mechanisms include autophagic cell death and phagoptosis being one cell devoured by another (Ferrer and Planas, 2003; Linnik et al., 1993; Puyal et al., 2013). Nevertheless, and although major interest exist in distinguish different types of cell death, so far no methodology can accurately distinguish between apoptosis and necrosis. Methodological problems may lead to misuse of terms or ambiguous concepts regarding cell death in stroke literature (Ferrer and Planas, 2003; Galluzzi et al., 2012).

Before neuroimaging and modern molecular biology, visualization of cell death was only possible in histological *postmortem* samples where morphological characteristics were associated with cell death. In the beginning of the 20th Century, many histological descriptions of different types of necrosis like "selective neuronal necrosis" or "incomplete necrosis" were described; later, necrotic cell death included also swelling of the organelles and disruption of the cell membrane. Only in the early seventies, Kerr and collaboraters described apoptosis, characterized by cells that show nuclear fragmentation with chromatin condensation without cell membrane rupture (Kerr et al., 1972). Years later, the morphological aspects of apoptosis after cerebral ischemia were confirmed by electron microscopy (Li et al., 1995). Finally, molecular and biochemical markers of cell dead were identified and assigned to either apoptosis or necrosis. However, the distinction is not yet as accurately as expected, despite current guidelines on definitions and nomenclature for cell death (Galluzzi et al., 2012; Zille et al., 2012).

Both histological and biomolecular markers identify cell death at a definite time point but not always coincidently. Additionally, *in vivo* imaging shows regions of interest (ROI) that will progress either to cell death or back towards normal tissue homeostasis. While it would be desirable that acute imaging tools in the context of acute brain focal ischemia would match perfectly with immunohistochemical data and relate ultimately to visualization of cell death, current descriptions of brain lesions in acute stroke imaging still represent only a surrogate for diagnosis of tissue fate.

Imaging techniques used in acute stroke include magnetic resonance imaging (MRI) and nuclear imaging techniques like positron emission tomography (PET) and single photon emission computed tomography (SPECT) (Zille et al., 2012). MRI uses very strong magnetic fields and radio waves inducing different states of excitation in the nuclei or protons of hydrogen atoms. Resulting images represent specific pathological changes in tissue water content. In the acute ischemic setting, the ability of calculating infarct volume has been used as a correlate of cell death, namely using T2-weighted image sequence and diffusion-weighted imaging (DWI).

DWI is a sequence very sensitive to Brownian water motion. Regions of restricted diffusion appear very intense and present a very low diffusion coefficient. In the setting of acute ischemia, the hyperintensity signal in DWI is attributed to disintegration of ion homeostasis and intracellular accumulation of water associated with cytotoxic edema (Fisher et al., 1992). Furthermore, the sequence of apparent diffusion coefficient (ADC) allows obtaining a quantitative measure of the level of water restriction. This quantification permits comparisons in permanent models of focal ischemia of imaging and biomolecular pathophysiological events in acute ischemia. So far, DWI can still be considered the best imaging method to diagnose acute cerebral ischemia, although it represents an indirect measure of damage without resolution at the cellular level.

MRI can also measure cerebral brain flow (CBF), cerebral blood volume (CBV) and mean transient time (MTT), using perfusion weighted imaging MRI (PWI). The "mismatch" between areas of blood perfusion and water diffusion in the ischemic territory represents the *gold standard* in brain image of the classical concept of "penumbra", a region at risk of definitive infarct but still potentially salvable, in opposition to "core" that has been described as one where tissue is irremediably lost. Limitations of the mismatch concept include the lack of penumbra threshold within the oligoemia region, the overestimation of the final infarct volume and the possible reversibility of PWI images if blood flow is restored. As such, initial PWI may not fully predict the final core (Kidwell et al., 2000).

Biomolecular correlates of penumbra include preserved ATP synthesis, synthesis of heat-shock proteins, general decrease of protein synthesis, and the capacity to elicit an unfolded protein response (Sharp et al., 2000).

The switch from “penumbra” to "core" follows an injury progression if reperfusion is not reestablished. PET studies suggested that injury progression occurs in three different stages. Initial acute ischemic injury begins within minutes after stroke onset, with a CBF below the threshold needed for energy metabolism; then it is followed by a subacute phase where "core" expands into "penumbra". Oxygen extraction fraction is still maintained despite decreased CBF and O_2 metabolism. Finally, a delayed injury

phase lasts from days to weeks. However, about half of the “penumbra” area expands to “core” within the first 3 hours, and after 6 – 8 hours, almost all ischemic area will appear as core if perfusion is not restored, both in animal models and in humans (del Zoppo et al., 2011; Heiss, 2000; Ramos-Cabrer et al., 2011).

4.3. "MICRO CORES AND MICRO PENUMBRAS"

An advance in the concept of penumbra that better expresses the variability within the ischemic injury is the theory of multiple *micro penumbras* and *micro cores* inside the ischemic territory (del Zoppo et al., 2011). Contrary to the original conception of penumbra as a concentric model of flow-related changes in evoked potentials within the ischemic injury around a core of permanent injury (Astrup et al., 1977), new data suggest that the central "core" is not dead since it can express genes that do not relate to the ischemic cascade (Ramos-Cejudo et al., 2012). Consequently, “core” may develop heterogeneously and only with time will coalesce into a homogeneous area when not reperfused in due time (and if electrical silence will not recover).

An important factor that influences differences in ischemic tissue fate consists in the variability in response of local microcirculation. Although it is generally accepted that the regulation of microvasculature plays an important role in acute ischemia, its role is not yet completely understood. In brain arteries, the blood conductance is operated by the macrocirculation, whereas the regulation of blood flow depends more on the microcirculation, including pial and penetrating arterioles, capillaries, and venules. During ischemia and after changes in endothelial cells and the breakdown of the BBB, capillaries and venules maximally dilate until no further response is obtained, and represent, in ischemic conditions, a major component of vascular resistance. Previous studies suggest a dynamic response of the microvasculature to acute focal ischemia suggestive of the presence of multiple cores. These changes support the concept that microvascular integrity is modified in a heterogeneous but consistent pattern (Tagaya et al., 2001). In consequence, a temporal relationship seems to exist between brain tissue integrity, regional CBF and electrical failure that define regions of reversible or permanent injury after acute brain ischemia (Kulik et al., 2008).

5. ISCHEMIC TOLERANCE: HYPOTHERMIA AND HIBERNATION

5.1 LACK OF CEREBRAL BLOOD FLOW WITHOUT PERMANENT NEUROLOGICAL DEFICIT

In nature, there are exceptions to the rule that lack of cerebral blood flow during a prolonged period inexorably leads to ischemia and irreversible brain damage. Examples include cardiac arrest from extreme cold (Dobson and Burgess, 1996) and hibernation (Rouble et al., 2013) where, despite very severe brain oligoemia or no cerebral blood flow at all, survival without permanent neurological deficit is possible (Dave et al., 2012; Schwartz et al., 2013; Storey and Storey, 2010). The prevention of severe brain damage in these cases, characterized by a markedly reduced cerebral blood flow during long periods, may serve as a model that can contribute to our understanding of new pharmacological targets in acute ischemic stroke treatment and to preserve brain tissue before reperfusion is achieved.

5.1.1. HYPOTHERMIA

Extreme cold is a condition where despite severe cerebral hypoperfusion or no perfusion at all, irreversible neurological damage can be avoided. Patients rescued from cardiac arrest in iced mountains or induced cold cardioplegia in the context of cardiac surgery illustrate that brain (and other tissues) can be preserved despite lack of blood flow. Consequently, there is a rational for the induction of hypothermia in acute stroke, since it may reduce deterioration if induced early enough after the onset of symptoms and maintained for an adequate period.

Two levels of externally induced decrease in body temperature are considered of therapeutic significance for translational studies: mild hypothermia (33ºC – 35ºC) and moderate hypothermia (30ºC – 33ºC). Mild hypothermia is safer, technically easier to perform (Buchan and Pulsinelli, 1990) and can be achieved in humans without sedation or mechanical ventilation. However, the neuroprotective effect varies with temperature and the time from symptom onset to hypothermia induction. A maximal

efficacy was observed with moderate cooling, maintained during a prolonged period (12h to 48h) (Corbett et al., 2000). Nonetheless, even a small decrease of basal body temperature of around 2ºC or less has a protective effect and its histological and behavioral evidence could be shown. However, external hypothermia was only effective if applied 5 min after hypoperfusion begun and not when it was delayed more than 30 min (Busto et al., 1989). Therefore, the extent of decrease in body temperature, the time from stroke onset, and the duration of hypothermia exposure contribute to outcome.

In animal models of acute ischemia, induced hypothermia showed benefit by reducing infarct size and ameliorating functional outcome (Campos et al.,2012). A meta-analysis of experimental data, including more than 100 experiments, confirmed that induced hypothermia after focal brain ischemia diminished infarct size and improved functional outcome. Yet, a very wide array of temperatures, duration of exposure and intervals between stroke onset and the initiation of hypothermia was tested, making it difficult to conclude for the most adequate subset of conditions. Overall, the hypothermia effect was more pronounced with lower temperatures, although still present in mild hypothermia as long as temperature was decreased below 35ºC (van der Worp et al., 2007). In the translational context, the induction of lower temperatures requires intensive care support, not universally available for the treatment of a highly prevalent disease like ischemic stroke.

The mechanisms by which hypothermia may protect brain tissue from ischemia are not yet entirely understood. In regard to mild hypothermia, protection was not only associated with the induced metabolic changes and reduction in metabolic needs, but also with inhibition of presumably protective biological processes, such as detoxification and repair, and the final balance between protective and non-protective mechanisms is difficult to establish. Nevertheless, some mechanisms are already acknowledged for their contribution to hypothermia brain protection. These include the decline of cerebral metabolic rate creating a more favorable balance between oxygen demand and supply, which represents a critical issue in acute ischemia. Furthermore, hypothermia promotes the decrease in arteriole permeability with development of less cerebral edema and a reduced brain-blood-barrier disruption with

less formation of free radicals and excitatory neurotransmitters (including glutamate), as well as a milder inflammatory response with reduced release of pro-inflammatory cytokines and leukocyte adhesion (Sinclair and Andrews, 2010). Thus, hypothermia induces changes in the CBF regulation, cell membrane stability, energetic metabolism and intracellular signaling, as well as modulation of excitotoxicity and acid-base balance, with interference in apoptotic mechanisms (Schaller and Graf, 2003).

In the clinical context, physical or pharmacological induction of hypothermia after acute stroke can trigger complications like bradycardia, shivering, and an increase in pneumonia occurrence, with controversial benefit in death rate. A Cochrane meta-analysis showed no evidence supporting the routine use of reducing temperature after acute ischemic stroke (Den Hertog et al., 2009). However, recent clinical trials showed benefit reducing unfavorable functional outcome at 3 months (Piironen et al., 2014). A large multicenter randomized phase III trial is under way to further clarify this issue (van der Worp et al., 2014).

5.1.2. DORMANCY AND HIBERNATION

Hibernation is a molecular, physiological, and behavioral adaptation of some mammalian species in periods of unpredictable or shortage of food availability. During states of dormancy and hibernation, mammals are able to survive with metabolic rates as low as 2% of their usual needs, without irreversible brain lesions. During these periods, animals need to carry out adaptive transformations, including mechanisms of metabolic suppression by actively decreasing body temperature and depressing immune functions, but also increased oxidative resistance (Drew et al., 2007; Zhou et al., 2001).

CNS regulation of hibernation is poorly understood but comprises a "circannually regulated hibernating protein complex". This protein complex allows metabolic flexibility regulated via neuronal pathways. Central sites for regulation include the hippocampus, hypothalamus, and nuclei of the autonomic nervous system. Wide-ranging sympathetic activation is suppressed and parasympathetic inhibition of

metabolic pathways promoted. The decreased demands in CNS metabolism cause a decrease in body temperature that assists further cooling by temperature-dependent mechanism. The mechanisms of metabolic suppression in hibernation include a reversible reduction in cellular needs for oxygen and other nutrients, better fitting the metabolic demand with the supply (Drew et al., 2007). Knowledge about the mechanisms used by hibernating animals to decrease metabolic demand may have translation potential for stroke therapy (Drew et al., 2007; Storey and Storey, 2010).

5.2 NITRIC OXIDE, CARBON MONOXIDE, AND HYDROGEN SULFIDE

Nitric oxide (NO) and carbon monoxide (CO) are signaling gaseous molecules of the central nervous and cardiovascular system with cytoprotective properties in the context of brain and heart ischemia (Elrod et al., 2006). Lately, particular attention has been paid to the potential biological significance of hydrogen sulfide (H_2S), initially known for its toxic environmental properties (Abe and Kimura, 1996; Beauchamp et al., 1984). These 3 labile biological mediators (NO, CO e H_2S) have common characteristics like being able to cross cell membranes without the need of membrane transporters, thus having easy and prompt access to intracellular pathways.

Interestingly, Blackstone and coworkers induced a condition similar to hibernation in mammals that normally do not hibernate by H_2S inhalation in their study published in 2005. They called this condition the “suspended animation-like state”. Mice exposed to a H_2S enriched atmosphere showed a significant decrease in their metabolic rates (measured through O_2 consumption and CO_2 elimination) and body temperature. After 6 hours of exposure to H_2S, animals started to breathe normal atmosphere and returned spontaneously to normal metabolic rates and body temperature, with no changes in health condition in short and long-term follow-up (Blackstone et al., 2005).

Hydrogen sulfide is a gas that results from bacterial breakdown of organic matter in anaerobic conditions. Small amounts are produced in the human body and used as signaling molecule. H_2S is present in the central nervous system at relatively concentrations (50 to 160 microM) in comparison to other organs which suggests that

it may have a localized physiological function (Abe and Kimura, 1996; Kimura and Kimura, 2004). Nevertheless, controversy still exists about measuring methods (Olson et al., 2014). H_2S is a vasodilator of the cerebral arterioles via activation of K(ATP) channels (Leffler et al., 2011), but its biological functions extent far beyond its direct effects on vasotonus.

H_2S is synthesized in mammals in different organs through two major L-cysteine metabolic pathways that depend on pyridoxal-5'-phosphate enzymes: cystathionine beta-synthase (CBS) and cystathionine gamma-lyase (CSE). L-cysteine can originate from food sources (like yogurt, oat flakes, and eggs), or be synthesized from L-methionine through the transsulfuration pathway, with homocysteine acting as intermediary in the process. The biological effects of exposure to H_2S seem to depend largely on its capacity to inhibit mitochondrial oxidative phosphorylation. H_2S is a potent inhibitor of brain cytochrome oxidase activity and suppresses metabolism since it is an inhibitor of cellular oxidative phosphorylation (Wallace and Starkov, 2000). Consequently, metabolic suppression precedes the decrease in body temperature that is observed after H_2S inhalation (Blackstone et al., 2005). This characteristically differentiates H_2S from other methods to induce hypothermia where the decrease in temperature precedes the hypometabolic effect.

Regarding temperature regulation in hibernation, the decrease in CNS activation and metabolic demand facilitates the drop in body temperature. Cooling can then boost further metabolic suppression by down-regulating temperature-dependent mechanisms including neuronal activity (Drew et al., 2007). Thus, the biologic effect of H_2S can be compared to the mechanisms described in the torpor phases of hibernation where reduced metabolism also seems to be accomplished by synergistic effects of both passive (temperature-dependent) and active (temperature-independent) mechanisms that provide a decrease in oxygen demand.

H_2S is endogenously produced in different organs including the brain (Mani et al., 2013) and regulates oxygen consumption by competing with O_2 in binding to cytochrome C oxydase at the mitochondrial electron transport chain (Wagner et al., 2009). A suggested mechanism for the regulation of H_2S refers to the observation that

the concentration of biologically active H_2S is regulated by the simple balance between constitutive H_2S production and its oxidation by the mitochondria (Olson, 2013; Olson et al., 2014). The potential of H_2S as a pharmacological tool in acute brain ischemia may also relate to its role as an oxygen sensor (Olson et al., 2013) and its properties concerning the regulation of neuronal and glial communication (Mikami et al., 2011) and of local vasotone (Leffler et al., 2011). Being an oxygen sensor H_2S may contribute to monitoring environmental oxygen and ensuring adequate delivery to tissues.

However, the biological effects of H_2S are still controversial and depend, among other factors, on the dosage and duration of the exposure. At micromolecular concentrations, H_2S appears to have a neuroprotective role, not only by interference with oxidative stress and cell death pathways but by modulation of the activity of the N-metil-d-aspartate (NMDA) receptors in physiological concentrations (Kimura and Kimura, 2004). Furthermore, induction and upregulation of cytoprotective and anti-inflammatory genes, including heme oxygenase-1 (HO_1) which allows the production of CO with renowned cytoprotective and anti-inflammatory properties, was attributed to H_2S (Nagai et al., 2004). Thus, exogenous administration of H_2S may also be cytoprotective in the context of acute experimental ischemia.

5.3. PREVIOUS WORKS WITH H_2S AFTER EXPERIMENTAL STROKE

Since the publication of an article in Science in 2005, showing that the inhalation of a mixture of atmosphere and H2S induced a dramatic reduction in oxygen consumption to less than 15% of normal metabolic rates without irreversible neurological deficits (Blackstone et al., 2005), the potential benefit of H_2S in the context of acute ischemia started to be investigated.

Despite multiple potentially protective mechanisms of H_2S, data regarding the benefit of H_2S in the context of acute ischemic stroke were few and conflicting when we designed the present research project. A first report on H_2S in acute ischemic stroke in a rodent model showed no benefit in functional outcome (Qu et al., 2006). Later, other studies including older rats or permanent and reperfusion models and prolonged

exposure to H_2S, demonstrated a clear benefit, both in functional outcome and in lesion size (Florian et al., 2008; Gheibi et al., 2014; Joseph et al., 2012). These results were in concordance with the data from experimental ischemic models of other organs like the heart and the kidney where similar benefits were observed using H_2S gas or liquid vials with H_2S donors (Bannenberg and Vieira, 2009; Hosgood and Nicholson, 2010; Simon et al., 2008; Sodha et al., 2009). Consequently, a rational for the potential translational interest of H_2S or H_2S donors in the context of acute stroke was established.

Nevertheless, the controversy about the cytoprotective role of H_2S in the context of acute ischemia persists and neurotoxic effects have been described in rodents. These discrepancies in the action of H_2S have been observed within the same specie (Qu et al., 2006) , between distinct species (mouse and piglets) (Li et al., 2008), and between distinct organs (heart and brain) (Hayashida et al., 2008). The reasons for this discrepancy in existing data include the fact that H_2S protective effects are dose–dependent, probably even at micro doses (ppM), as suggested by studies in myocardial ischemia (Johansen et al., 2006). Furthermore, results of H_2S administration also depend on exposure time for the purpose of hypometabolic effects, particularly in mammals with large body size.

The induction of hypometabolic conditions after the onset of acute cerebral ischemia by reducing metabolic needs and diminishing the difference between energy production and demand may theoretically contribute to prevention of ischemic injury, enlarging the time window until spontaneous reperfusion occurs or therapeutic reperfusion is available. If confirmed in experimental and clinical setting, the induction of hypometabolism may represent an option to increase the therapeutic window and a chance for thrombolysis in patients that are currently excluded from reperfusion therapy.

6. REFERENCES

Abe, K., Kimura, H., 1996. The possible role of hydrogen sulfide as an endogenous neuromodulator. J. Neurosci. 16, 1066–71.

Alberts, M.J., Latchaw, R.E., Selman, W.R., Shephard, T., Hadley, M.N., Brass, L.M., Koroshetz, W., Marler, J.R., Booss, J., Zorowitz, R.D., Croft, J.B., Magnis, E., Mulligan, D., Jagoda, A., O'Connor, R., Cawley, C.M., Connors, J.J., Rose-DeRenzy, J.A., Emr, M., Warren, M., Walker, M.D., 2005. Recommendations for comprehensive stroke centers: a consensus statement from the Brain Attack Coalition. Stroke. 36, 1597–616.

Arrick, D.M., Sharpe, G.M., Sun, H., Mayhan, W.G., 2007. nNOS-dependent reactivity of cerebral arterioles in Type 1 diabetes. Brain Res. 1184, 365–71.

Astrup, J., Siesjö, B.K., Symon, L., 1981. Thresholds in cerebral ischemia - the ischemic penumbra. Stroke. 12, 723–5.

Astrup, J., Symon, L., Branston, N.M., Lassen, N.A., 1977. Cortical evoked potential and extracellular K+ and H+ at critical levels of brain ischemia. Stroke. 8, 51–7.

Bannenberg, G.L., Vieira, H.L. a, 2009. Therapeutic applications of the gaseous mediators carbon monoxide and hydrogen sulfide. Expert Opin. Ther. Pat. 19, 663–82.

Baron, J.C., 1999. Mapping the ischaemic penumbra with PET: implications for acute stroke treatment. Cerebrovasc. Dis. 9, 193–201.

Baron, J.C., 2001. Mapping the ischaemic penumbra with PET: a new approach. Brain 124, 2–4.

Beauchamp, R.O., Bus, J.S., Popp, J.A., Boreiko, C.J., Andjelkovich, D.A., 1984. A critical review of the literature on hydrogen sulfide toxicity. Crit. Rev. Toxicol. 13, 25–97.

Blackstone, E., Morrison, M., Roth, M.B., 2005. H2S induces a suspended animation-like state in mice. Science 308, 518.

Bluhmki, E., Chamorro, A., Dávalos, A., Machnig, T., Sauce, C., Wahlgren, N., Wardlaw, J., Hacke, W., 2009. Stroke treatment with alteplase given 3.0-4.5 h after onset of acute ischaemic stroke (ECASS III): additional outcomes and subgroup analysis of a randomised controlled trial. Lancet Neurol. 8, 1095–102.

Buchan, A., Pulsinelli, W.A., 1990. Hypothermia but not the N-methyl-D-aspartate antagonist, MK-801, attenuates neuronal damage in gerbils subjected to transient global ischemia. J. Neurosci. 10, 311–6.

Busto, R., Dietrich, W.D., Globus, M.Y., Ginsberg, M.D., 1989. Postischemic moderate hypothermia inhibits CA1 hippocampal ischemic neuronal injury. Neurosci. Lett. 101, 299–304.

Campos, F., Blanco, M., Barral, D., Agulla, J., Ramos-Cabrer, P., Castillo, J., 2012. Influence of temperature on ischemic brain: basic and clinical principles. Neurochem. Int. 60, 495–505.

Caplan, L.R., Arenillas, J., Cramer, S.C., Joutel, A., Lo, E.H., Meschia, J., Savitz, S., Tournier-Lasserve, E., 2011. Stroke-related translational research. Arch. Neurol. 68, 1110–23.

Cheng, B., Brinkmann, M., Forkert, N.D., Treszl, A., Ebinger, M., Köhrmann, M., Wu, O., Kang, D.-W., Liebeskind, D.S., Tourdias, T., Singer, O.C., Christensen, S., Luby, M., Warach, S., Fiehler, J., Fiebach, J.B., Gerloff, C., Thomalla, G., 2013. Quantitative measurements of relative fluid-attenuated inversion recovery (FLAIR) signal intensities in acute stroke for the prediction of time from symptom onset. J. Cereb. Blood Flow Metab. 33, 76–84.

Corbett, D., Hamilton, M., Colbourne, F., 2000. Persistent neuroprotection with prolonged postischemic hypothermia in adult rats subjected to transient middle cerebral artery occlusion. Exp. Neurol. 163, 200–6.

Correia, M., Magalhães, R., Silva, M.R., Matos, I., Silva, M.C., 2013. Stroke types in rural and urban northern portugal: incidence and 7-year survival in a community-based study. Cerebrovasc. Dis. Extra 3, 137–49.

Correia, M., Silva, M.R., Matos, I., Magalhães, R., Lopes, J.C., Ferro, J.M., Silva, M.C., 2004. Prospective community-based study of stroke in Northern Portugal: incidence and case fatality in rural and urban populations. Stroke. 35, 2048–53.

Dave, K.R., Christian, S.L., Perez-Pinzon, M.A., Drew, K.L., 2012. Neuroprotection: lessons from hibernators. Comp. Biochem. Physiol. B. Biochem. Mol. Biol. 162, 1–9.

Del Zoppo, G.J., Sharp, F.R., Heiss, W.-D., Albers, G.W., 2011. Heterogeneity in the penumbra. J. Cereb. Blood Flow Metab. 31, 1836–51.

Den Hertog, H.M., van der Worp, H.B., Tseng, M.-C., Dippel, D.W., 2009. Cooling therapy for acute stroke. Cochrane database Syst. Rev. CD001247.

Díez-Tejedor, E., Fuentes, B., 2012. Stroke: Bringing care to the patient--quick treatment at any cost? Nat. Rev. Neurol. 8, 362–3.

Dirnagl, U., 2006. Bench to bedside: the quest for quality in experimental stroke research. J. Cereb. Blood Flow Metab. 26, 1465–78.

Dobson, J.A., Burgess, J.J., 1996. Resuscitation of severe hypothermia by extracorporeal rewarming in a child. J. Trauma 40, 483–5.

Drew, K.L., Buck, C.L., Barnes, B.M., Christian, S.L., Rasley, B.T., Harris, M.B., 2007. Central nervous system regulation of mammalian hibernation: implications for metabolic suppression and ischemia tolerance. J. Neurochem. 102, 1713–26.

Drummond, A.E.R., Pearson, B., Lincoln, N.B., Berman, P., 2005. Ten year follow-up of a randomised controlled trial of care in a stroke rehabilitation unit. BMJ 331, 491–2.

Elrod, J.W., Duranski, M.R., Langston, W., Greer, J.J.M., Tao, L., Dugas, T.R., Kevil, C.G., Champion, H.C., Lefer, D.J., 2006. eNOS gene therapy exacerbates hepatic ischemia-reperfusion injury in diabetes: a role for eNOS uncoupling. Circ. Res. 99, 78–85.

Endres, M., Dirnagl, U., 2002. Ischemia and stroke. Adv. Exp. Med. Biol. 513, 455–73.

Evenson, K.R., Rosamond, W.D., Morris, D.L., 2001. Prehospital and in-hospital delays in acute stroke care. Neuroepidemiology 20, 65–76.

Feigin, V.L., Lawes, C.M.M., Bennett, D.A., Anderson, C.S., 2003. Stroke epidemiology: a review of population-based studies of incidence, prevalence, and case-fatality in the late 20th century. Lancet Neurol. 2, 43–53.

Ferrer, I., Planas, A.M., 2003. Signaling of cell death and cell survival following focal cerebral ischemia: life and death struggle in the penumbra. J. Neuropathol. Exp. Neurol. 62, 329–39.

Ferro, J.M., 1997. [Is hospital admission urgent in stroke?]. Rev. Neurol. 25, 1110–2.

Ferro, J.M., Dávalos, A., 2006. Other neuroprotective therapies on trial in acute stroke. Cerebrovasc. Dis. 21 Suppl 2, 127–30.

Fisher, M., Sotak, C.H., Minematsu, K., Li, L., 1992. New magnetic resonance techniques for evaluating cerebrovascular disease. Ann. Neurol. 32, 115–22.

Florian, B., Vintilescu, R., Balseanu, A.T., Buga, A.-M., Grisk, O., Walker, L.C., Kessler, C., Popa-Wagner, A., 2008. Long-term hypothermia reduces infarct volume in aged rats after focal ischemia. Neurosci. Lett. 438, 180–5.

Fukuda, S., del Zoppo, G.J., 2003. Models of focal cerebral ischemia in the nonhuman primate. ILAR J. 44, 96–104.

Galluzzi, L., Vitale, I., Abrams, J.M., Alnemri, E.S., Baehrecke, E.H., Blagosklonny, M. V, Dawson, T.M., Dawson, V.L., El-Deiry, W.S., Fulda, S., Gottlieb, E., Green, D.R., Hengartner, M.O., Kepp, O., Knight, R.A., Kumar, S., Lipton, S.A., Lu, X., Madeo, F., Malorni, W., Mehlen, P., Nuñez, G., Peter, M.E., Piacentini, M., Rubinsztein, D.C., Shi, Y., Simon, H.-U., Vandenabeele, P., White, E., Yuan, J., Zhivotovsky, B., Melino,

G., Kroemer, G., 2012. Molecular definitions of cell death subroutines: recommendations of the Nomenclature Committee on Cell Death 2012. Cell Death Differ. 19, 107–20.

Gheibi, S., Aboutaleb, N., Khaksari, M., Kalalian-Moghaddam, H., Vakili, A., Asadi, Y., Mehrjerdi, F.Z., Gheibi, A., 2014. Hydrogen Sulfide Protects the Brain Against Ischemic Reperfusion Injury in a Transient Model of Focal Cerebral Ischemia. J. Mol. Neurosci.

Goldstein, L.B., 2003. Editorial comment--Advertising strategies to increase the public knowledge of the warning signs of stroke. Stroke. 34, 1968–9.

Gomez, C.R., Malkoff, M.D., Sauer, C.M., Tulyapronchote, R., Burch, C.M., Banet, G.A., 1994. Code stroke. An attempt to shorten inhospital therapeutic delays. Stroke. 25, 1920–3.

Gutiérrez-Fernández M, Rodríguez-Frutos B, Ramos-Cejudo J, Otero-Ortega L, Fuentes B, Díez-Tejedor E. Stem cells for brain repair and recovery after stroke. Expert Opin Biol Ther. 2013 Nov;13(11):1479-83

Hacke, W., Kaste, M., Bluhmki, E., Brozman, M., Dávalos, A., Guidetti, D., Larrue, V., Lees, K.R., Medeghri, Z., Machnig, T., Schneider, D., von Kummer, R., Wahlgren, N., Toni, D., 2008. Thrombolysis with alteplase 3 to 4.5 hours after acute ischemic stroke. N. Engl. J. Med. 359, 1317–29.

Hacke, W., Kaste, M., Fieschi, C., Toni, D., Lesaffre, E., von Kummer, R., Boysen, G., Bluhmki, E., Höxter, G., Mahagne, M.H., 1995. Intravenous thrombolysis with recombinant tissue plasminogen activator for acute hemispheric stroke. The European Cooperative Acute Stroke Study (ECASS). JAMA 274, 1017–25.

Hayashida, K., Sano, M., Ohsawa, I., Shinmura, K., Tamaki, K., Kimura, K., Endo, J., Katayama, T., Kawamura, A., Kohsaka, S., Makino, S., Ohta, S., Ogawa, S., Fukuda, K., 2008. Inhalation of hydrogen gas reduces infarct size in the rat model of myocardial ischemia-reperfusion injury. Biochem. Biophys. Res. Commun. 373, 30–5.

Heiss, W.D., 2000. Ischemic penumbra: evidence from functional imaging in man. J. Cereb. Blood Flow Metab. 20, 1276–93.

Hill, M.D., Barber, P.A., Demchuk, A.M., Sevick, R.J., Newcommon, N.J., Green, T., Buchan, A.M., 2000. Building a “brain attack” team to administer thrombolytic therapy for acute ischemic stroke. CMAJ 162, 1589–93.

Hosgood, S.A., Nicholson, M.L., 2010. Hydrogen sulphide ameliorates ischaemia-reperfusion injury in an experimental model of non-heart-beating donor kidney transplantation. Br. J. Surg. 97, 202–9.

Hussein, H.M., Georgiadis, A.L., Vazquez, G., Miley, J.T., Memon, M.Z., Mohammad, Y.M., Christoforidis, G.A., Tariq, N., Qureshi, A.I., 2010. Occurrence and predictors of futile recanalization following endovascular treatment among patients with acute ischemic stroke: a multicenter study. AJNR. Am. J. Neuroradiol. 31, 454–8.

Iadecola, C., Davisson, R.L., 2008. Hypertension and cerebrovascular dysfunction. Cell Metab. 7, 476–84.

Indredavik, B., Bakke, F., Slordahl, S.A., Rokseth, R., Hâheim, L.L., 1999. Stroke unit treatment. 10-year follow-up. Stroke. 30, 1524–7.

Johansen, D., Ytrehus, K., Baxter, G.F., 2006. Exogenous hydrogen sulfide (H2S) protects against regional myocardial ischemia-reperfusion injury--Evidence for a role of K ATP channels. Basic Res. Cardiol. 101, 53–60.

Joseph, C., Buga, A.-M., Vintilescu, R., Balseanu, A.T., Moldovan, M., Junker, H., Walker, L., Lotze, M., Popa-Wagner, A., 2012. Prolonged gaseous hypothermia prevents the upregulation of phagocytosis-specific protein annexin 1 and causes low-amplitude EEG activity in the aged rat brain after cerebral ischemia. J. Cereb. Blood Flow Metab. 32, 1632–42.

Kerr, J.F., Wyllie, A.H., Currie, A.R., 1972. Apoptosis: a basic biological phenomenon with wide-ranging implications in tissue kinetics. Br. J. Cancer 26, 239–57.

Kidwell, C.S., Saver, J.L., Mattiello, J., Starkman, S., Vinuela, F., Duckwiler, G., Gobin, Y.P., Jahan, R., Vespa, P., Kalafut, M., Alger, J.R., 2000. Thrombolytic reversal of acute human cerebral ischemic injury shown by diffusion/perfusion magnetic resonance imaging. Ann. Neurol. 47, 462–9.

Kimura, Y., Kimura, H., 2004. Hydrogen sulfide protects neurons from oxidative stress. FASEB J. 18, 1165–7.

Kulik, T., Kusano, Y., Aronhime, S., Sandler, A.L., Winn, H.R., 2008. Regulation of cerebral vasculature in normal and ischemic brain. Neuropharmacology 55, 281–8.

Langhorne, P., Dennis, M.S., 2004. Stroke units: the next 10 years. Lancet 363, 834–5.

Lapchak, P.A., Zhang, J.H., Noble-Haeusslein, L.J., 2013. RIGOR guidelines: escalating STAIR and STEPS for effective translational research. Transl. Stroke Res. 4, 279–85.

Lees, K.R., Bluhmki, E., von Kummer, R., Brott, T.G., Toni, D., Grotta, J.C., Albers, G.W., Kaste, M., Marler, J.R., Hamilton, S.A., Tilley, B.C., Davis, S.M., Donnan, G.A., Hacke, W., Allen, K., Mau, J., Meier, D., del Zoppo, G., De Silva, D.A., Butcher, K.S., Parsons, M.W., Barber, P.A., Levi, C., Bladin, C., Byrnes, G., 2010. Time to treatment with intravenous alteplase and outcome in stroke: an updated pooled analysis of ECASS, ATLANTIS, NINDS, and EPITHET trials. Lancet 375, 1695–703.

Leffler, C.W., Parfenova, H., Basuroy, S., Jaggar, J.H., Umstot, E.S., Fedinec, A.L., 2011. Hydrogen sulfide and cerebral microvascular tone in newborn pigs. Am. J. Physiol. Heart Circ. Physiol. 300, H440–7.

Li, J., Zhang, G., Cai, S., Redington, A.N., 2008. Effect of inhaled hydrogen sulfide on metabolic responses in anesthetized, paralyzed, and mechanically ventilated piglets. Pediatr. Crit. Care Med. 9, 110–2.

Li, Y., Sharov, V.G., Jiang, N., Zaloga, C., Sabbah, H.N., Chopp, M., 1995. Ultrastructural and light microscopic evidence of apoptosis after middle cerebral artery occlusion in the rat. Am. J. Pathol. 146, 1045–51.

Liang, D., Dawson, T.M., Dawson, V.L., 2004. What have genetically engineered mice taught us about ischemic injury? Curr. Mol. Med. 4, 207–25.

Linnik, M.D., Zobrist, R.H., Hatfield, M.D., 1993. Evidence supporting a role for programmed cell death in focal cerebral ischemia in rats. Stroke. 24, 2002–8; discussion 2008–9.

Lo, E.H., 2008. A new penumbra: transitioning from injury into repair after stroke. Nat. Med. 14, 497–500.

Mani, S., Li, H., Untereiner, A., Wu, L., Yang, G., Austin, R.C., Dickhout, J.D., Lhoták, S., Meng, Q.H., Wang, R., 2013. Decreased Endogenous Production of Hydrogen Sulfide Accelerates Atherosclerosis. Circulation 127, 2523–34.

Mergenthaler, P., Dirnagl, U., Meisel, A., 2004. Pathophysiology of stroke: lessons from animal models. Metab. Brain Dis. 19, 151–67.

Mikami, Y., Shibuya, N., Kimura, Y., Nagahara, N., Yamada, M., Kimura, H., 2011. Hydrogen sulfide protects the retina from light-induced degeneration by the modulation of Ca2+ influx. J. Biol. Chem. 286, 39379–86.

Moskowitz, M.A., Lo, E.H., Iadecola, C., 2010. The science of stroke: mechanisms in search of treatments. Neuron 67, 181–98.

Moustafa, R.R., Baron, J.-C., 2008. Pathophysiology of ischaemic stroke: insights from imaging, and implications for therapy and drug discovery. Br. J. Pharmacol. 153 Suppl , S44–54.

Nagai, Y., Tsugane, M., Oka, J.-I., Kimura, H., 2004. Hydrogen sulfide induces calcium waves in astrocytes. FASEB J. 18, 557–9.

Olmez, I., Ozyurt, H., 2012. Reactive oxygen species and ischemic cerebrovascular disease. Neurochem. Int. 60, 208–12.

Olson, K.R., 2013. Hydrogen sulfide as an oxygen sensor. Clin. Chem. Lab. Med. 51, 623–32.

Olson, K.R., Deleon, E.R., Gao, Y., Hurley, K., Sadauskas, V., Batz, C., Stoy, G.F., 2013. Thiosulfate: a Readily Accessible Source of Hydrogen Sulfide in Oxygen Sensing. Am. J. Physiol. Regul. Integr. Comp. Physiol.

Olson, K.R., DeLeon, E.R., Liu, F., 2014. Controversies and Conundrums in Hydrogen Sulfide Biology. Nitric Oxide.

Organised inpatient (stroke unit) care for stroke., 2013. . Cochrane database Syst. Rev. 9, CD000197.

Pacher, P., Beckman, J.S., Liaudet, L., 2007. Nitric oxide and peroxynitrite in health and disease. Physiol. Rev. 87, 315–424.

Piironen, K., Tiainen, M., Mustanoja, S., Kaukonen, K.-M., Meretoja, A., Tatlisumak, T., Kaste, M., 2014. Mild hypothermia after intravenous thrombolysis in patients with acute stroke: a randomized controlled trial. Stroke. 45, 486–91.

Puyal, J., Ginet, V., Clarke, P.G.H., 2013. Multiple interacting cell death mechanisms in the mediation of excitotoxicity and ischemic brain damage: a challenge for neuroprotection. Prog. Neurobiol. 105, 24–48.

Qu, K., Chen, C.P.L.H., Halliwell, B., Moore, P.K., Wong, P.T.-H., 2006. Hydrogen sulfide is a mediator of cerebral ischemic damage. Stroke. 37, 889–93.

Radermacher, K.A., Wingler, K., Kleikers, P., Altenhöfer, S., Jr Hermans, J., Kleinschnitz, C., Hhw Schmidt, H., 2012. The 1027th target candidate in stroke: Will NADPH oxidase hold up? Exp. Transl. Stroke Med. 4, 11.

Ramos-Cabrer, P., Campos, F., Sobrino, T., Castillo, J., 2011. Targeting the ischemic penumbra. Stroke. 42, S7–11.

Ramos-Cejudo, J., Gutiérrez-Fernández, M., Rodríguez-Frutos, B., Expósito Alcaide, M., Sánchez-Cabo, F., Dopazo, A., Díez-Tejedor, E., 2012. Spatial and temporal gene expression differences in core and periinfarct areas in experimental stroke: a microarray analysis. PLoS One 7, e52121.

Recommendations for clinical trial evaluation of acute stroke therapies., 2001. . Stroke. 32, 1598–606.

Recommendations for standards regarding preclinical neuroprotective and restorative drug development., 1999. . Stroke. 30, 2752–8.

Rouble, A.N., Hefler, J., Mamady, H., Storey, K.B., Tessier, S.N., 2013. Anti-apoptotic signaling as a cytoprotective mechanism in mammalian hibernation. PeerJ 1, e29.

Sarti, C., Rastenyte, D., Cepaitis, Z., Tuomilehto, J., 2000. International trends in mortality from stroke, 1968 to 1994. Stroke. 31, 1588–601.

Saver, J.L., 2006. Time is brain--quantified. Stroke. 37, 263–6.

Saver, J.L., Albers, G.W., Dunn, B., Johnston, K.C., Fisher, M., 2009. Stroke Therapy Academic Industry Roundtable (STAIR) recommendations for extended window acute stroke therapy trials. Stroke. 40, 2594–600.

Schaller, B., Graf, R., 2003. Hypothermia and stroke: the pathophysiological background. Pathophysiology 10, 7–35.

Schulz, E., Jansen, T., Wenzel, P., Daiber, A., Münzel, T., 2008. Nitric oxide, tetrahydrobiopterin, oxidative stress, and endothelial dysfunction in hypertension. Antioxid. Redox Signal. 10, 1115–26.

Schwartz, C., Hampton, M., Andrews, M.T., 2013. Seasonal and regional differences in gene expression in the brain of a hibernating mammal. PLoS One 8, e58427.

Sharp, F.R., Lu, A., Tang, Y., Millhorn, D.E., 2000. Multiple molecular penumbras after focal cerebral ischemia. J. Cereb. Blood Flow Metab. 20, 1011–32.

Shuaib, A., Butcher, K., Mohammad, A.A., Saqqur, M., Liebeskind, D.S., 2011. Collateral blood vessels in acute ischaemic stroke: a potential therapeutic target. Lancet Neurol. 10, 909–21.

Silver, F.L., Rubini, F., Black, D., Hodgson, C.S., 2003. Advertising strategies to increase public knowledge of the warning signs of stroke. Stroke. 34, 1965–8.

Simon, F., Giudici, R., Duy, C.N., Schelzig, H., Oter, S., Gröger, M., Wachter, U., Vogt, J., Speit, G., Szabó, C., Radermacher, P., Calzia, E., 2008. Hemodynamic and metabolic effects of hydrogen sulfide during porcine ischemia/reperfusion injury. Shock 30, 359–64.

Sinclair, H.L., Andrews, P.J., 2010. Bench-to-bedside review: Hypothermia in traumatic brain injury. Crit. Care 14, 204.

Sodha, N.R., Clements, R.T., Feng, J., Liu, Y., Bianchi, C., Horvath, E.M., Szabo, C., Stahl, G.L., Sellke, F.W., 2009. Hydrogen sulfide therapy attenuates the inflammatory response in a porcine model of myocardial ischemia/reperfusion injury. J. Thorac. Cardiovasc. Surg. 138, 977–84.

Storey, K.B., Storey, J.M., 2010. Metabolic rate depression: the biochemistry of mammalian hibernation. Adv. Clin. Chem. 52, 77–108.

Tadros, A., Crocco, T., Davis, S.M., Newman, J., Mullen, J., Best, R., Teets, A., Maxwell, C., Slaughter, B., Teter, S., 2009. Emergency medical services-based community stroke education: pilot results from a novel approach. Stroke. 40, 2134–42.

Tagaya, M., Haring, H.P., Stuiver, I., Wagner, S., Abumiya, T., Lucero, J., Lee, P., Copeland, B.R., Seiffert, D., del Zoppo, G.J., 2001. Rapid loss of microvascular integrin expression during focal brain ischemia reflects neuron injury. J. Cereb. Blood Flow Metab. 21, 835–46.

The World Health Organization MONICA Project (monitoring trends and determinants in cardiovascular disease): a major international collaboration. WHO MONICA Project Principal Investigators., 1988. . J. Clin. Epidemiol. 41, 105–14.

Tissue plasminogen activator for acute ischemic stroke. The National Institute of Neurological Disorders and Stroke rt-PA Stroke Study Group., 1995. . N. Engl. J. Med. 333, 1581–7.

Traystman, R.J., 2003. Animal models of focal and global cerebral ischemia. ILAR J. 44, 85–95.

Truelsen, T., Piechowski-Jóźwiak, B., Bonita, R., Mathers, C., Bogousslavsky, J., Boysen, G., 2006. Stroke incidence and prevalence in Europe: a review of available data. Eur. J. Neurol. 13, 581–98.

Van der Worp, H.B., Macleod, M.R., Bath, P.M.W., Demotes, J., Durand-Zaleski, I., Gebhardt, B., Gluud, C., Kollmar, R., Krieger, D.W., Lees, K.R., Molina, C., Montaner, J., Roine, R.O., Petersson, J., Staykov, D., Szabo, I., Wardlaw, J.M., Schwab, S., 2014. EuroHYP-1: European multicenter, randomized, phase III clinical trial of therapeutic hypothermia plus best medical treatment vs. best medical treatment alone for acute ischemic stroke. Int. J. Stroke 9, 642–5.

Van der Worp, H.B., Sena, E.S., Donnan, G.A., Howells, D.W., Macleod, M.R., 2007. Hypothermia in animal models of acute ischaemic stroke: a systematic review and meta-analysis. Brain 130, 3063–74.

Wagner, F., Asfar, P., Calzia, E., Radermacher, P., Szabó, C., 2009. Bench-to-bedside review: Hydrogen sulfide--the third gaseous transmitter: applications for critical care. Crit. Care 13, 213.

Wallace, K.B., Starkov, A.A., 2000. Mitochondrial targets of drug toxicity. Annu. Rev. Pharmacol. Toxicol. 40, 353–88.

Zhou, F., Zhu, X., Castellani, R.J., Stimmelmayr, R., Perry, G., Smith, M.A., Drew, K.L., 2001. Hibernation, a model of neuroprotection. Am. J. Pathol. 158, 2145–51.

Zille, M., Farr, T.D., Przesdzing, I., Müller, J., Sommer, C., Dirnagl, U., Wunder, A., 2012. Visualizing cell death in experimental focal cerebral ischemia: promises, problems, and perspectives. J. Cereb. Blood Flow Metab. 32, 213–31.

AIMS AND SCOPE OF INVESTIGATION

AIMS AND SCOPE OF INVESTIGATION

We studied the hypothesis that exposure to hydrogen sulfide after acute cerebral ischemia has a protective effect regarding brain damage and functional outcome in an animal model of focal cerebral ischemia, addressing in particular the following questions:

1. Does current literature support further research concerning the role of oxidative phosphorylation inhibitors in the context of acute stroke treatment?

2. Does exposure to H_2S after acute ischemic stroke diminish infarct size and enhance recovery?

3. Does the effect of H_2S relate to brain protection or repair mechanisms, involving either modulation of post-ischemic oxidative stress and the expression of reactive oxygen species or promotion of post-ischemic repair?

4. Is it possible to use in vivo brain imaging to predict outcome in experimental stroke?

We analyzed the effects of H_2S exposure in a permanent middle cerebral artery occlusion (pMCAO) model in rodents and measured functional outcome and infarct size in vivo and post-mortem. Furthermore, we investigated mechanisms of cytoprotection and repair and compared data from in vivo brain imaging with post-mortem immunohistochemical evidence.

Our research shall contribute to the understanding of the potential role of H_2S in the context of acute ischemic stroke and clarify underlying processes involved in presumed ischemic tissue preservation. In the future, we shall expect a major translational benefit if the hypothetic potential of H_2S donors in acute brain ischemia is confirmed.

1. ACUTE BRAIN ISCHEMIA, HYPOTHERMIA AND HIBERNATION: THE ROLE OF OXIDATIVE PHOSPHORYLATION INHIBITORS

Part of this chapter was published in the following article

Isabel Henriques, Maria Gutiérrez, Exuperio Diez-Tejedor. Acute brain ischemia, hypothermia and hibernation: the role of oxidative phosphorylation inhibitors. *News @fmul, 2010, 18: December, 2010.*
http://news.fm.ul.pt/Content.aspx?tabid=67&mid=442&cid=1329

and presented as a poster at the 20th European Stroke Conference, 2011

Henriques I, Gutiérrez-Fernández M, Rodríguez-Frutos B, Exposito-Alcaide M Alvarez-Grech J, Ferro J , Díez-Tejedor E. Inhibitors of oxidative phosphorylation in acute stroke: preliminary data in rats. Cerebrovasc Dis 2011; 31(suppl 2): 131

1. ACUTE BRAIN ISCHEMIA, HYPOTHERMIA AND HIBERNATION: THE ROLE OF OXIDATIVE PHOSPHORYLATION INHIBITORS

INTRODUCTION

Current treatment of acute ischemic cerebrovascular accidents (CVA) includes arterial reperfusion using rt-PA (recombinant tissue-plasminogen activator) and treatment at CVA Units. During the last decades, numerous neuroprotective substances have been promising in pre-clinical studies, both in terms of ischemic volume and functional outcome. Regrettably, none has demonstrated unequivocal clinical benefit.

Reasons for the difficulties of extrapolation to humans include the need for very quick administration of drugs which presents difficulties within a clinical context, the disparity of measurement instruments including functional scales (Richard Green et al., 2003), or the differences in the acquisition of imaging techniques during the acute stage and the definition of penumbra (Fisher et al., 2007; Weinstein et al., 2004).

There is evidence that, if untreated, the penumbra area bordering the ischemic lesion will soon become part of the infarct zone (core), increasing the volume of the initial lesion and worsening functional prognosis.

> The rational for the recommendation to treat stroke as an emergency is that early reperfusion is associated with functional improvement by preventing irreversible brain damage. Unfortunately, the therapeutic window between symptoms onset and useful reperfusion is short, and measures that permit the widening of the therapeutically window may allow to include an important number of patients that arrive too late to benefit from brain reperfusion therapies. Procedures aiming to slow down or interrupt the metabolic processes involved in the so-called “ischemic cascade” have potential of extending the time available to perform arterial reperfusion.

HYPOTHERMIA

Inducing a drop in body temperature may reduce deterioration following the acute ischemic lesion if induced early enough after the beginning of ischemic symptoms and if the duration is also appropriate. The use of moderate external hypothermia in the context of the acute stage of stroke is currently under research in Phase II clinical trials.

In animal models of acute ischemia, induced hypothermia has proved benefit, both in terms of reducing infarct size and improving functional outcome.

There are two different levels of decrease in body temperature that have therapeutic interest for translational studies: mild hypothermia (33ºC – 35ºC) and moderate hypothermia (30ºC - 33ºC). Mild hypothermia is safer and technically easier to perform (Buchan and Pulsinelli, 1990). In humans, it is possible to reach the desired temperature without the need of sedation or mechanical ventilation which is an advantage for translation into clinical context. Nonetheless, the neuroprotective effect is different for different temperatures and for different intervals between ischemia and hypothermia induction; it was noted that maximum efficacy occurs when cooling is moderate (≤31ºC) and exposition is long (12 to 48h) (Corbett et al., 2000).

However, even small reductions of basal body temperature of around 2ºC or less seem to have a neuroprotective effect with histological and behavioural evidence (Busto et al., 1989).

The mechanisms by which hypothermia is neuroprotective are not entirely understood. With regard to mild hypothermia, neuroprotection was exclusively associated with the induced metabolic changes (the drop in temperature reduces metabolic needs). However, protective biological processes, such as detoxification and repair, would also be inhibited, which makes the final balance difficult to establish. Currently, there seems to be evidence that the pathophysiology of hypothermia includes also changes in cerebral blood flow, cell membrane stability, energetic and calcium metabolism, intracellular signalling, excitotoxicity mechanisms, acid-base balance, formation of free radicals, and in apoptotic mechanisms (Schaller and Graf, 2003). Therefore, hypothermia is considered a tissue protector due to the fact that it

boosts resistance to deleterious effects including interfering with glucose metabolism diverging it from the glycolysis pathway to the pentose phosphate pathway which is potentially a neuroprotective pathway and reducing the levels of tissular lactate and intracellular acidosis. It frees excitatory amino acids, the formation of free radicals, the mitochondrial release of cytochrome C and kinase C, the activation of microglia, and improves the behaviour of the hematoencephalic barrier by reducing its deterioration and rupture. Hypothermia induces also the inhibition of at least one cell death pathway, covering several lesion mechanisms and contributing to the preservation of both cell function and structure, thus improving tissue preservation (Minard and Grant, 1982).

NITRIC OXIDE, CARBON MONOXIDE AND HYDROGEN SULFIDE

Nitric Oxide (NO) and Carbon Monoxide (CO) are signalling gaseous molecules of the central nervous and cardiovascular system, which have proved cytoprotective benefits in the context of brain and heart ischemia (Elrod et al., 2006). Lately, particular attention has been paid to the potential biological significance of hydrogen sulphide (H_2S) (Abe and Kimura, 1996), first known for its environmental toxic properties (Beauchamp et al., 1984). These three gaseous labile biological mediators (NO, CO e H_2S) are able to cross cell membranes without the need of specific transporters, what facilitates their quick interference in the regulation of intracelular mechanisms.

H_2S is synthesized in mammals in several tissues through two main metabolic pathways of the L-Cysteine, that depend on pyridoxal-5'-phosphate enzymes: cystathionine beta-synthase (CBS) and cystathionine gamma-lyase (CSE). L-Cysteine can originate from food sources or be synthesized from L-Methionine through a transsulfuration pathway, homocysteine acting as the intermediary in the process.

The biological effects of exposure to H_2S seem to depend, in particular, on its capacity to inhibit mitochondrial oxidative phosphorylation and hypothermia induction. Nonetheless, they are controversial and depend, among other factors, on the dosage and duration of the exposure. In micro molecular concentrations, hydrogen sulphide

appears to have a neuronal protective role in oxidative stress (Kimura and Kimura, 2004), with modulation of the intracellular caspase and kinase pathways, influencing the activity of the N-metil-d-aspartate (NMDA) receptors in physiological concentrations and modifying the induction of long term potentiation (LTP) (Nagai et al., 2004). It can also induces an upregulation of cytoprotective and anti-inflammatory genes, including Heme oxygenase-1 (HO_1), which promotes the production of CO, that has cytoprotective and anti-inflammatory behaviour.

H_2S is present in the central nervous system in relatively high concentration levels (50 to 160 microM), by comparison with other organs, which suggest it may have a localized physiological function (Abe and Kimura, 1996) .

OXIDATIVE PHOSPHORYLATION INHIBITORS AND HYBERNATION

During states of dormancy such as hibernation, mammals are able to survive with metabolism rates as low as 2% of their usual needs, without suffering irreversible brain lesions, despite very low CBF. During these periods, animals need to carry out adaptive transformations at brain level. These adaptations include not only mechanisms of metabolic suppression, but also of increased oxidative defence, in addition to lowering body temperature and immune functions (Drew et al., 2007). Knowledge on the regulation mechanisms and reversible adaptative induction in case of extreme hypometabolic conditions can contribute to a better understanding of some crucial aspects of ischemic lesion, namely how brain cells can sustain homeostasis despite very low CBF. .

Remarkably, it was exactly with H_2S that it was possible, in 2005, to induce a condition similar to hibernation in mammals that normally do not hibernate. This condition was called "*suspended animation-like state*" (Blackstone et al., 2005). After inhalation of an H_2S enriched atmosphere mixture, mice had a significant drop in body temperature and in metabolic rates (measured through O_2 consumption and CO_2 elimination). After 6 hours of exposure, rats returned to breathe normal atmosphere, with quick and spontaneous recovery of their normal metabolic rates and body temperature, without

changes in their health condition in the short or medium follow-up. Therefore, the potential role of H_2S, as a neuroprotective agent and hypometabolic inductor was enhanced. Mechanisms involved included H_2S tamponading effect in oxygen consumption, changes the intracellular redox environment, and prevention of further imbalance between energy sources and needs (Blackstone and Roth, 2007). The proposed mechanism, that may regulated the consumption of cell O_2 by H_2S, appears to be centred on inhibiting cytochrome C oxidase, which, at the level of the brain, reduces oxygen consumption and inhibits the recapture of the L-glutamate, an excitatory neurotransmitter.

Concerning the cytoprotective role of hypothermia, its potential benefit has been demonstrated in animal models of acute brain ischemia, not just for outcomes regarding infarct size, but also at functional recovery.

Regarding the cytoprotective role of H_2S, controversy persists, with some studies showing neurotoxic effects. These discrepancies in the action of H_2S have been observed within the same species (Qu et al., 2006), between distinct species (small mouse and piglets) (Li et al., 2008) and between distinct organs (brain ischemia and cardiac ischemia) (Hayashida et al., 2008). The explanation for these differences concerning the expression of hypometabolic effects may relate to dose and exposition time differences (Johansen et al., 2006), and body mass effect, especially for ischemic models using larger mammals.,

Severe hypothermia and hibernation are two extreme metabolic conditions where, despite the presence of much reduced metabolic rates, it is possible to recover without irreversible cerebral lesion.

The possibility of inducing hypometabolic states following acute cerebral ischemia by lowering body temperature as well as oxygen consumption and other metabolic needs, may help increase the window of therapeutic opportunity of thrombolysis, thus helping to make it accessible to an increased number of patients with ischemic CVA.

CONCLUSION

Severe hypothermia and hibernation are two extreme metabolic conditions where, despite the presence of severely reduced metabolic rates, it is possible to recover without irreversible cerebral lesion. The possibility of inducing hypometabolic states following acute cerebral ischemia by lowering body temperature as well as oxygen consumption may help increase the window of therapeutic opportunity of thrombolysis, thus contributing to making it accessible to a larger number of patients with ischemic stroke.

REFERENCES

Abe, K., Kimura, H., 1996. The possible role of hydrogen sulfide as an endogenous neuromodulator. J. Neurosci. 16, 1066–71.

Beauchamp, R.O., Bus, J.S., Popp, J.A., Boreiko, C.J., Andjelkovich, D.A., 1984. A critical review of the literature on hydrogen sulfide toxicity. Crit. Rev. Toxicol. 13, 25–97.

Blackstone, E., Morrison, M., Roth, M.B., 2005. H2S induces a suspended animation-like state in mice. Science 308, 518.

Blackstone, E., Roth, M.B., 2007. Suspended animation-like state protects mice from lethal hypoxia. Shock 27, 370–2.

Buchan, A., Pulsinelli, W.A., 1990. Hypothermia but not the N-methyl-D-aspartate antagonist, MK-801, attenuates neuronal damage in gerbils subjected to transient global ischemia. J. Neurosci. 10, 311–6.

Busto, R., Dietrich, W.D., Globus, M.Y., Ginsberg, M.D., 1989. Postischemic moderate hypothermia inhibits CA1 hippocampal ischemic neuronal injury. Neurosci. Lett. 101, 299–304.

Corbett, D., Hamilton, M., Colbourne, F., 2000. Persistent neuroprotection with prolonged postischemic hypothermia in adult rats subjected to transient middle cerebral artery occlusion. Exp. Neurol. 163, 200–6.

Drew, K.L., Buck, C.L., Barnes, B.M., Christian, S.L., Rasley, B.T., Harris, M.B., 2007. Central nervous system regulation of mammalian hibernation: implications for metabolic suppression and ischemia tolerance. J. Neurochem. 102, 1713–26.

Elrod, J.W., Duranski, M.R., Langston, W., Greer, J.J.M., Tao, L., Dugas, T.R., Kevil, C.G., Champion, H.C., Lefer, D.J., 2006. eNOS gene therapy exacerbates hepatic ischemia-reperfusion injury in diabetes: a role for eNOS uncoupling. Circ. Res. 99, 78–85.

Fisher, M., Hanley, D.F., Howard, G., Jauch, E.C., Warach, S., 2007. Recommendations from the STAIR V meeting on acute stroke trials, technology and outcomes. Stroke. 38, 245–8.

Hayashida, K., Sano, M., Ohsawa, I., Shinmura, K., Tamaki, K., Kimura, K., Endo, J., Katayama, T., Kawamura, A., Kohsaka, S., Makino, S., Ohta, S., Ogawa, S., Fukuda, K., 2008. Inhalation of hydrogen gas reduces infarct size in the rat model of myocardial ischemia-reperfusion injury. Biochem. Biophys. Res. Commun. 373, 30–5.

Johansen, D., Ytrehus, K., Baxter, G.F., 2006. Exogenous hydrogen sulfide (H2S) protects against regional myocardial ischemia-reperfusion injury--Evidence for a role of K ATP channels. Basic Res. Cardiol. 101, 53–60.

Kimura, Y., Kimura, H., 2004. Hydrogen sulfide protects neurons from oxidative stress. FASEB J. 18, 1165–7.

Li, J., Zhang, G., Cai, S., Redington, A.N., 2008. Effect of inhaled hydrogen sulfide on metabolic responses in anesthetized, paralyzed, and mechanically ventilated piglets. Pediatr. Crit. Care Med. 9, 110–2.

Minard, F.N., Grant, D.S., 1982. Hypothermia as a mechanism for drug-induced resistance to hypoxia. Biochem. Pharmacol. 31, 1197–203.

Nagai, Y., Tsugane, M., Oka, J.-I., Kimura, H., 2004. Hydrogen sulfide induces calcium waves in astrocytes. FASEB J. 18, 557–9.

Qu, K., Chen, C.P.L.H., Halliwell, B., Moore, P.K., Wong, P.T.-H., 2006. Hydrogen sulfide is a mediator of cerebral ischemic damage. Stroke. 37, 889–93.

Richard Green, A., Odergren, T., Ashwood, T., 2003. Animal models of stroke: do they have value for discovering neuroprotective agents? Trends Pharmacol. Sci. 24, 402–8.

Schaller, B., Graf, R., 2003. Hypothermia and stroke: the pathophysiological background. Pathophysiology 10, 7–35.

Weinstein, P.R., Hong, S., Sharp, F.R., 2004. Molecular identification of the ischemic penumbra. Stroke. 35, 2666–70.

2. EXPOSURE TO HYDROGEN SULFIDE DIMINISHES INFARCT SIZE AND ENHANCES RECOVERY: EXPERIMENTAL DATA IN A pMCAO MODEL IN RODENTS

Part of this chapter will be published in the following article

Isabel Henriques,, María Gutiérrez-Fernández, Berta Rodríguez-Frutos, Jaime Ramos-Cejudo, Laura Otero-Ortega, Teresa Navarro Hernanz, Sebastián Cerdán, José Ferro, Exuperio Díez-Tejedor. Short-term hydrogen sulfide exposure after stroke is protective to the brain by lowering oxidative stress. *(under review)*

and was presented as an oral communication at the 21st European Stroke Conference, 2012

Isabel Henriques, Maria Gutiérrez-Fernández, Berta Rodríguez-Frutos, Jaime Ramos-Cejudo, Mercedes Exposito-Alcaide, Julia Alvarez-Grech, José Ferro, Exuperio Díez-Tejedor. Exposure to Hydrogen sulphide diminishes infarct size and enhances recovery: experimental data in a MCAO model in rodents. Cerebrovasc Dis 2012: 32(suppl 2): 11

2. EXPOSURE TO HYDROGEN SULFIDE DIMINISHES INFARCT SIZE AND ENHANCES RECOVERY: EXPERIMENTAL DATA IN A pMCAO MODEL IN RODENTS

INTRODUCTION

There are exceptions in nature to the rule that lack of cerebral blood flow during a prolonged period of time inexorably leads to ischemia and irreversible brain damage. Two examples are cardiac arrest from extreme cold (Dobson and Burgess, 1996) and hibernation (Rouble et al., 2013) where, despite very low or no cerebral blood flow at all, survival is possible without permanent neurological damage (Schwartz et al., 2013; Storey and Storey, 2010). These examples show that severe brain damage may be prevented even in the absence of cerebral blood flow during long periods. This observation may contribute to new strategies in acute stroke therapy.

The induction of a “hibernation-like” state in mice using the inorganic gas hydrogen sulfide (H_2S) suggested its potential in the context of acute ischemia (Szabó, 2007), promoting a dramatic reduction in oxygen consumption to less than 15% of normal metabolic rates, without subsequent irreversible neurological deficits (Blackstone et al., 2005).

H_2S regulates oxygen consumption by competing with O_2 in binding to cytochrome C oxidase at the mitochondrial electron transport chain level, inhibiting the electron transport chain by binding stronger than O_2 to the Fe-Cu center in cytochrome C oxidase. H_2S is also involved in neuronal and glial communication (Mikami et al., 2011) and local vasotone regulation.

Despite of these potential beneficial effects, data about the benefit of H_2S in the context of acute ischemic stroke was modest and conflicting when we designed this study. First reports showed no functional benefit (Qu et al., 2006), whereas others demonstrated improvement in functional outcome and lesion size (Joseph et al., 2012). Data from experimental models in the context of acute ischemia in other organs like heart and kidney showed clear benefits of H_2S exposure (both with the gas itself or with liquid vials with H_2S donors) (Hosgood and Nicholson, 2010; Snijder et al., 2013).

We here hypothesized that inducing a reversible hypometabolic state after acute cerebral ischemia through exposure to H_2S could limit acute ischemic brain damage.

In the present section, we investigated the effects of short-term H_2S exposure after permanent middle cerebral artery occlusion (pMCAO) by analyzing the functional outcome and infarct size.

MATERIALS AND METHODS

All experiments were designed to minimize animal suffering in compliance with the ARRIVE criteria and our medical school's Ethical Committee for the Care and Use of Animals in Research (EU directives 86/609/CEE and 2003/65/CE). Regarding all procedures, researchers were blinded to group allocation after randomization. Male 8 - 12 weeks old Sprague-Dawley rats (250 to 320g) (Charles River©, Spain) were randomly assigned to three groups: sham (craniotomy, n=13), control (craniotomy + pMCAO, n=23) and treated (craniotomy + pMCAO + exposure to 40 ppm H2S, n=28). Rats were anesthetized with the halogenated general inhalation anesthetic drug Sevoflurane {[fluoromethyl 2, 2, 2,-trifluoro-1-(trifluoromethyl) ethyl ether] [1, 1, 1, 3, 3, 3-hexafluoro-2-(fluoromethoxy) propane]}. Its median alveolar concentration (the concentration at which half of the subjects do not move in response to a skin incision) is 2.5 (+/-0.3) volumen %. We performed pMCAO after a small craniotomy above the rhinal fissure over the branch of the right middle cerebral artery (MCA), exposing MCA and permanently ligated with a 9-0 silk suture before its bifurcation, in order to enhance reproducibility. After MCAO, both common carotid arteries were temporarily occluded for 60 min with a lace of a 6-0 silk suture. Scar size and location were equal for all groups, animal cages had no information about group allocation, and codes were used in *post mortem* samples, in order to maintain blinded data collection and analysis. Body temperature and glycemia were measured throughout procedures. Rats were sacrificed at 24h and 14d after surgery.

Gas mixtures

Treated animals were exposed to H_2S, 3 hours after acute ischemia and breathed a mixture of atmosphere with hydrogen sulfide [Gasin medical bottles, 40 ppm H_2S in nitrogen (N_2: 99, 9%)] during 24 min inside a Plexiglas® chamber (9.5 x 20 x 10 cm = Volume 1,900 cm^3). Pressure output of hydrogen sulfide was 1 bar/30s. Control and sham animals breathed normal atmosphere in the same temperature and humidity conditions.

When this study was designed, no data was available regarding time and dosage of H_2S exposure and its efficacy in pMCAO. Thus, we established an effective dose by exposing healthy rats to progressive doses of H_2S. Our variables were H_2S concentration (40 and 80 ppm), time of exposure (from 1 to 90 min), and output pressure (1 or 2 bar). We used rectal temperature before and after exposure as an indirect measure of change into lower metabolism. Finally, we established an exposure time of 24 minutes under a concentration of 40ppm with an output pressure of 1 bar/30s as standard dosage.

Ischemic lesion size

Lesion size was evaluated *in vivo* at 24h and 14d with T2-weighted sequence MRI and *post mortem* by hematoxylin and eosin (H&E) stains, as previously described (Gutiérrez-Fernández et al., 2011).

Magnetic Resonance Imaging

The extension of ischemic lesions was analyzed *in vivo* at 24h (group sacrificed at 24h) and twice, at 24h and 14d (group sacrificed at 14d), using T2-weighted images. The observer was blinded to allocation of animals in all cases. After contrast adjustment, the contours of the hemispheres were traced manually on each slice. Data analysis was performed using Image J software from NIH Image, slice-by-slice contouring at lesion

site and in the contralateral hemisphere in the same location. Only lesions larger than 2mm x 2mm x 2mm were analyzed to minimize partial volume effects. We used JPG® region of interest (ROI) to measure infarct size. To correct for brain edema effect, lesion size was determined by an indirect method: (infarct area) = (area of the intact contralateral hemisphere) – (area of the intact ipsilateral hemisphere). Lesion size was expressed as percentage of total size of the ipsilateral hemisphere. Exclusion criteria were no measurable lesion on MRI except for the sham group. These animals were sacrificed and excluded from the sample (n=3). We therefore used T_2 MRI at 24h as confirmation tool for successful ischemic lesion induction.

MRI images were acquired on a 7 Tesla/16 cm Bruker Avance III system (Bruker Medical Gmbh, Ettlingen, Germany) at the MR Imaging Facility (SIERMAC, http://www.siermac.es) from the Institute for Biomedical Research "Alberto Sols" CSIC/UAM, Madrid, Spain. The magnet was equipped with a ^{1}H selective birdcage resonator for rat head (38mm) and a gradient coil insert (90 mm, maximum intensity 36 G/cm). Anesthesia was induced in a plexiglass chamber with 2%-3% isoflurane mixed with oxygen and maintained during the experiment through a nose mask. The physiological state of the rats was monitored during MRI acquisitions with a Biotrig physiological monitor (Bruker) depicting on-line the respiratory rate.

Axial T_2-weighted spin echo images were obtained using a rapid acquisition with relaxation enhancement (RARE) sequence in axial and coronal orientations using the following parameters: Number of echo images 2 (TE: 29.54ms and 88.61ms), TR = 3000 ms, RARE factor = 4, Av = 3, FOV = 3.5 cm, acquisition matrix = 256 × 256 corresponding to an in-plane resolution of 136 × 136 μm^2, slice thickness = 1.00 mm without gap.

Diffusion-weighted magnetic resonance images (DWI) were obtained in three ortoghonal orientations as defined by the read, phase and slice encoding gradients using a multishot spin-echo echo planar imaging (EPI) sequence. Acquisition conditions were; diffusion gradient duration spin-echo echo planar imaging (EPI) sequence. TR: 3000ms; TE: 50ms, FOV: 3.8cm; axial slices (1.5mm thickness) and three b values: 100,

400 and 1000 s/mm^2; acquisition matrix = 128 × 128 corresponding to an in-plane resolution of 296 × 296 μm^2.

Dynamic susceptibility contrast – Magnetic Resonance Imaging (DSC MRI) was performed using a bolus injection of paramagnetic contrast agent (Gd-DTPA; Magnevist, Bayer Schering Pharma AG, Leverkusen, Germany; 0.3mmol/Kg i.v.). Dynamic changes in signal intensity were used to calculate CBF (cerebral blood flow), CBV (cerebral blood volume, the fraction of tissue volume occupied by blood) and MTT (mean transit time: MTT=CBF/CBV, the time it takes for blood to pass through the vasculature within the tissue of interest). Dynamic T2* Weighted images were acquired using a spin-echo single shot echo planar imaging (EPI) sequence with the following scan parameters: TR/TE of 250/7ms; Flip angle: 30º; Number of repetitions: 150; slice thickness and interslice gap: 1.5mm and 0.1mm; number of slices: 6; FOV: 3.8cm and matrix size: 86x8. After an initial baseline period of 10s, a rapid bolus injection of Gd-DTPA was administered intravenously in the tail vein.

ADC, CBF, CBV and MTT pixel by pixel maps were generated with a homemade software application (MatLab ®, 2007a). ADC value was computed for each voxel using the exponential model according to the expression: $S_b = S_0\, e^{-b*ADC}$, where S_b is signal intensity with the different b weightings and S_o the signal intensity for b=0. Perfusion parameters were calculated based on the premise that ΔR* is proportional to the contrast agent concentration according to the curve equation: ΔR*= -K. ln [S(t) / So (t)], where S(t) is de signal intensity at time t, So baseline signal intensity and, K a constant. The transit curve was then fitted to a gamma variant function.

The mean and standard deviation of ADC of the central and peripheral lesion area were determined, and the same measurement performed in the same anatomic location as the lesion but in the normal contralateral hemisphere. These three regions of interests (ROIs) are easy to identify on color coded ADC maps and drawn manually over the maps. The ROIs were applied on all affected ADC slices from each rat with a maximum number of five slices. The mean ADC values of central and peripheral lesion areas were divided by the value in the contralateral normal hemisphere and expressed as a relative ADC (rADC).

Perfusion weighted MR imaging was performed using bolus tracking and resulting data used to generate CBF, CBV and MTT maps. In these maps, only two ROIs were investigated: ischemic lesion and contralateral normal hemisphere, because of the smaller matrix size (86*86) than in ADC maps, hindering the selection of central and peripheral lesion areas. The mean CBF values of the ischemic region were divided by the value of the contralateral normal hemisphere used as reference region and expressed as relative CBF (rCBF).

Functional evaluation scales

Functional evaluation was performed using Rotarod and Rogers tests by a blinded observer at baseline, 24h and at 14d after surgery. The latency to fall from a rotator cylinder (accelerating at 4-40 rpm) was measured and recorded. Motor function by Rogers test was scored: 0, no deficit; 1, failure to extend contralateral forepaw fully; 2, decreased grip of the contralateral forelimb while tail gently pulled; 3, spontaneous movement in all directions, contralateral circling only if pulled by the tail; 4, circling or walking to the right; 5, walks only when stimulated; 6, unresponsive to stimulation; and 7, dead (Gutiérrez-Fernández et al., 2011).

Statistical analysis

Quantitative data is shown as mean ± standard error of the mean (SEM) and presented as box and whiskers plots. As data followed a non-normal distribution, the Mann–Whitney test was used to compare two samples and the Kruskal–Wallis test to compare more than two samples in the same group or more than two groups (SPSS 16 for Windows®). Values of $p<0.05$ were considered significant at a 95% confidence level.

RESULTS

Functional outcome after exposure to hydrogen sulfide

We measured functional outcome before procedure, at 24h and 14d. At baseline, Rogers Modified Scale was zero for all animals and the latency to fall in the Rotarod test was >120 seconds. The sham-operated group showed no functional deficit. A better functional outcome was observed at 24h in animals exposed to H_2S compared to control group regarding Rogers Modified Scale (1.73 ± 0.23, *vs.* 3.29 ± 0.18, p= 0.001) and Rotarod test (65 ± 5.97, *vs.* 37 ± 7.14, p=0.03). At 14d, the functional benefit observed in treated animals was sustained in both tests: Rogers Modified Scale (1.18±0.17 *vs.* 1.82± 0.20, p=0.03), and Rotarod (55.25±5.17 *vs.* 31.5±7.79, p=0.04) (Figure 2.1A).

Infarct size after exposure to hydrogen sulfide

At 24 hours after pMCAO, lesion size measured by T2-weighted MRI did not differ significantly between treated and control groups (9.69±1.67 *vs.* 15.45±1.06, p= 0.054). However, H&E stains showed a reduced infarct size in the treated group (6.69±1.38 *vs.* 23.20±3.05, p= 0.008). At day 14, both T_2-weighted MRI and H&E showed smaller infarct size in treated compared to control rats (6.13±0.62 vs. 11.56±0.4, p=0.0004, and 4.94±0.92 vs. 11.63±1.99, p=0.002). Sham operated rats showed no cerebral lesion and the maximum lesion size was observed in the control group (Figure 2.1B).

MRI heterogeneities in ischemic territory after exposure to hydrogen sulfide

In treated rats, we observed heterogeneities inside the ischemic lesions on MRI ADC maps at 24h (Figure 2.2, upper right image and graph). These heterogeneities were observed inside the ischemic area, including central and peripheral areas, presenting central areas with a higher diffusion coefficient than peripheral ones. In animals treated with H_2S, the relative ADC (rADC) coefficients were similar in central and

peripheral areas (Figure 2.2, lower left images and graph). Finally, using perfusion MRI, the differential CBF (Δ CBF) between the lesion side and contralateral hemisphere was lower in treated rats (Figure 2.2, lower right image and graph).

Physiological parameters

Glycemia was assessed immediately after starting the procedure and during surgery and was similar in all groups. Body temperature was significantly lower after induction of anesthesia in all groups ($p<0.05$). After an exposure time to H_2S of 24 minutes, body temperature decreased by 1.85 ºC (mean) but quickly recovered after animals started to inhale normal atmosphere; no difference in body temperature was observed at 2 hours after exposure (Figure 2.3).

DISCUSSION

We report on the role of short-term exposure to H_2S in acute ischemic brain damage. Our results show that exposure to hydrogen sulfide after pMCAO improves functional outcome and decreases infarct size. DWI MRI ADC maps revealed intralesional heterogeneity compared to controls and PWI MRI showed higher intralesional cerebral blood flow. Significant benefit is likely to occur before major tissue damage develops.

H_2S exposure improved functional outcome after pMCAO

A main goal of acute stroke treatment is the improvement of functional outcome. In the present study, a better functional outcome in animals exposed to H_2S was observed at 24h and 14 days. A similar benefit in functional outcome has been reported in studies that used H_2S in the context of ischemia reperfusion (Lin et al., 2012), in global brain ischemia (Yin et al., 2013), and in cardiac and kidney ischemia (Shibuya et al., 2013; Szabó et al., 2011). In our model, functional benefit from H_2S

exposure was not limited to short term, but sustained until day 14. This observation is supported by our in vivo imaging data that showed improved brain tissue preservation and smaller lesion size.

H_2S exposure decreased lesion size after pMCAO

Concerning infarct size, a previous publication using a H_2S donor (NaHS) in an ischemic electrocauterization model did not show reduction in lesion size (Qu et al., 2006). However, others reported smaller infarcts using longer H_2S exposure times, higher doses (Joseph et al., 2012) or reversible MCAO models (Lin et al., 2012). Our data showed that lower dose and shorter exposure (40 ppm, during 24 min) were able to decrease infarct size after pMCAO.

Despite of finding smaller infarcts at day 14, differences between infarct sizes assessed by T2-weighted MRI at 24h were not significant, possibly due to acute post ischemic brain edema that increases brain volume. However, H&E staining at 24h showed significant reduction in lesion size in treated rats. This discrepancy may be related to the process of H&E staining that includes tissue exsiccation steps. Interestingly, MRI ADC maps at 24h in treated rats revealed heterogeneity, with spotty areas inside ischemic lesion with higher ADC coefficients, both in central and peripheral areas that may reflect partial brain tissue preservation within the ischemic area. This may contribute to better understand the discrepancy between *in vivo* lesion size and better functional outcome at 24h. Nevertheless, infarct size as single outcome measure seems to be insufficient to serve as evidence for protection, and demonstration of ischemic size should not be interpreted independently from other endpoints (Balkaya et al., 2013).

H_2S exposure induces heterogeneities within the ischemic lesion in brain MRI

Previous studies from our group showed that gene expression exists inside the ischemic lesion, including CNS development and trophic factors within the lesion core, until at least 24h after pMCAO, suggesting the presence of surviving areas within the ischemic core (Ramos-Cejudo et al., 2012). At 24h, ADC maps showed heterogeneities in the central part of the ischemic lesion, revealing different rates of water diffusion and underlying brain tissue integrity. These heterogeneities may represent previously described "mini-cores and mini-penumbras" (del Zoppo et al., 2011). Finally, when we compared CBF in both hemispheres in treated and control groups, less difference between CBF in affected and non-affected hemispheres was observed in treated rats. This suggests that better perfusion may be achieved by mechanisms that include microvasoregulation, a known property of H_2S (Zhao et al., 2001). In our study, heterogeneity in ADC maps corresponded to better functional outcome as well as smaller lesions and better ischemic tissue preservation in treated rats. Consequently, in a translational context where acute imaging is crucial for acute therapeutic decisions, prognostic relevance of ADC heterogeneities may be assumed and merits further research.

H_2S exposure during 24 min is effective with minor interference with body temperature

Hypothermia, when not induced from external sources, is a result of hypometabolism and not the cause of metabolic changes. H_2S modulation in the context of acute stroke has been associated with induction of hypothermia, especially in protocols that included prolonged exposure times (Joseph et al., 2012). In our study, after an exposure time of 24 minutes, a mean decrease of 1.85ºC in body temperature was observed. Body temperature fully recovered in less than 120 min (Figure 2.3). Consequently, hypothermia appears to be a side effect of hypometabolism induced by H_2S and other mechanisms must be involved since the effects of H_2S administration were observed until day 14. In the present study, a shorter exposure time than

previously reported was effective and the reduced effect on body temperature represents an important finding in a translational context since minor changes in body temperature will not require patient management in intensive care units.

Study limitations

We designed this study to fulfill the most recent recommendations for research in translational stroke. Animals were randomized and all procedures except surgery were performed in a blinded manner to avoid observational bias regarding functional outcome, MRI image evaluation, and in-bench procedures, by using codes not known to observers. Detailed data is shown to facilitate reproducibility.

Unfortunately, dosage of H2S in the present study was the same in all animals and different dosages might produce distinct effects on outcome. Due to a limited budget and the preliminary nature of our study, we were not able to include female or older animals or animals with co-morbidities in this study. In the setting of an experimental study using rodents, clinical outcome was only assessed by evaluation of motor skills. However, we used MRI at 24h as a confirmation tool of successful pMCAO. As such, no bias in results can be attributable to surgical failure. The long-term results of H_2S exposure were not investigated, as study design included comparison of *in vivo* and *post mortem* data in the acute setting at 24h and after 14d only.

CONCLUSIONS

In our pMCAO model of ischemic stroke, early exposure to hydrogen sulfide after focal brain ischemia improved functional outcome and decreased infarct size. Regarding brain imaging, perfusion MRI in rats exposed to H_2S revealed improved cerebral blood flow, while diffusion MRI showed spots of heterogeneity inside ischemic lesions in ADC maps, including central regions. Heterogeneity in ADC maps corresponded to better functional outcome as well as smaller lesions and better ischemic tissue preservation

in treated rats. Consequently, in a translational context where acute imaging is crucial for acute therapeutic decisions, prognostic relevance of ADC heterogeneities may be assumed and merits further research (please refer to *Section 4*).

FIGURES

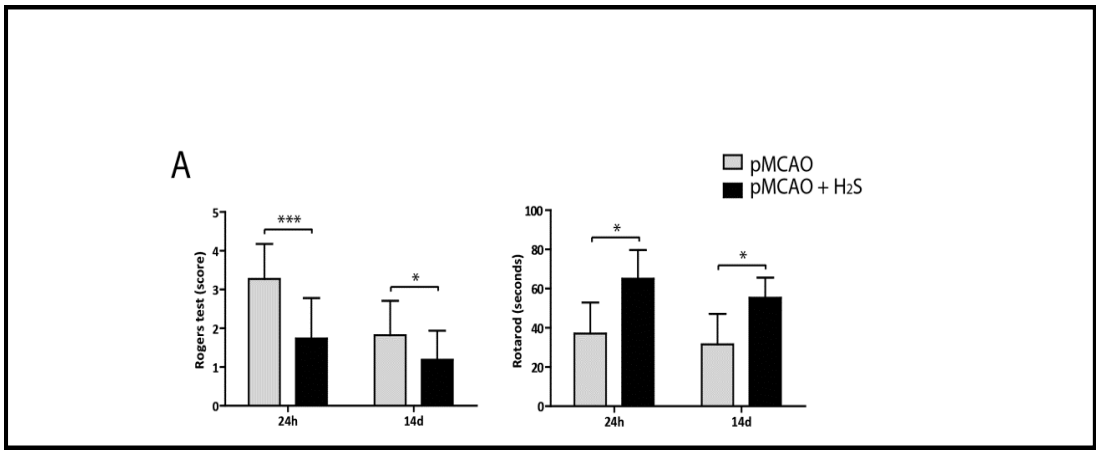

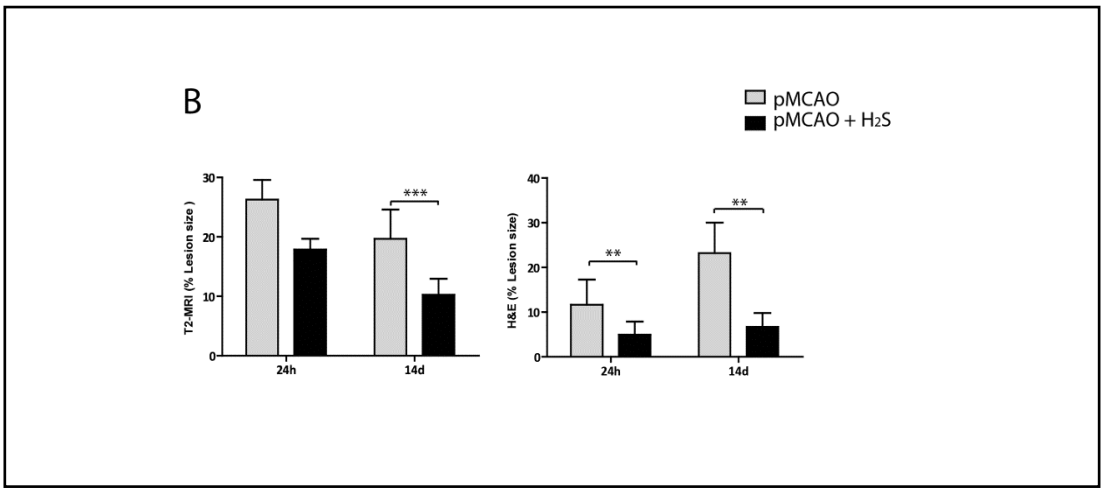

Figure 2.1. *RATS EXPOSED TO H_2S SHOW BETTER FUNCTIONAL OUTCOME AND SMALLER LESION SIZE*. **A.** Rats exposed to H_2S (black bars) had significantly lower score in Rogers scale (left graph)) at 24h (****P*<0.001) and at 14d (**P*<0.05) and more latency to fall from Rotarod (right graph) at 24h (**P*<0.05) and at 14d (**P*<0.05). **B.** At 14d rats exposed to H_2S (black bars) had significantly smaller ischemic lesion size, both in MRI (T2 weighted sequence) (left graph) (****P*<0.001) and H&E stain (right graph) (***P*<0.01). At 24h, MRI showed a lower but non-significant difference in lesion size (left graph), whereas H&E showed a significantly smaller ischemic lesion after H_2S exposure (***P*<0.01)(right graph).

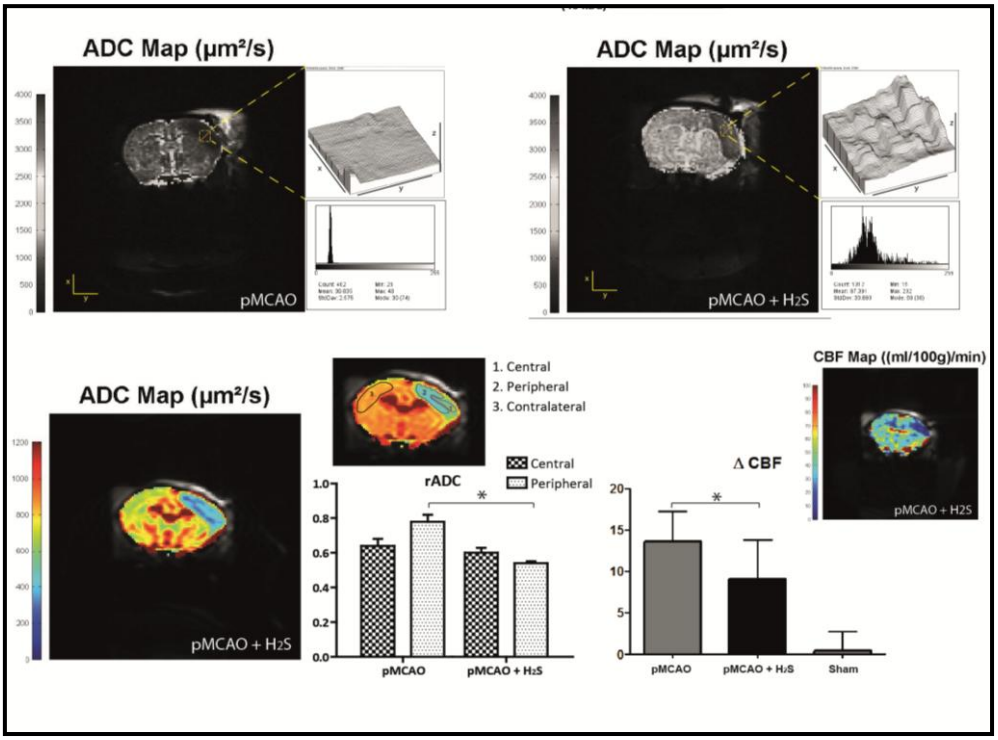

Figure 2.2. *RATS EXPOSED TO H_2S SHOW BETTER INTRALESIONAL CBF AT 24H*. **Upper and lower left**: Diffusion-weighted imaging MRI (ADC maps). Rats exposed to H_2S showed heterogeneities in ADC maps (upper right) whereas control rats showed homogeneous ischemic lesions (upper left). ADC maps in rats exposed to H_2S showed islands of ADC diffusion coefficient in central lesion area, similar to ADC observed in peripheral areas (lower left big image). For quantification, three manually designed Region of Interest (ROIs) were considered on ADC maps: ROI 1, ischemic central lesion area; ROI 2, peripheral lesion area; ROI 3, contralateral hemisphere (lower left small image). Animals exposed to H_2S showed similar differential ADC coefficients (rADC) in central and peripheral lesion areas. In controls, rADC was lower in central lesion area (lower left graph).**Lower right:** Perfusion-weighted imaging MRI (CBF). CBF showed improved intralesional perfusion in rats exposed to H_2S (lower right image), being the difference between intralesional and contralateral hemisphere CBF (ΔCBF) significantly smaller in comparison to controls (*P<0.05) (lower right graph).

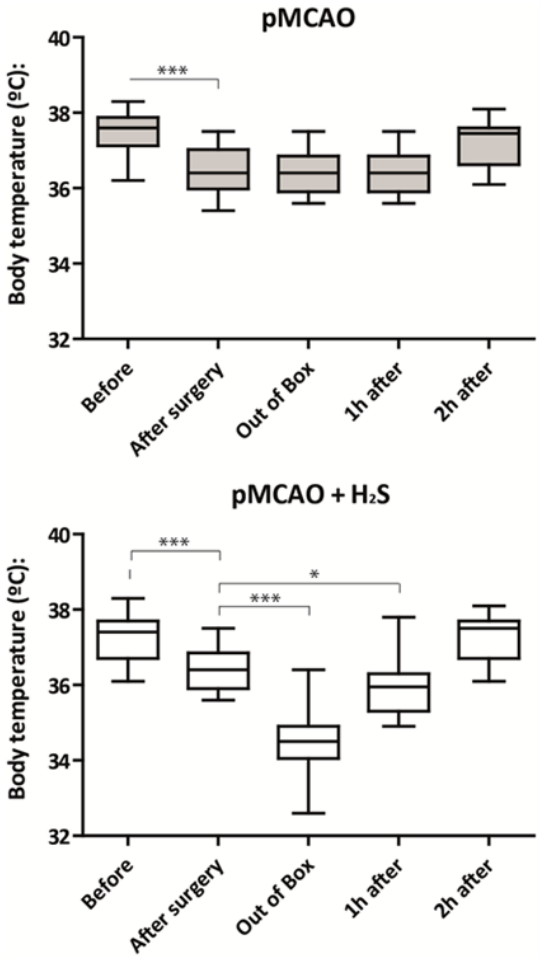

Figure 2.3. *BODY TEMPERATURE DURING EXPERIMENTS IN RATS EXPOSED TO H2S (LOWER GRAPH) AND CONTROLS (UPPER GRAPH).* No difference in body temperature 2h after exposure to hydrogen sulfide was observed. AXIS LEGEND: **Before**: rectal temperature in awake rats before starting surgery; **After surgery**: rectal temperature after surgery, before entering the box with atmosphere enriched with 40 ppm H2S (please see Methods for exposure to H2S conditions). **Out of Box**: Rectal temperature after getting out of the box, 24 minutes later. **1h after** and **2h after**: rectal temperature one and two hours after exposure to H2S. All rats showed significant

REFERENCES

Balkaya, M., Kröber, J.M., Rex, A., Endres, M., 2013. Assessing post-stroke behavior in mouse models of focal ischemia. J. Cereb. Blood Flow Metab. 33, 330–8.

Blackstone, E., Morrison, M., Roth, M.B., 2005. H2S induces a suspended animation-like state in mice. Science 308, 518.

Del Zoppo, G.J., Sharp, F.R., Heiss, W.-D., Albers, G.W., 2011. Heterogeneity in the penumbra. J. Cereb. Blood Flow Metab. 31, 1836–51.

Dobson, J.A., Burgess, J.J., 1996. Resuscitation of severe hypothermia by extracorporeal rewarming in a child. J. Trauma 40, 483–5.

Gutiérrez-Fernández, M., Rodríguez-Frutos, B., Alvarez-Grech, J., Vallejo-Cremades, M.T., Expósito-Alcaide, M., Merino, J., Roda, J.M., Díez-Tejedor, E., 2011. Functional recovery after hematic administration of allogenic mesenchymal stem cells in acute ischemic stroke in rats. Neuroscience 175, 394–405.

Hosgood, S.A., Nicholson, M.L., 2010. Hydrogen sulphide ameliorates ischaemia-reperfusion injury in an experimental model of non-heart-beating donor kidney transplantation. Br. J. Surg. 97, 202–9.

Joseph, C., Buga, A.-M., Vintilescu, R., Balseanu, A.T., Moldovan, M., Junker, H., Walker, L., Lotze, M., Popa-Wagner, A., 2012. Prolonged gaseous hypothermia prevents the upregulation of phagocytosis-specific protein annexin 1 and causes low-amplitude EEG activity in the aged rat brain after cerebral ischemia. J. Cereb. Blood Flow Metab. 32, 1632–42.

Lin, X., Yu, S., Chen, Y., Wu, J., Zhao, J., Zhao, Y., 2012. Neuroprotective effects of diallyl sulfide against transient focal cerebral ischemia via anti-apoptosis in rats. Neurol. Res. 34, 32–7.

Mikami, Y., Shibuya, N., Kimura, Y., Nagahara, N., Yamada, M., Kimura, H., 2011. Hydrogen sulfide protects the retina from light-induced degeneration by the modulation of Ca2+ influx. J. Biol. Chem. 286, 39379–86.

Qu, K., Chen, C.P.L.H., Halliwell, B., Moore, P.K., Wong, P.T.-H., 2006. Hydrogen sulfide is a mediator of cerebral ischemic damage. Stroke. 37, 889–93.

Ramos-Cejudo, J., Gutiérrez-Fernández, M., Rodríguez-Frutos, B., Expósito Alcaide, M., Sánchez-Cabo, F., Dopazo, A., Díez-Tejedor, E., 2012. Spatial and temporal gene expression differences in core and periinfarct areas in experimental stroke: a microarray analysis. PLoS One 7, e52121.

Rouble, A.N., Hefler, J., Mamady, H., Storey, K.B., Tessier, S.N., 2013. Anti-apoptotic signaling as a cytoprotective mechanism in mammalian hibernation. PeerJ 1, e29.

Schwartz, C., Hampton, M., Andrews, M.T., 2013. Seasonal and regional differences in gene expression in the brain of a hibernating mammal. PLoS One 8, e58427.

Shibuya, N., Koike, S., Tanaka, M., Ishigami-Yuasa, M., Kimura, Y., Ogasawara, Y., Fukui, K., Nagahara, N., Kimura, H., 2013. A novel pathway for the production of hydrogen sulfide from D-cysteine in mammalian cells. Nat. Commun. 4, 1366.

Snijder, P.M., de Boer, R.A., Bos, E.M., van den Born, J.C., Ruifrok, W.-P.T., Vreeswijk-Baudoin, I., van Dijk, M.C.R.F., Hillebrands, J.-L., Leuvenink, H.G.D., van Goor, H., 2013. Gaseous hydrogen sulfide protects against myocardial ischemia-reperfusion injury in mice partially independent from hypometabolism. PLoS One 8, e63291.

Storey, K.B., Storey, J.M., 2010. Metabolic rate depression: the biochemistry of mammalian hibernation. Adv. Clin. Chem. 52, 77–108.

Szabó, C., 2007. Hydrogen sulphide and its therapeutic potential. Nat. Rev. Drug Discov. 6, 917–35.

Szabó, G., Veres, G., Radovits, T., Gero, D., Módis, K., Miesel-Gröschel, C., Horkay, F., Karck, M., Szabó, C., 2011. Cardioprotective effects of hydrogen sulfide. Nitric Oxide 25, 201–10.

Yin, J., Tu, C., Zhao, J., Ou, D., Chen, G., Liu, Y., Xiao, X., 2013. Exogenous hydrogen sulfide protects against global cerebral ischemia/reperfusion injury via its anti-oxidative, anti-inflammatory and anti-apoptotic effects in rats. Brain Res. 1491, 188–96.

Zhao, W., Zhang, J., Lu, Y., Wang, R., 2001. The vasorelaxant effect of H(2)S as a novel endogenous gaseous K(ATP) channel opener. EMBO J. 20, 6008–16.

3. HYDROGEN SULPHIDE PROTECTION AFTER ACUTE ISCHEMIC STROKE INCLUDES REACTIVE OXYGEN SPECIES MODULATION WITH DECREASED EXPRESSION OF NOX-4

Part of this chapter will be published in the following article

Isabel Henriques,, María Gutiérrez-Fernández, Berta Rodríguez-Frutos, Jaime Ramos-Cejudo, Laura Otero-Ortega, Teresa Navarro Hernanz, Sebastián Cerdán, José Ferro, Exuperio Díez-Tejedor. Short-term hydrogen sulfide exposure after stroke is protective to the brain by lowering oxidative stress. *(under review)*

and was presented as an oral communication at the 22nd European Stroke Conference, 2013

Henriques I, Gutiérrez-Fernández M, Rodríguez-Frutos B, Ramos J, Ferro J, Díez-Tejedor E. Hydrogen sulphide reduces infarct size and enhances recovery in a rat model: protection mechanism includes NOX-4 downregulation. Cerebrovasc Dis 2013: 33 (suppl 3): 79

3. HYDROGEN SULPHIDE PROTECTION AFTER ACUTE ISCHEMIC STROKE INCLUDES REACTIVE OXYGEN SPECIES (ROS) MODULATION WITH DECREASED EXPRESSION OF NOX-4

INTRODUCTION

H_2S is endogenously produced in different organs including the brain (Mani et al., 2013) and regulates oxygen consumption by competing with O_2 in binding to cytochrome C oxidase at the mitochondrial electron transport chain (Szabó, 2007). H_2S is also involved in neuronal and glial communication (Mikami et al., 2011) and in local vasotone regulation (Leffler et al., 2011). Being a gas, it can diffuse and cross membranes, allowing quick interaction with intracellular mechanisms. Its role as an oxygen sensor further enhances its potential as a pharmacological tool in ischemic stroke (Olson et al., 2013). Yet, data about the potential benefit of H_2S in the context of acute ischemic stroke is scarce and conflicting.

We hypothesized that inducing a reversible hypometabolic state after acute cerebral ischemia through exposure of H_2S after pMCAO, could limit acute ischemic brain damage. We showed that short-term exposure to H_2S after pMCAO improves functional outcome and decreases infarct size. Interestingly, DWI MRI ADC maps revealed a different intralesional pattern compared to controls and PWI MRI showed higher intralesional cerebral blood flow. To better understand if, and when, H_2S can be protective in the context of acute ischemic stroke, it is needed to dissecate the mechanisms by which H_2S modulates brain ischemia.

In the current study, we investigated the effects of short-term H_2S exposure after permanent middle cerebral artery occlusion (pMCAO) by analyzing markers of cytoprotection and repair. We completed the study with *in vivo* brain imaging (MRI) and compared it to *post-mortem* immunohistochemical analysis.

MATERIALS AND METHODS

All experiments were designed to minimize animal suffering in compliance with the ARRIVE criteria and our medical school's Ethical Committee for the Care and Use of Animals in Research (EU directives 86/609/CEE and 2003/65/CE). Regarding all procedures, researchers were blinded to group allocation after randomization. Male 8 - 12 weeks old Sprague-Dawley rats (250 to 320g) (Charles River©, Spain) were randomly assigned to three groups: sham (craniotomy, n=13), control (craniotomy + pMCAO, n=23) and treated (craniotomy + pMCAO + exposure to 40 ppm H2S, n=28). Rats were anesthetized with the halogenated general inhalation anesthetic drug Sevoflurane {[fluoromethyl 2, 2, 2,-trifluoro-1-(trifluoromethyl) ethyl ether] [1, 1, 1, 3, 3, 3-hexafluoro-2-(fluoromethoxy) propane]}. Its median alveolar concentration (the concentration at which half of the subjects do not move in response to a skin incision) is 2.5 (+/-0.3) volumen %. We performed pMCAO after a small craniotomy above the rhinal fissure over the branch of the right middle cerebral artery (MCA), exposing MCA and permanently ligated with a 9-0 silk suture before its bifurcation, in order to enhance reproducibility. After MCAO, both common carotid arteries are temporarily occluded for 60 min with a lace of a 6-0 silk suture. Scar size and location were equal for all groups, animal cages had no information about group allocation, and codes were used in *post mortem* samples, in order to maintain blinded data collection and analysis. Body temperature and glycemia were measured throughout procedures. Rats were sacrificed at 24h and 14d after surgery.

Gas mixtures

Treated animals were exposed to H_2S 3 hours after acute ischemia and breathed a mixture of atmosphere with hydrogen sulfide [Gasin medical bottles, 40 ppm H2S in nitrogen (N_2: 99, 9%)] during 24 min inside a closed box (9.5 x 20 x 10 cm = Volume 1,900 cm^3). Pressure output of hydrogen sulfide was 1 bar/30s. Control and sham animals breathed normal atmosphere in the same temperature and humidity conditions. When this study was designed, no data was available regarding time and

dosage of H_2S exposure and its efficacy in pMCAO. Thus, we established an effective dose by exposing healthy rats to progressive doses of H2S. Our variables were H_2S concentration (40 and 80 ppm), time of exposure (from 1 to 90 min), and output pressure (1 to 2 bar). We used rectal temperature before and after exposure as an indirect measure of change into hypometabolism and established an exposure time of 24 minutes under a concentration of 40ppm with an output pressure of 1 bar/30s as standard dosage.

Ischemic lesion size

Lesion size was evaluated *in vivo* at 24h and 14d *using* T2-weighted sequence MRI and *post mortem* by hematoxylin and eosin (H&E) stains, as previously described (Gutiérrez-Fernández et al., 2011).

Magnetic Resonance Imaging

The extension of ischemic lesions was analyzed non-invasively after 24h (group sacrificed at 24h) and twice, after 24h and 14d (group sacrificed at 14d), using T2-weighted images. The observer was blinded to allocation of animals in all cases. After contrast adjustment, the contours of the hemispheres were traced manually on each slice. Data analysis was performed using Image J software from NIH Image, slice-by-slice contouring at lesion site and in the contralateral hemisphere in the same location. Only lesions larger than 2mm x 2mm x 2mm were analyzed to minimize partial volume effects. We used JPG® region of interest (ROI) to measure infarct size. To correct for brain edema effect, lesion size was determined by an indirect method: (infarct area) = (area of the intact contralateral hemisphere) – (area of the intact ipsilateral hemisphere). Lesion size was expressed as percentage of total size of the ipsilateral hemisphere. Exclusion criteria were no measurable lesion on MRI except for the sham group, and animals were sacrificed and excluded from the sample (n=3). We therefore

used T2-weighted MRI at 24h as confirmation tool for successful ischemic lesion induction.

MRI images were acquired on a 7 Tesla/16 cm Bruker Avance III system (Bruker Medical Gmbh, Ettlingen, Germany) at the MR Imaging Facility (SIERMAC, http://www.siermac.es) from the Institute for Biomedical Research "Alberto Sols" CSIC/UAM, Madrid, Spain. The magnet was equipped with a ^{1}H selective birdcage resonator for rat head (38mm) and a gradient coil insert (90 mm, maximum intensity 36 G/cm). Anestesia was induced in a plexiglass chamber with 2%-3% isoflurane mixed with oxygen and maintained during the experiment through a nose mask. The physiological state of the rats was monitored during MRI acquisitions with a Biotrig physiological monitor (Bruker) depicting on-line the respiratory rate.

Axial T2-weighted spin echo images were obtained using a rapid acquisition with relaxation enhancement (RARE) sequence in axial and coronal orientations using the following parameters: Number of echo images 2 (TE: 29.54ms and 88.61ms), TR = 3000 ms, RARE factor = 4, Av = 3, FOV = 3.5 cm, acquisition matrix = 256 × 256 corresponding to an in-plane resolution of 136 × 136 μm^2, slice thickness = 1.00 mm without gap.

Diffusion-weighted magnetic resonance images (DWI) were obtained in three ortoghonal orientations as defined by the read, phase and slice encoding gradients using a multishot spin-echo echo planar imaging (EPI) sequence. Acquisition conditions were; diffusion gradient duration □: 3ms; diffusion gradient separation □: 18ms; TR: 3000ms; TE: 50ms, FOV: 3.8cm; axial slices (1.5mm thickness) and 3 b values: 100, 400 and 1000 s/mm^2; acquisition matrix = 128 × 128 corresponding to an in-plane resolution of 296 × 296 μm^2.

Dynamic susceptibility contrast – Magnetic Resonance Imaging (DSC MRI) was performed using a bolus injection of paramagnetic contrast agent (Gd-DTPA; Magnevist, Bayer Schering Pharma AG, Leverkusen, Germany; 0.3mmol/Kg i.v.). Dynamic changes in signal intensity were used to calculate CBF (cerebral blood flow), CBV (cerebral blood volume, the fraction of tissue volume occupied by blood) and MTT

(mean transit time: MTT=CBF/CBV, the time it takes for blood to pass through the vasculature within the tissue of interest). Dynamic T2-weighted images were acquired using a spin-echo single shot echo planar imaging (EPI) sequence with the following scan parameters: TR/TE of 250/7ms; Flip angle: 30º; Number of repetitions: 150; slice thickness and interslice gap: 1.5mm and 0.1mm; number of slices: 6; FOV: 3.8cm and matrix size: 86x8. After an initial baseline period of 10s, a rapid bolus injection of Gd-DTPA was administered intravenously in the tail vein.

ADC, CBF, CBV and MTT pixel by pixel maps were generated with a homemade software application (MatLab®, 2007a). ADC value was computed for each voxel using the exponential model according to the expression: $S_b = S_0\, e^{-b*ADC}$, where S_b is signal intensity with the different b weightings and S_o the signal intensity for b=0. Perfusion parameters were calculated based on the premise that ΔR* is proportional to the contrast agent concentration according to the curve equation: ΔR*= -K. ln [S(t) / So (t)], where S(t) is de signal intensity at time t, So baseline signal intensity and, K a constant. The transit curve was then fitted to a gamma variant function.

The mean and standard deviation of ADC of the central and peripheral lesion area were determined, and the same measurement performed in the same anatomic location as the lesion but in the normal contralateral hemisphere. These three regions of interests (ROIs) are easy to identify on color coded ADC maps and drawn manually over the maps. The ROIs were applied on all affected ADC slices from each rat with a maximum number of five slices. The mean ADC values of central and peripheral lesion areas were divided by the value of the contralateral normal hemisphere and expressed as a relative ADC (rADC).

Perfusion-weighted MR imaging was performed using bolus tracking and resulting data used to generate CBF, CBV and MTT maps. In these maps only two ROIs were investigated: ischemic lesion and contralateral normal hemisphere, because of the smaller matrix size (86*86) than in ADC maps, hindering the selection of central and peripheral lesion areas. The mean CBF values of the ischemic region were divided by the value of the contralateral normal hemisphere used as reference region and expressed as relative CBF (rCBF).

Cell death

Cell death was assessed by TUNEL staining (biotin-dUTP nick end-labeling mediated by terminal deoxynucleotidyl transferase; TdT-FragEL DNA Fragmentation Detection Kit, Oncogene Research Products) following manufacturer's instructions. The number of positive cells was counted using a 40× objective and image analysis software (Image-Pro Plus 4.1®, Media Cybernetics) in the ischemic lesion. Blind access to group code was done in all microscopic observations and all samples were independently counted by at least two of the authors.

Immunohistochemistry, immunofluorescence and western blot

We used markers for NADPH oxidase 4 (NOX-4), neuronal nuclei (NeuN), astrocytes [glial fibrillary acid protein (GFAP)], vascular endothelial growth factor (VEGF), synaptophysin, superoxide dismutase 2 (SOD-2) and heat shock protein 27 (HSP-27). B-actine loading (1:400, Sigma-Aldrich) was used as control.

NOX-4

Pro-oxidant enzyme, NADPH oxidase 4 (NOX-4) primary polyclonal antibody anti-Nox-4 (1:1000, Abnova) was incubated for1 hour at room temperature.

Immunofluorescence

Serial coronal sections were cut at 10µm in a cryostat (Leica CM1950) and studied by immunofluorescence neuronal markers. Markers for neuronal nuclei (NeuN) (monoclonal antibody diluted 1:100, Millipore), astrocytes [glial fibrillary acid protein (GFAP) (monoclonal antibody diluted 1:400, Chemicon)], vascular growth [vascular endothelial growth factor (VEGF) marker (polyclonal antibody diluted 1:500, Millipore)], synaptogenesis [synaptophysin (monoclonal antibody diluted 1:200, Sigma

- Aldrich)], Superoxide dismutase 2 (SOD-2) (polyclonal antibody diluted 1:150, Abcam®), and Heat shock protein 27 (HSP-27) (monoclonal antibody diluted 1:200, Abcam®), followed by goat anti-mouse Alexa Fluor 488 and anti-rabbit Alexa Fluor 594 (1: 750, Molecular Probes, Invitrogen) were used.

Sections were mounted with a H-1200 VectaShield® mounting medium for fluorescence with DAPI (ATOM). Samples were examined using a spectral confocal microscope Leica TCS SPE (Leica Microsystems®, Heidelberg, Germany) and the confocal images were analyzed using Leica software LAS AF, version 2.0.1, build 2043. The images were acquired at maximum confocal projection.

Western Blot

Animals (n=4 per group) were decapitated and the proteins of the peri-infarct tissue and their concentrations were determined using a BCA protein assay kit (Pierce). Western-Blot for β-actin (monoclonal antibody diluted 1:400, Sigma Aldrich), NADPH oxidase 4 (NOX-4)(polyclonal antibody 1:2000, Abnova), SOD-2 (polyclonal antibody diluted 1:5000, Abcam), HSP27 (monoclonal antibody diluted 1:1000, Abcam), GFAP (monoclonal antibody diluted 1:500, Chemicon), VEGF (polyclonal antibody diluted 1:500, Millipore) and synaptophysin (monoclonal antibody diluted 1:400, Sigma) were measured in all groups. To reduce differences between animals, at least three Western blots were performed for each animal. In addition, at least three repeated samples were always included in every set of experimental samples as internal standards.

Statistical analysis

Quantitative data are shown as mean ± standard error of the mean (SEM) and presented as box and whiskers plots. As data followed a non-normal distribution, the Mann–Whitney test was used to compare two samples and the Kruskal–Wallis test to

compare more than two samples of the same group or more than 2 groups (SPSS 16 for Windows®). Values of $p<0.05$ were considered significant at a 95% confidence level.

RESULTS

Cell death after exposure to hydrogen sulfide

Treated rats showed significantly less TUNEL positive cells, both at 24h (367.5 ± 78.03 *vs.* 901.25 ± 217.45 p=0.047) and 14d (42.7 ± 7.76 *vs.* 53.71 ± 6.75 p=0.04) (Figure 3.1A, Figure 3.2A) in comparison to controls. No sham operated rats showed TUNEL positive cells.

Exposure to hydrogen sulfide does not increase brain repair but enhances markers associated with brain protection

At day 14, the group treated with H_2S showed no increase in expression of VEGF (0.75 ± 0.22 *vs.* 0.79 ± 0.18 p= 0.88) or synaptophysin (1.40 ± 0.39 *vs.*1.29 ± 0.30 p=0.50) compared to control group (Figure 3.2B). GFAP showed significantly lower levels at day 14 in treated animals compared to control (0.36 ± 0.16 *vs. 0.77* ± 0.43, p=0.027) (Figure 3.2B and C). The levels of SOD2 at day 14 were lower than in the control group (0.66 ± 0.06 *vs. 1.07* ± 0.14, p= 0.05) (Figure 3.2C), but not at 24h (0.788±0.13 *vs*. 0.90±0.3 p=0.11) (Figure 3.1B). The levels of NOX-4 were lower in treated rats compared to the control group at 24h (0.50 ± 0.12 *vs.* 1.11 ± 0.28 p=0.03) (Figure 3.1A) and day 14 (0.47 ± 0.21 *vs.* 1.40 ± 0.46 p=0.049) (Figure 3.2A). HSP-27 levels were lower at 24h in treated rats compared to control animals (0.41 ± 0.12 *vs.* 0.81 ± 0.11 p=0.49) but not at day 14 (0.84 ± 0, 51 *vs*. 1,056 ±0, 55 p= 0.24) (Figure 3.1B and Figure 3.2B).

Physiological parameters

Glycemia was assessed immediately after starting the procedure and during surgery and was similar in all groups. Body temperature was significantly lower after induction of anesthesia in all groups ($p<0.05$). After an exposure time to H_2S of 24 minutes, body temperature decreased by 1.85 ºC (mean) but quickly recovered after animals started to breathe normal atmosphere; no difference in body temperature was observed at 2 hours after exposure (Figure 3.3).

DISCUSSION

We report on the role of short-term exposure to H_2S in acute ischemic brain damage. Our previous results have shown that exposure to hydrogen sulfide after pMCAO improves functional outcome and decreases infarct size and cell death. Now, we conclude for that H_2S may act very early in the ischemic process, since there were lower levels of acute injury-related markers at 24h without enhancement of repair-associated markers for vasculogenesis, angiogenesis or synaptogenesis at day 14. Significant benefit is likely to occur then before major tissue damage develops, including modulation of NOX-4, a major generator of reactive oxygen species (ROS) and mediator of endothelial dysfunction.

H_2S exposure during 24 min is effective with minor interference with body temperature

Hypothermia, when not induced from external sources, is a result of hypometabolism and not the cause of metabolic changes. H_2S modulation in the context of acute stroke has been associated with induction of hypothermia, especially in protocols that included prolonged exposure times (Joseph et al., 2012). In our study, after an exposure time of 24 minutes, a mean decrease of 1.85ºC in body temperature was observed. Body temperature fully recovered in less than 120 min (Figure 3.3).

Consequently, hypothermia appears to be a side effect of hypometabolism induced by H_2S and other mechanisms must be involved since hypothermia during 2 hours may not explain all the effects of H_2S administration observed at least until day 14. In the present study, a shorter exposure time than previously reported was effective and the reduced effect on body temperature represents an important finding in a translational context since minor changes (less than 2º Celsius) in body temperature will not require stroke patient management in intensive care units.

H_2S exposure protects brain tissue and does not enhance repair markers after pMCAO

Previous *in vitro* studies have shown that the use of D-cysteine (a biosynthetic pathway for H_2S production) was associated with attenuation of ischemia-reperfusion injury in the kidney (Shibuya et al., 2013). Also in a murine primary cortical neuron preparation ischemic neuronal death was prevented using a H_2S-releasing NMDA receptor antagonist (Marutani et al., 2012). Additionally, rats pre-treated with diallyl sulfide showed a significant decrease in TUNEL positive cell count (Lin et al., 2012). Our study confirmed that markers for cell death depict significantly less expression in treated animals.

HSP27 is a stress-related protein known to be differentially expressed after stroke (Stetler et al., 2012). Genomic studies have already highlighted that several chaperones including HSP27 were upregulated at 24h, both in the core and peri-infarct areas (Ramos-Cejudo et al., 2012). Others reported that neuronal expression of another HSP (HSP 70) was associated with ischemic penumbra and core, using a reporter mice model (de la Rosa et al., 2013). Also a study with reperfusion in cardiac ischemia showed that HSP27 expression was lower in H_2S-treated pigs (Osipov et al., 2009). In the present study, we observed less expression of HSP27 at 24h after pMCAO in rats exposed to H_2S, associated with markers of tissue preservation, reflecting an additional indication of a possible protective role for H_2S.

It is known that oxidative stress causes tissue damage in the context of acute brain ischemia with ROS expressed above physiological levels (Kleinschnitz et al., 2010; Moskowitz et al., 2010). ROS downregulation after exposure to H_2S was reported in ischemia-reperfusion models, after hemorrhagic shock (Ganster et al., 2010), and during lung transplantation (George et al., 2012). NOX-4 is a major source of oxidative stress in ischemic stroke (Kleinschnitz et al., 2010). In our study, NOX-4 levels were lower at 24h and day 14 in treated rats. Thus, the protective effect of H_2S after acute brain ischemia is maintained in time and may modulate early ROS expression. Interestingly, also less expression of SOD2 was observed at day 14, which could be related to reduced ROS production during the acute phase of ischemic stroke.

Finally, GFAP levels were lower in rats exposed to H_2S, suggesting that early protection may be related to preservation of tissue structure and less glial scar, since we did not find increased levels of repair-associated markers implicated in synaptogenesis, vasculogenesis or angiogenesis at day 14.

CONCLUSIONS

In our pMCAO model of ischemic stroke, early exposure to hydrogen sulfide after focal brain ischemia decreased cell death expression through processes that involve modulation of NOX-4, a major enzyme generator of reactive oxygen species. H_2S probably acts very early after administration, since lower levels of acute injury-related markers were present at 24h, without increase of repair-associated markers for vasculogenesis, angiogenesis or synaptogenesis at day 14. Significant benefit is likely to occur before major tissue damage has taken place. Since H_2S donors exist already for other clinical purposes, clinical trials in a translational context deserve further consideration.

FIGURES

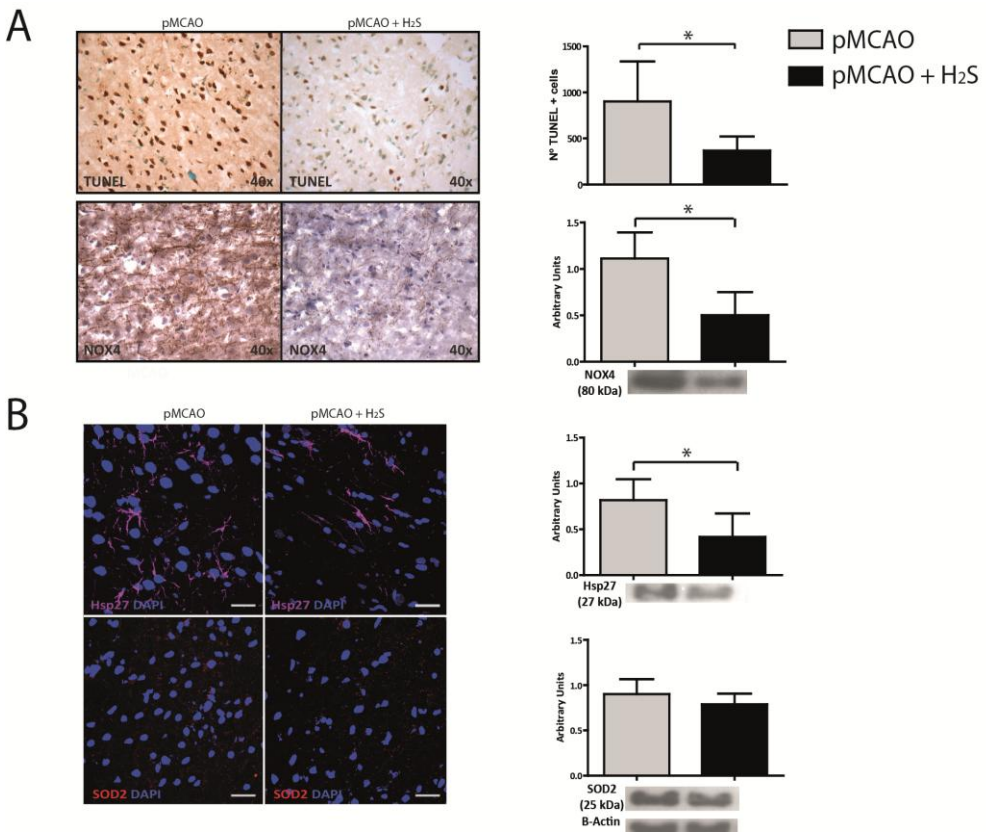

Figure 3.1. *RATS EXPOSED TO H_2S AFTER pMCAO SHOW LOWER EXPRESSION OF CELL DEATH, NOX-4 AND HSP27 AT 24H*. **A.** Decreased expression of cell death (**P*<0.05) and of NOX-4 in rats exposed to H_2S. **B.** Decreased expression of heat shock protein 27 (HSP 27) in treated rats (**P*<0.05). No differences in superoxide dismutase-2 (SOD-2) expression levels.

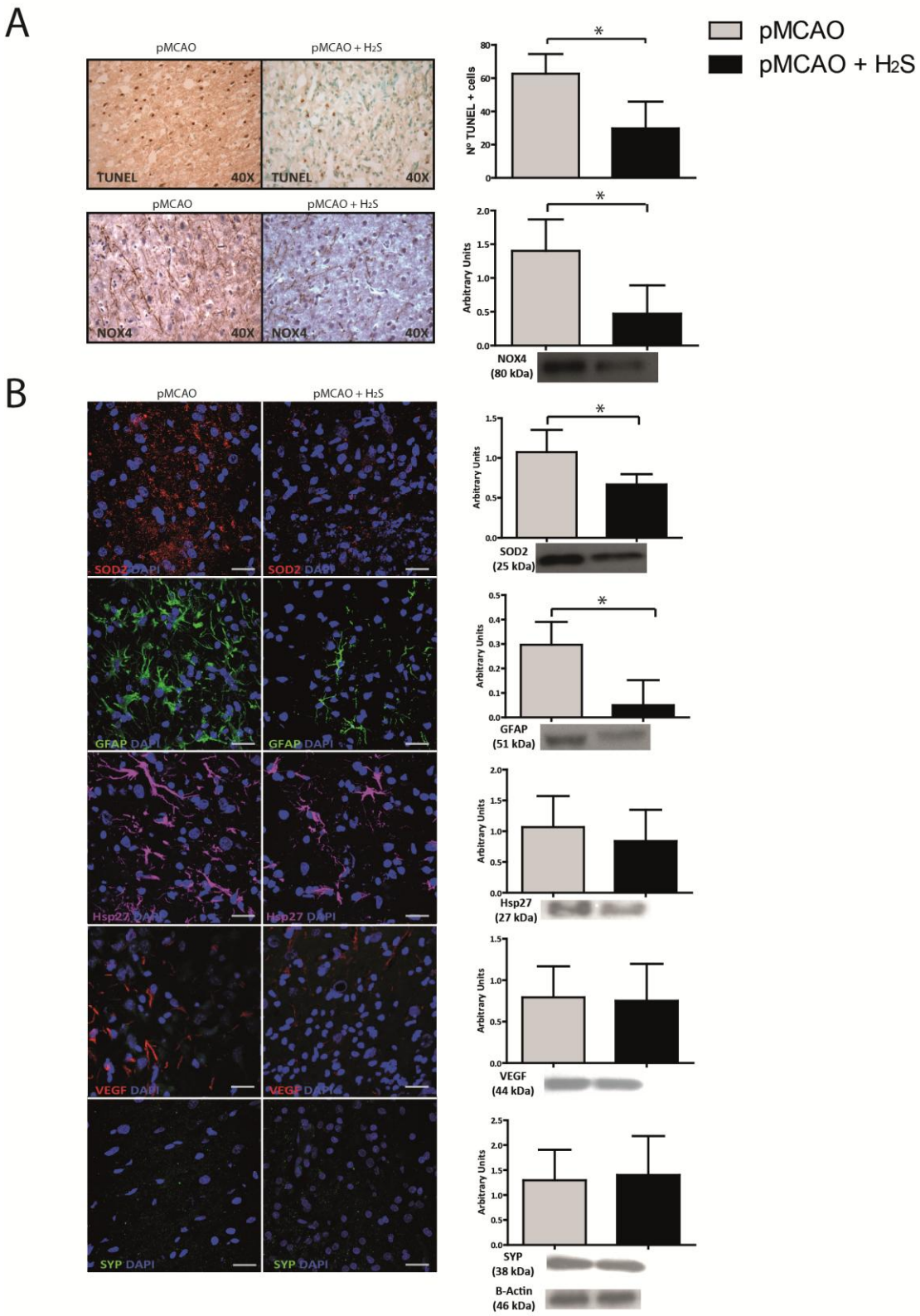
A
pMCAO
pMCAO + H2S
TUNEL
40X
NOX4
B
SOD2 DAPI
GFAP DAPI
Hsp27 DAPI
VEGF DAPI
SYP DAPI
Nº TUNEL + cells
Arbitrary Units
NOX4 (80 kDa)
SOD2 (25 kDa)
GFAP (51 kDa)
Hsp27 (27 kDa)
VEGF (44 kDa)
SYP (38 kDa)
B-Actin (46 kDa)

Figure 3.2. *DECREASED EXPRESSION OF CELL DEATH AND ROS GENERATING ENZYME NOX-4 AT 14D IN RATS EXPOSED TO H_2S* **A.** At 14d, cell death (**P*<0.05) and NOX-4 expression levels (**P*<0.05) were significantly lower in rats exposed to H_2S **B.** Significant lower levels of NOX-4 (**P*<0.05), SOD2 (**P*<0.05) and GFAP (**P*<0.05) were present at day14 in rats exposed to H_2S. No significant differences were observed in HSP27, VEGF or synaptophisin expression levels detected at day 14.

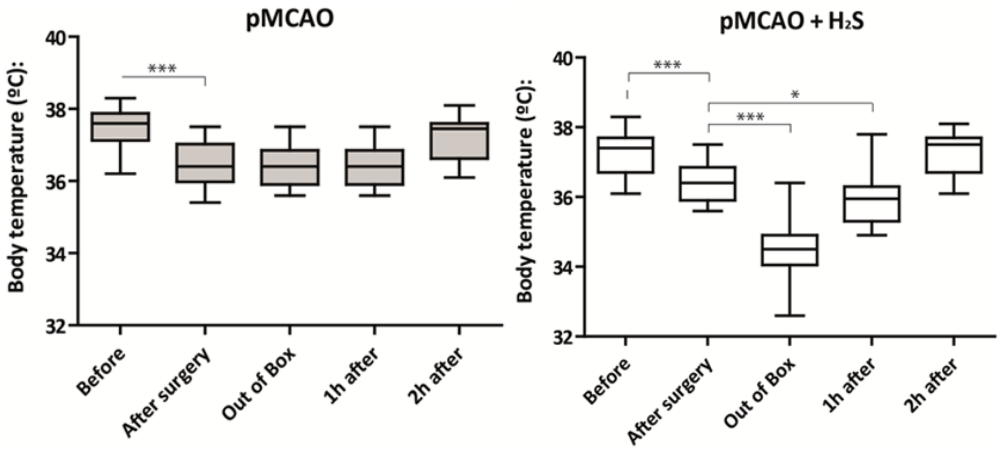

Figure 3.3. *BODY TEMPERATURE DURING EXPERIMENTS IN RATS EXPOSED TO H2S (RIGHT GRAPH) AND CONTROLS (LEFT GRAPH).* No difference in body temperature 2h after exposure to hydrogen sulfide was observed. GRAPH LEGEND: **Before**: rectal temperature in awake rats before starting surgery; **After surgery**: rectal temperature after surgery, before entering the box with atmosphere enriched with 40 ppm H2S (please see Methods for exposure to H2S conditions). **Out of Box**: Rectal temperature after getting out of the box, 24 minutes later. **1h after** and **2h after**: rectal temperature one and two hours after exposure to H2S. All rats showed significant differences before and after surgery (***p<0.0001). Rats exposed to H_2S showed a significant decrease in body temperature after surgery (***p<0.0001) until one hour (*p<0.05). No difference in rectal temperature was observed 2h after exposure.

REFERENCES

De la Rosa, X., Santalucía, T., Fortin, P.-Y., Purroy, J., Calvo, M., Salas-Perdomo, A., Justicia, C., Couillaud, F., Planas, A.M., 2013. In vivo imaging of induction of heat-shock protein-70 gene expression with fluorescence reflectance imaging and intravital confocal microscopy following brain ischaemia in reporter mice. Eur. J. Nucl. Med. Mol. Imaging 40, 426–38.

Ganster, F., Burban, M., de la Bourdonnaye, M., Fizanne, L., Douay, O., Loufrani, L., Mercat, A., Calès, P., Radermacher, P., Henrion, D., Asfar, P., Meziani, F., 2010. Effects of hydrogen sulfide on hemodynamics, inflammatory response and oxidative stress during resuscitated hemorrhagic shock in rats. Crit. Care 14, R165.

George, T.J., Arnaoutakis, G.J., Beaty, C.A., Jandu, S.K., Santhanam, L., Berkowitz, D.E., Shah, A.S., 2012. Hydrogen sulfide decreases reactive oxygen in a model of lung transplantation. J. Surg. Res. 178, 494–501.

Gutiérrez-Fernández, M., Rodríguez-Frutos, B., Alvarez-Grech, J., Vallejo-Cremades, M.T., Expósito-Alcaide, M., Merino, J., Roda, J.M., Díez-Tejedor, E., 2011. Functional recovery after hematic administration of allogenic mesenchymal stem cells in acute ischemic stroke in rats. Neuroscience 175, 394–405.

Joseph, C., Buga, A.-M., Vintilescu, R., Balseanu, A.T., Moldovan, M., Junker, H., Walker, L., Lotze, M., Popa-Wagner, A., 2012. Prolonged gaseous hypothermia prevents the upregulation of phagocytosis-specific protein annexin 1 and causes low-amplitude EEG activity in the aged rat brain after cerebral ischemia. J. Cereb. Blood Flow Metab. 32, 1632–42.

Kleinschnitz, C., Grund, H., Wingler, K., Armitage, M.E., Jones, E., Mittal, M., Barit, D., Schwarz, T., Geis, C., Kraft, P., Barthel, K., Schuhmann, M.K., Herrmann, A.M., Meuth, S.G., Stoll, G., Meurer, S., Schrewe, A., Becker, L., Gailus-Durner, V., Fuchs, H., Klopstock, T., de Angelis, M.H., Jandeleit-Dahm, K., Shah, A.M., Weissmann, N., Schmidt, H.H.H.W., 2010. Post-stroke inhibition of induced NADPH oxidase type 4 prevents oxidative stress and neurodegeneration. PLoS Biol. 8.

Leffler, C.W., Parfenova, H., Basuroy, S., Jaggar, J.H., Umstot, E.S., Fedinec, A.L., 2011. Hydrogen sulfide and cerebral microvascular tone in newborn pigs. Am. J. Physiol. Heart Circ. Physiol. 300, H440–7.

Lin, X., Yu, S., Chen, Y., Wu, J., Zhao, J., Zhao, Y., 2012. Neuroprotective effects of diallyl sulfide against transient focal cerebral ischemia via anti-apoptosis in rats. Neurol. Res. 34, 32–7.

Mani, S., Li, H., Untereiner, A., Wu, L., Yang, G., Austin, R.C., Dickhout, J.D., Lhoták, S., Meng, Q.H., Wang, R., 2013. Decreased Endogenous Production of Hydrogen Sulfide Accelerates Atherosclerosis. Circulation 127, 2523–34.

Marutani, E., Kosugi, S., Tokuda, K., Khatri, A., Nguyen, R., Atochin, D.N., Kida, K., Van Leyen, K., Arai, K., Ichinose, F., 2012. A novel hydrogen sulfide-releasing N-methyl-D-aspartate receptor antagonist prevents ischemic neuronal death. J. Biol. Chem. 287, 32124–35.

Mikami, Y., Shibuya, N., Kimura, Y., Nagahara, N., Yamada, M., Kimura, H., 2011. Hydrogen sulfide protects the retina from light-induced degeneration by the modulation of Ca2+ influx. J. Biol. Chem. 286, 39379–86.

Moskowitz, M.A., Lo, E.H., Iadecola, C., 2010. The science of stroke: mechanisms in search of treatments. Neuron 67, 181–98.

Olson, K.R., Deleon, E.R., Gao, Y., Hurley, K., Sadauskas, V., Batz, C., Stoy, G.F., 2013. Thiosulfate: a readily accessible source of hydrogen sulfide in oxygen sensing. Am. J. Physiol. Regul. Integr. Comp. Physiol. 305, R592–603.

Osipov, R.M., Robich, M.P., Feng, J., Liu, Y., Clements, R.T., Glazer, H.P., Sodha, N.R., Szabo, C., Bianchi, C., Sellke, F.W., 2009. Effect of hydrogen sulfide in a porcine model of myocardial ischemia-reperfusion: comparison of different administration regimens and characterization of the cellular mechanisms of protection. J. Cardiovasc. Pharmacol. 54, 287–97.

Ramos-Cejudo, J., Gutiérrez-Fernández, M., Rodríguez-Frutos, B., Expósito Alcaide, M., Sánchez-Cabo, F., Dopazo, A., Díez-Tejedor, E., 2012. Spatial and temporal gene expression differences in core and periinfarct areas in experimental stroke: a microarray analysis. PLoS One 7, e52121.

Shibuya, N., Koike, S., Tanaka, M., Ishigami-Yuasa, M., Kimura, Y., Ogasawara, Y., Fukui, K., Nagahara, N., Kimura, H., 2013. A novel pathway for the production of hydrogen sulfide from D-cysteine in mammalian cells. Nat. Commun. 4, 1366.

Stetler, R.A., Gao, Y., Zhang, L., Weng, Z., Zhang, F., Hu, X., Wang, S., Vosler, P., Cao, G., Sun, D., Graham, S.H., Chen, J., 2012. Phosphorylation of HSP27 by protein kinase D is essential for mediating neuroprotection against ischemic neuronal injury. J. Neurosci. 32, 2667–82.

Szabó, C., 2007. Hydrogen sulphide and its therapeutic potential. Nat. Rev. Drug Discov. 6, 917–35.

4. INTRALESIONAL PATTERN OF MRI ADC MAPS PREDICT OUTCOME IN EXPERIMENTAL STROKE

Part of this chapter will be published in the following article:

Henriques I, Gutiérrez-Fernández M, Rodríguez-Frutos B, Ramos J, Otero-Ortega L, Teresa Navarro Hernanz, Sebastián Cerdán, Ferro J , Díez-Tejedor E. Intralesional pattern of MRI ADC maps predict outcome in experimental stroke. (under review)

And was presented as an oral communication at the 23rd European Stroke Conference, Nice, France, 2014

Isabel Henriques, María Gutiérrez-Fernández, Berta Rodríguez-Frutos, Jaime Ramos-Cejudo, Laura Otero-Ortega, Teresa Navarro Hernanz, Sebastián Cerdán, José Ferro, Exuperio Díez-Tejedor. ADC heterogeneities within acute ischemic lesion predicted better functional outcome. Cerebrovasc Dis 2014; 34 (suppl 1): 51

4. INTRALESIONAL PATTERN OF MRI ADC MAPS PREDICT OUTCOME IN EXPERIMENTAL STROKE

INTRODUCTION

After acute ischemia, viable tissue at risk of infarction can be detected by perfusion weighted imaging/diffusion weighted imaging (PWI/DWI) mismatch but the time needed to process PWI limits its use in the acute clinical setting. However, acute ischemic stroke can produce different types of intralesional patterns in DWI (Rivers et al., 2006). In ADC maps, those patterns can be either homogeneous or patchy and heterogeneous. Since DWI is highly sensitive to tissue damage, we hypothesized that these two patterns in ADC maps represent ischemic areas with a different potential for recovery after acute ischemia and consequently predict functional outcome after acute ischemia.

In the present study, we evaluated the correlation between different patterns in MRI ADC maps, functional outcome, and immunohistochemical markers of tissue damage to further confirm that different patterns relate to a distinct potential for brain tissue recovery despite the same infarct size and interval after permanent middle cerebral artery occlusion (pMCAO).

MATERIAL AND METHODS

Ethical committee, animal rights

All procedures were carried out at our Cerebrovascular and Neuroscience Research Laboratory at La Paz University Hospital, Universidad Autónoma de Madrid, Spain, and at the Animal Imaging Department (SIERMAC®, Consejo Superior de Investigación Científica), Madrid, Spain. All experiments were performed in compliance with the Ethical Committee for the Care and Use of Animals in Research rules following the International Guidelines for the Care and Use of Laboratory Animals (Royal Decree (R.D.)1201/2005 and European Directive 2010/ 63/UE). The experiments were

designed to use the smallest number of animals possible and to minimize their suffering in accordance with the ethical standards of the Helsinki Declaration of 1975. We included post-surgery analgesia for all groups until sacrifice at 24h. All operated rats (sham and pMCAO) had a cranial suture of the same dimension and on the same side (right craniotomy), and we used group allocation codes in order to keep observation blinded to group allocation while collecting functional data and performing molecular and histological procedures.

EXPERIMENTAL PROCEDURES

Surgical model of pMCAO

Rats were anesthetized using halogenated general inhalation anesthesia with Sevoflurane® {[fluoromethyl 2, 2, 2,-trifluoro-1-(trifluoromethyl) ethyl ether] [1, 1, 1, 3, 3, 3-hexafluoro-2-(fluoromethoxy) propane]}. We performed pMCAO after a small craniotomy above the rhinal fissure over the branch of the right middle cerebral artery (MCA). We exposed the homolateral MCA and permanently ligated it with a 9-0 silk suture immediately before its bifurcation, in order to enhance reproducibility including similar lesion size. After MCAO, both common carotid arteries were temporarily occluded during 60 min with a lace of a 6-0 silk suture.

Subject selection criteria & data collection tools

Animals

Adult male Sprague-Dawley rats, 10 to 12 weeks old, with an average body weight of 250 to 320 g (Charles River® S.L., Barcelona, Spain) were housed with free access to standard rat chow and water. Room temperature was maintained at 21±2°C, with a relative humidity of 45±15% and a light/dark cycle of 12/12 h (7:00h to 19:00h/19:00h to 7:00h). Rats were randomly assigned to the following groups: sham surgery (craniotomy) and permanent middle cerebral artery occlusion (pMCAO). At 24h, T2-

weighted MRI was performed in order to confirm complete MCAO infarct and evaluate infarct size in animals submitted to pMCAO. Rats submitted to pMCAO were then further divided into 2 groups according to the result of the DWI MRI ADC maps: group 1 if heterogeneities were present inside the ischemic lesion at least in more than 2/3 of the lesion in ADC maps (subgroup "heterogeneous"), and group 2 if DWI showed a homogenous lesion in ADC maps (subgroup "homogeneous"). The number of rats submitted to surgery was progressively increased until a minimum of 12 animals was reached in both groups.

Functional evaluation scales

Functional evaluation scales were performed before procedures at baseline and at 24h. All rats were evaluated using a variant of the Rogers' scale and the Rotarod performance test™ (accelerating course of 4- 40 rpm). We used previously validated functional scales to minimize observational bias in semi-quantitative scales by maintaining blindness to allocation group in all observations. We performed similar size cranial and neck scars for all groups and used cage codes regarding group allocation.

Ischemic lesion size measurements

Lesion size was measured at 24h, *in vivo* by T2-weighted magnetic resonance imaging (MRI) and *post-mortem* by hematoxylin and eosin (H&E) stain after processing of tissue samples. We used Image J® software to analyze and measure the Regions of Interest (ROI), employing an 8-bit grayscale or indexed color, 16-bit unsigned integers, 32-bit floating-points and RGB color.

Measurement of ischemic size by hematoxylin & eosin (H&E) staining

Post-mortem lesion size was estimated by H&E stain of brain sections at 24h. Brains were sectioned at the optic chiasm and at the infundibular stalk. A digitalized image was obtained from these slices (Epson® Perfection 1260 scanner) to automatically measure the ischemic area (Image Pro plus 4.0, Media Cybernetics, USA), as previously described (Gutiérrez-Fernández et al., 2011).

Magnetic resonance imaging

We used T2 sequence diffusion-weighted imaging (DWI) including apparent diffusion coefficiency (ADC) maps and tractography, as well as perfusion-weighted imaging (PWI) with determination of cerebral blood flow (CBF), cerebral blood volume (CBV), and mean transient time (MTT).

The extension of the ischemic lesions was analyzed at 24h using T2-weighted images. After contrast adjustment, the contours of the hemispheres were traced manually on each slice. Analysis of the data was performed using Image J® software from NIH Image, slice- by-slice lesion contouring of the lesion and the contralateral hemisphere in the same location as the lesion. Only lesions larger than 2mm x 2mm x 2mm were analyzed to minimize partial volume effects. We used JPG Region of Interest (ROI) to measure infarct size. To correct for the brain edema effect, lesion size was determined by an indirect method: infarct area = area of the intact contralateral hemisphere – area of the intact ipsilateral hemisphere (Swanson et al., 1990; van der Worp et al., 2001). Lesion size was expressed as a percentage of the ipsilateral hemisphere. Exclusion criteria was no lesion on the 24h MRI except for the sham group. When complete MCAO was not confirmed on T2-weighted MRI at 24h, animals were sacrificed and excluded from the sample (n=3). We therefore used MRI at 24h as a confirmation tool of successful ischemic lesion induction.

The MRI images were acquired on a 7 Tesla Bruker Pharmascan system (Bruker Medical GmbH, Ettlingen, Germany) in the local High Field Magnetic Resonance

Spectroscopy and Imaging Facility (SIERMAC®) of the Institute of Biomedical Research "Alberto Sols" CSIC/UAM, Madrid, Spain. The system is equipped with a ^{1}H selective birdcage resonator of 38mm and a 90mm Bruker gradient coil insert (maximum intensity 36 G/cm). Rats were anesthetized with 2% - 3% Isoflurane® mixed with oxygen and anesthesia was maintained during the experiment employing a mask. The physiological state of the rats was monitored using a Biotrig physiological monitor (Bruker) that controlled the respiratory rate.

T2-weighted spin echo images were generated using rapid acquisition with relaxation enhancement (RARE) sequence in axial and coronal orientations and the following parameters: Number of echo images 2 (TE: 29.54ms and 88.61ms), TR = 3000 ms, RARE factor = 4, Av = 3, FOV = 3.5 cm, acquisition matrix = 256 × 256, corresponding to an in-plane resolution of 136 × 136 μm^2, slice thickness = 1.00 mm, without gap.

Diffusion-weighted (DW) magnetic resonance images were obtained with three different directions defined by the read, phase and slice encoding gradients using a multishot spin-echo echo planar imaging (EPI) sequence. Acquisition conditions were diffusion gradient duration: 3ms; diffusion gradient separation: 18ms; TR: 3000ms; TE: 50ms, FOV: 3.8cm; axial slices (1.5mm thickness) and 3 b values: 100, 400 and 1000 s/mm^2; acquisition matrix = 128 × 128.

Tractography

Diffusion tensor imaging and fiber tractography were constructed from DTI datasets acquired with 30 noncollinear directions for diffusion weighted gradient scheme. At 24h after pMCAO, data were acquired with a spin echo single shot echo planar imaging (EPI) pulse sequence. The receiver bandwith was 300KHz; b factor of 1000 sec/mm^2; repetition time 8s; echo time: 35ms; 18 contiguous slices with a slice thickness of 1.5mm; field of view of 3.5 cm x 3.5cm; 128x128 image matrix and a total acquisition time was 56 min.

We employed DSC (Dynamic susceptibility contrast) MRI with a bolus injection of paramagnetic contrast agent (Gd-DTPA; Magnevist, Bayer Schering Pharma AG, Leverkusen, Germany; 0.3mmol/Kg i.v.). Changes in signal intensity for dynamic data were used to calculate CBF (cerebral blood flow), CBV (cerebral blood volume: as fraction of tissue volume occupied by blood) and MTT (mean transit time; MTT=CBF/CBV, as time that it takes for blood to pass through the vasculature within the tissue of interest). Dynamic T2-weighted images were acquired using a spin-echo single shot echo planar imaging (EPI) pulse sequence with the following scan parameters: TR/TE of 250/7ms; flip angle: 30º; number of repetitions: 150; slice thickness and interslice gap: 1.5mm and 0.1mm; number of slices: 6; FOV: 3.8cm and matrix size: 86x86. After an initial baseline period of 10s, a rapid bolus of Gd-DTPA was administered intravenously.

ADC, CBF, CBV, and MTT maps were generated with a homemade software application (MatLab, R2007a), and tractography with MedINRIA software (MedINRIA Ver. 2.0.1, available free at http://www-sop.inria.fr/asclepios/software/MedINRIA/).

ADC value was computed for each voxel using the exponential model according to the expression: $\mathbf{S_b} = \mathbf{S_0 e^{-b*ADC}}$, Sb: signal intensity versus the b factor and So: signal intensity versus b=0. Perfusion parameters were calculated based on the premise that ΔR* is proportional to the contrast agent concentration according to the curve equation: $\Delta R^* = -K \ln [S(t) / S_o (t)]$, where S is de intensity signal at time, S_o baseline intensity signal and K a constant. The curve was fitted to a gamma variant function.

ADC values of the central and peripheral lesion area of acute DWI were measured and the mean and standard error of the mean (SEM) calculated. The same measurement was done in the normal contralateral hemisphere in the same anatomic location as the lesion. The three regions of interests (ROI) are easy to identify on color ADC maps and were drawn manually on maps. The ROI were applied at all affected ADC slices in each rat with a maximum number of five slices. The mean ADC values of central and peripheral lesion areas were divided by the value in the contralateral normal hemisphere and expressed as a relative ADC (rADC) of the region.

As described above, MRI PWI was performed using bolus tracking and resulting data were used to obtain CBF, CBV and MTT maps. Here, we only used two ROI: ischemic lesion and the contralateral normal hemisphere, as the matrix size (86*x86) was smaller than in ADC maps, making it impossible to select the central and peripheral lesion areas. The mean CBF value of the ischemic region was divided by the value from the contralateral normal hemisphere as reference region and expressed as relative CBF (rCBF).

We calculated PWI/DWI mismatch by the standard volumetric model (mismatch = %PWI-%DWI volume) since co-registrations of PWI and DWI are not possible.

Immunohistochemistry

Cell death

Cell death was detected by TUNEL staining (biotin-dUTP nick end-labeling mediated by terminal deoxynucleotidyl transferase; TdT-FragEL DNA Fragmentation Detection Kit, Oncogene Research Products) following the methodology indicated by the manufacturer. Blind access to group code was employed in all microscopic observations and all samples were independently counted by at least two of the authors.

NOX-4

Pro-oxidant enzyme, NADPH oxidase 4 (NOX-4) primary polyclonal antibody anti-Nox-4 (1:1000, Abnova, Heidelberg, Germany) was incubated for one hour at room temperature. The slides were then incubated with a secondary antibody (donkey anti-rabbit antibody diluted 1:50) conjugated with horseradish peroxidase (Chemicon International, Temecula, CA, USA) and incubated with 3',3'-diaminobenzidine (Invitrogen).

Immunofluorescence

Serial coronal sections were cut at 10µm in a cryostat (Leica CM1950) and studied by immunofluorescence neural markers. Markers for neuronal nuclei (NeuN) (monoclonal antibody diluted 1:100, Millipore), astrocytes [glial fibrillary acid protein (GFAP) (monoclonal antibody diluted 1:400, Chemicon)], vascular growth [vascular endothelial growth factor (VEGF) marker (polyclonal antibody diluted 1:500, Millipore)], synaptogenesis [synaptophysin (monoclonal antibody diluted 1:200, Sigma - Aldrich)], Superoxide dismutase 2 (SOD-2) (polyclonal antibody diluted 1:150, Abcam®), and Heat shock protein 27 (HSP-27) (monoclonal antibody diluted 1:200, Abcam®), followed by goat anti-mouse Alexa Fluor 488 and anti-rabbit Alexa Fluor 594 (1: 750, Molecular Probes, Invitrogen) were used.

All sections were mounted with H-1200 VectaShield mounting medium for fluorescence with DAPI (ATOM). Samples were examined using a spectral confocal microscope Leica TCS SPE (Leica Microsystems, Heidelberg, Germany) and the confocal images were analyzed using Leica software LAS AF, version 2.0.1 build 2043. The images were acquired at confocal maximum projection.

Western Blot

Brain proteins levels were measured in the infarct zone of animals (n=4 per group) and its concentration was determined using a BCA protein assay kit (Pierce). Western-Blot for NADPH oxidase 4 (NOX-4)(polyclonal antibody 1:2000, Abnova), SOD-2 (polyclonal antibody diluted 1:5000, Abcam), HSP27 (monoclonal antibody diluted 1:1000, Abcam), GFAP (monoclonal antibody diluted 1:500, Millipore), VEGF (polyclonal antibody diluted 1:500, Millipore) and synaptophysin (monoclonal antibody diluted 1:400, Sigma) were measured in all groups. The units were normalized based on B-actin levels (1:400, Sigma-Aldrich). To reduce methodological bias, at least three Western blots were performed for each animal.

.

Statistical analysis

Functional evaluation scores, lesion size, cell death, and protein levels are described as mean and standard error of the mean (SEM) and presented as box and whisker plots. Since data followed a non-normal distribution in the Shapiro-Wilk test, we selected non-parametric tests for data comparison between groups. The Mann–Whitney test was used to compare two samples and the Kruskal–Wallis test was employed to compare more than two samples in the same group or the same variable in more than two groups. Values of $p<0.05$ were considered significant at a 95% confidence level. We used SPSS 16 for Windows for statistical analysis.

RESULTS

Physiological parameters

Glycemia was assessed immediately after starting the procedure and during surgery and was similar in all groups. Rectal temperature was significantly lower after induction of anesthesia in all groups ($p<0.05$) and maintained at 37±0.5ºC. Mean $PaCO_2$ and PaO_2 were not significantly different before and after surgical proceedings.

Same lesion size and time after pMCAO: homogeneous *versus* heterogeneous ADC infarct pattern

At 24 hours after pMCAO, lesion size measured by T2-weighted MRI did not differ between groups (heterogeneous *vs.* homogeneous: 28.99 ± 2.27 *vs.* 29.55 ±2.72, p= 0.418). Sham animals showed no ischemic lesion (Figure 4.1B).

Better functional outcome in heterogeneous ADC pattern

Functional assessment was performed before the procedure and at 24h. At baseline, Rogers Modified Scale was zero for all animals and the latency to fall in the Rotarod test was >120 seconds. Sham-operated animals did not show any functional deficit at 24h. A better functional outcome was observed at 24h in animals with a heterogeneous ADC pattern when compared to animals with a homogeneous pattern regarding the latency to fall in the Rotarod test (118.37 ± 31.43 *vs.* 51.25 ± 30.87, p= 0.032). No significant differences were observed in the Rogers test (3.43 ± 0.48 *vs.* 3.57 ± 0.41, p=0.158) (Figure 4.1C).

Less cell death after pMCAO in heterogeneous ADC pattern

Animals with a heterogeneous ADC pattern expressed significantly less TUNEL positive cells at 24h, in comparison to animals a homogeneous ADC pattern (56.25 ± 13.75 *vs.* 170.5 ± 61.0, p=0.014) (Figure 4.2A). Sham operated rats did not show TUNEL positive cells.

Brain protection associated markers: homogeneous *versus* heterogeneous ADC pattern

NOX-4 showed significantly lower expression levels in animals with heterogeneous intralesional ADC pattern when compared to homogeneous pattern (2.1 ± 0.367 *vs.* 4.693 ± 1.31, p=0.0063) (Figure 4.2B above and Figure 4.2C). The levels of SOD2 at 24h were significantly higher in animals with a heterogeneous intralesional ADC type when compared to animals with a homogeneous pattern (4.84 ± 1.049 *vs.* 2.906 ± 0.368, p= 0.0039) (Figure 4.2B middle and Figure 4.2C). At 24h, the group with a heterogeneous intralesional ADC pattern showed a decreased expression of GFAP when compared to animals with a homogeneous pattern; however, the difference was not significant (2.52 ± 0.53 *vs.* 4.04 ± 0.71, p= 0,068) (Figure 4.2B below and Figure 4.2C).

DWI: Apparent diffusion coefficients and tractographies - homogeneous *versus* heterogeneous ADC pattern infarct

Mean relative apparent diffusion coefficients differed between the two different ADC patterns. Animals with a heterogeneous pattern showed the higher values and a wider variation (844.87 ± 155.402 *vs.* 537.33 ± 61.15, p= 0.0013). Furthermore, the lowest coefficient was observed in a homogeneous lesion and the highest value in a heterogeneous one. Additionally, the SEM of apparently diffusion coefficients was much larger in heterogeneous lesions (155.4 *vs.* 61.15) (Figure 4.3 A). DWI tractographies showed a more consistent preservation in the fiber reconstruction model of ischemic areas in the heterogeneous lesion type (Figure 4.3 B). We observed no heterogeneous patterns below an ADC of 600um2/s that in the present sample may be considered a cut-off value for irremiadetly lost brain tissue.

Higher intralesional cerebral blood flow in heterogeneous ADC pattern

CBF inside ischemic lesions differed between the two patterns. Animals with a heterogeneous pattern showed the higher values for CBF if compared to animals with homogeneous ADC patterns (79.66 ± 32.2 *vs.* 55.43 ± 16.0, p= 0.0026). The lowest value was observed in a homogeneous lesion (14 ml/100g/min) and the highest in a heterogeneous lesion (218 ml/100g/min) (examples are shown in Figure 4.3 C).

Larger PWI/DWI mismatch in heterogeneous ADC pattern

We calculated PWI/DWI mismatch by the standard volumetric model (mismatch = %PWI - %DWI volume), measured in each slice that showed the lesion. Then, we selected the slice that has the largest lesion size. The observed mismatch was higher in the heterogeneous type of pattern when compared to animals with homogeneous lesions (7.72 ± 1.94 *vs.* 2.35 ± 1.45, p=0.007) (examples are shown in in Figure 4.3 D)

DISCUSSION

In the present study we used a rodent model of pMCAO and identified distinct intralesional patterns in MRI ADC maps that predicted a different functional outcome in lesions of similar size and the same time after ischemic induction. Intralesional heterogeneity was related to less expression of cell death and markers of brain tissue protection. Animals with heterogeneous patterns in ADC maps showed also a higher potential for recovery after acute ischemic infarction when compared to animals with the homogeneous type. When assessing PWI/DWI mismatch, homogeneous lesions showed a smaller mismatch, allegedly related to a lower probability of recovery of ischemic penumbra and a higher probability of progression to definitive infarct. (Kakuda et al., 2008; Ogata et al., 2011; Sobesky, 2012).

In the clinical setting, it is known that acute lesions with the same interval after stroke onset and occurring in the same arterial territory do not always show a similar tissue fate in subacute imaging neither the same potential for functional recovery (Koyama et al., 2014; Malik et al., 2014). Reasons for this discrepancy include differences in vascular risk factors, age, preconditioning, and variability in collateral circulation and microcirculation response.

Since futile reperfusion should be avoided in order to minimize the risks of reperfusion when they may outweigh the potential benefit, the topic of acute image patterns that might differentiate brain tissue fate after acute stroke is a subject of intense debate, moreover with the advent of more resources for reperfusion. The introduction of mismatch measurement as inclusion criteria for reperfusion in clinical trials included significant differences in the definition of mismatch and a somewhat arbitrary volumetric difference of 20% between PWI and DWI. Nevertheless, no validation was performed that would support this threshold as a tool for stratifying patients or take into account that mismatch could serve as a surrogate measure of penumbra (Barber, 2013; Sobesky, 2012).

Mismatch between the lesion volume in DWI (attributed to ischemic and irreversibly tissue dead) and PWI (decaying but not yet irreversibly lost) has been used to define

penumbra (where CBF is reduced and the tissue is at risk of infarction), but the time needed to process PWI limits its use in the clinical context. In the present study, we were able to show that interpretation of distinct intralesional MRI DWI ADC patterns in lesions of the same size might offer useful pre-treatment information without the need of using contrast and losing valuable time while processing PWI (Mishra et al., 2010; Neumann-Haefelin et al., 1999).

In the present study, we observed that animals with heterogeneous intralesional ADC patterns showed higher CBF with larger variations inside the ischemic lesion that will reduce the risk for definite infarction. This observation is further supported by the better functional outcome in animals with a heterogeneous ADC pattern. Additionally, tractographies showed a better preservation in the heterogeneous type. In the clinical setting, tractography has also been used to show structural integrity of the corticospinal tract and was related to recovery of motor impairment (Borich et al., 2012; Park et al., 2013).

In our experimental setting, it was possible to control for the variables lesion size and interval after ischemic induction, since the same experimental protocol was used in all animals and T2-weighted MRI confirmed lesion size and involved territory. No differences between heterogeneous and homogeneous groups were observed concerning infarct size. However, we were able to observe significant differences in intralesional apparent diffusion coefficients in ischemic lesions of the same size and arterial territory. It is known that DWI sequences better reflect anatomical structure of tissues (del Zoppo et al., 2011). Moreover, MRI is a bridge between basic science and clinical assessment by representing a high resolution anatomical delineation of disease at an ionic and molecular level (Barber, 2013). As the heterogeneous type showed higher diffusion coefficients that represent a surrogate measure of better anatomical tissue preservation, an increased possibility of avoiding definite infarction and reversion to well perfused brain tissue can be assumed. Our findings support an improved preservation of the intralesional region when ADC maps show a heterogeneous pattern in lesions of MCA territory.

It would be desirable to identify an ADC threshold that distinguishes heterogeneous from homogeneous ADC maps. In our study, no heterogeneous samples were observed below 600um2/s ADC. If confirmed in the clinical context, this observation may proove usefull in identifying patients with irreversible ischemia, without indication for thrombolysis.

Animals with a heterogeneous pattern showed a better functional outcome measured by the latency to fall in Rotarod test. Also in the clinical setting, functional outcome after complete MCA occlusion is far from uniform. Several clinical studies demonstrated the variability of clinical recovery in patients with lesions of the same size and location (Honarmand et al., 2014; Lima et al., 2014). Several explanations for this diversity in functional outcome have been brought forward and include individual variability in collateral circulation, pre-conditioning, and microcirculation response after ischemic insult (Malik et al., 2014; Thompson et al., 2013). However, to our knowledge, the relation between heterogeneous patterns in ADC maps and functional outcome in the clinical setting has not yet been fully addressed.

As outlined above, DWI is the MRI sequence that more consistently reflects ionic and molecular tissue changes since the effect in the Brownian movement of water molecules is changed in the presence of abnormal anatomical features (Tsang et al., 2011). Genomic studies demonstrated yet that there is gene expression associated with trophic factors and CNS development within the lesion core at 24h after pMCAO, suggesting the existence of surviving areas inside the ischemic core (Ramos-Cejudo et al., 2012). These findings support the argument that the central region of the ischemic territory is not inexorably dead or irreversibly damaged. In the present study, we could show differences in the expression of cell death related to different patterns in ADC maps with significantly less expression in the group with a heterogeneous pattern. Consequently, present imaging data emphasize previous findings of genetic expression inside the central areas of the infarct, and, the relation between ADC patterns and tissue preservation requires further exploration.

Oxidative stress causes tissue damage after acute brain ischemia with overexpression of ROS above physiological levels (Kleinschnitz et al., 2010; Moskowitz et al., 2010). In

the present study, we analyzed the expression of major ROS producing enzyme NOX-4 in both groups of ADC patterns and observed significantly reduced expression of NOX-4 in animals with a heterogeneous pattern in ADC maps. At 24h, we also found a higher expression of SOD2, a major scavenger of mitochondrial superoxide, in the group with a heterogeneous ADC pattern. SOD2 is synthesized after brain infarction and tissue levels were related to lesion size (Murakami et al., 1998). We also observed a smaller expression of GFAP in the group with a heterogeneous pattern, albeit not significant. After a brain lesion, astrocytes occupy the space that becomes empty after phagocytosis has taken place, in order to fill up the empty space and maintain tissue structure. Reactive gliosis is part of the healing process but massive gliosis is related with worse outcome (Suma et al., 2008). Consequently, the reduced expression of GFAP in animals with the heterogeneous pattern is possibly related to a reduced ischemic injury.

Reperfusion of tissue that is no longer able to recover from oligemia to normoperfusion exposes stroke patients to risks and may worsen prognosis instead of contributing to improved functional outcome (Barlinn et al., 2014; Yoo et al., 2014). The penumbra concept includes the premise that acute stroke treatment can avoid that part of the ischemic region progresses into infarction. The mismatch lesion volume has been used as a surrogate marker of ischemic penumbra and is defined as the PWI map that exceeds the isotopic DWI lesion. In clinical practice, PWI/DWI mismatch has been employed to evaluate tissue that may recover from acute ischemia in order to avoid futile reperfusion (Barlinn et al., 2014; Foley et al., 2010). Previous clinical studies based on MRI mismatch profiles assessed its usefulness in predicting the clinical response to early reperfusion after rt-PA administration in humans (Albers et al., 2006). Unfortunately, overall benefit of mismatch as inclusion criteria for reperfusion failed to prove its clinical relevance (Kakuda et al., 2008; Nagakane et al., 2011).

Although our study did not address early reperfusion, we observed a pre-treatment DWI MRI pattern that distinguishes between improved and impaired functional outcome. We found increased PWI/DWI mismatch in ischemic MCA lesions with a

heterogeneous pattern in ADC maps indicating a higher potential for reversibility in these animals. On the other hand, in animals with a homogeneous pattern, CBF was not only below the functional threshold but became as low as 6-15 ml/100g/min. Despite the variability that may exist in CBF thresholds in different brain locations, gray or white matter, or different age groups, levels as low as 6-15ml/100g/ min correspond to thresholds of biochemical biomarkers of protein synthesis inhibition, preference for aerobic glycolysis, neurotransmitter release, impaired energy metabolism and terminal depolarization with potassium influx. We also observed coherence in our data concerning functional outcome and biochemical markers (with less expression of cell death and less expression of ROS markers) favoring the group with a heterogeneous pattern in ADC maps. Possibly, homogeneous ADC pattern indicate irreversible brain damage where reperfusion might be futile or even dangerous. However, research in the clinical setting is necessary to confirm our experimental data and validate the usefulness of intralesional ADC patterns to predict outcome and identify patients that may benefit from reperfusion. Nonetheless, the results of the present study represent a promising starting point and may indicate a new tool in pre-treatment decisions in the acute stroke setting.

Study limitations and potential bias

As shown by our experimental data in a pMCAO model of ischemic stroke, the heterogeneity in the coefficients of apparent diffusion inside the ischemic lesion represents areas with a different potential for recovery. Nevertheless, there is significant variability in ADC values depending on the coil systems, imagers, or field strengths used for MR imaging that may have to be taken into account when analyzing data from different MRI equipments. We used relative ADC values because they are more suitable for evaluating diffusion abnormalities than absolute ADC values. Moreover, their use in the experimental setting facilitates translational application.

We used a model of permanent MCAO with high reproducibility as confirmed by equal lesion size in both the heterogeneous and homogeneous group. However, our experimental model did not include vascular risk factors, older age or female sex.

Most importantly, we controlled for time after stroke onset and lesion size, but variability in preconditioning or individual variability in collateral circulation or intracranial pressure variations that may interfere with microcirculation are difficult to assess in an experimental model and may have impact on results.

CONCLUSIONS

Intralesional patterns of MRI ADC maps in an experimental model of ischemic stroke can be classified in heterogeneous and homogeneous patterns. Animals with the same infarct size and interval after ischemia but a heterogeneous intralesional ADC pattern showed a better functional outcome, a higher expression of markers of brain protection, and less expression of cell death. Animals with a homogeneous pattern showed a smaller PWI/DWI mismatch with lower probability of recovery from ischemic penumbra and an increased progression to definitive infarction. Applied to the clinical setting, early identification of tissue at increased risk of irreversible infarction through DWI ADC map patterns may assist in acute therapeutic decisions.

FIGURES

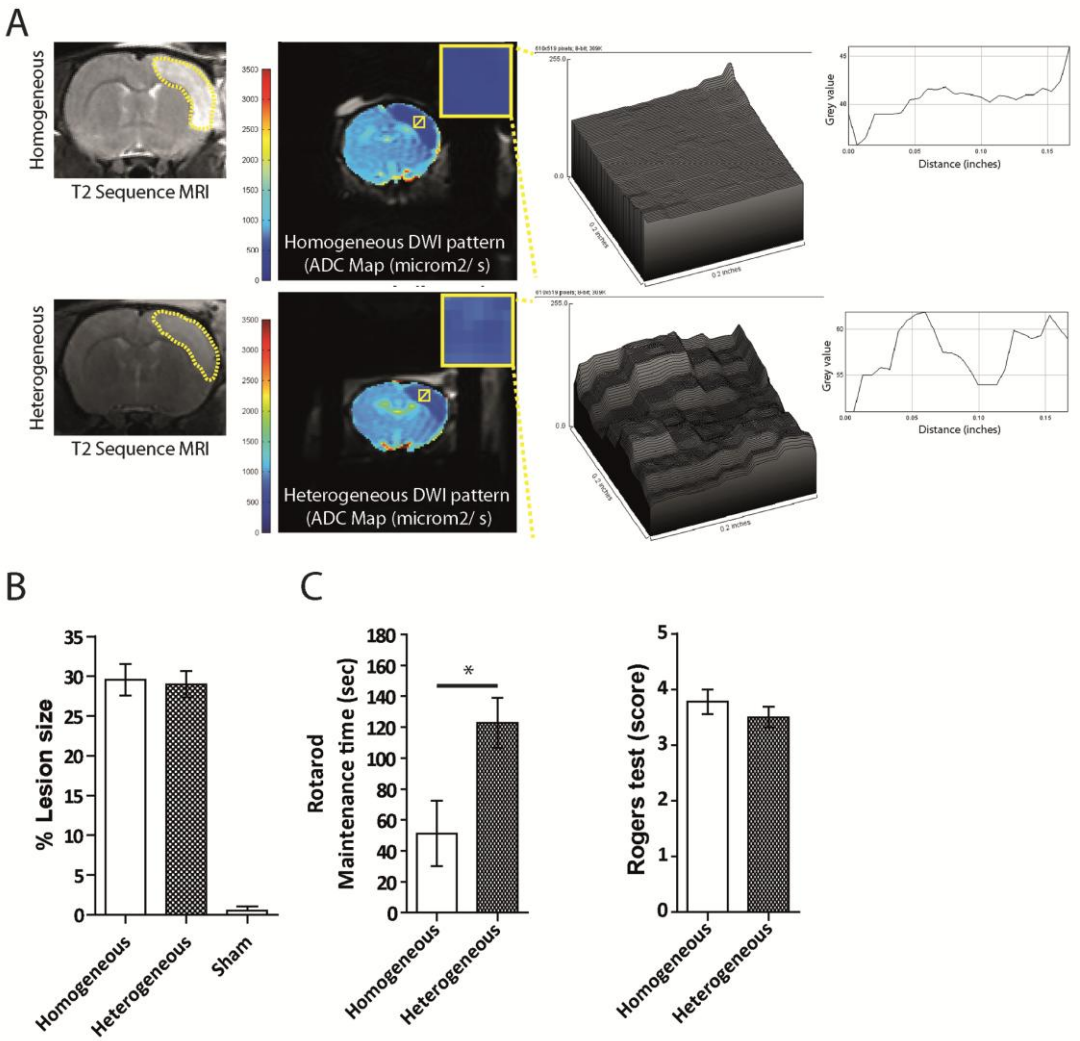

Figure 4.1. *LESION SIZE AND FUNCTIONAL OUTCOME OF TWO DIFFERENT INTRALESIONAL PATTERNS OF MRI ADC MAPS: HOMOGENEOUS AND HETEROGENEOUS.* A. T2 sequence MRI and DWI ADC maps of intralesional homogenous (upper images and graphs) and heterogeneous patterns (lower images and graphs). Heterogeneous and homogeneous showed the same infarct size (left images), but heterogeneous pattern showed an increased range of ADC coefficients (lower graphs)

B. Lesion size: homogeneous pMCAO, heterogeneous pMCAO and sham groups. For the same interval after stroke induction, lesion size was the same in rats with pMCAO and different ADC patterns.

C. Functional outcome in homogeneous and heterogeneous ADC patterns: Maintenance time (sec) in Rotarod test is significantly superior in heterogeneous ADC patterns (left graph). No difference observed with Rotarod test (right graph).

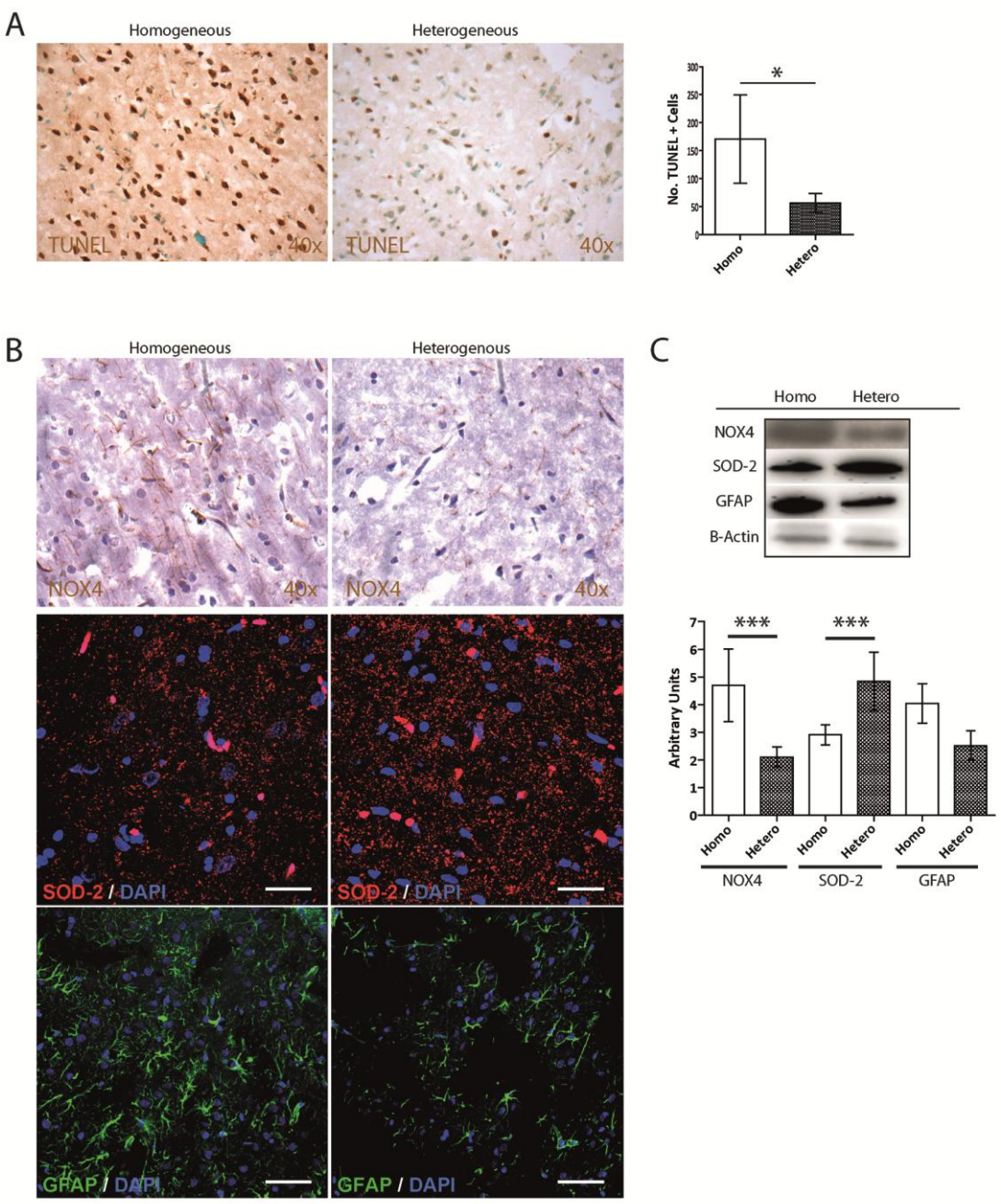

Figure 4.2. *EXPRESSION OF CELL DEATH AND IMMUNOHISTOCHEMICAL MARKERS AT 24H AFTER PMCAO IN TWO DIFFERENT INTRALESIONAL ADC PATTERNS: HOMOGENEOUS AND HETEROGENEOUS.*

A. Expression of cell death by TUNEL: less expression in heterogeneous ADC pattern (right image and graph).

B. Immunohistochemical markers and W/B: Upper images: less expression of NOX-4 in heterogeneous pattern (right image). Middle images: less expression of SOD-2 in

homogeneous type (left image and white bar in Figure 2 C). Lower images: less expression of GFAP in heterogeneous patterns (right image, grey bar in Figure 2 C).

C. Western-Blot of NOX-4, SOD-2 and GFAP 24h after pMCAO. Upper: W/B of NOX-4, SOD-2 and GFAP (image). Lower: W/B of NOX-4, SOD-2 and GFAP (graph).

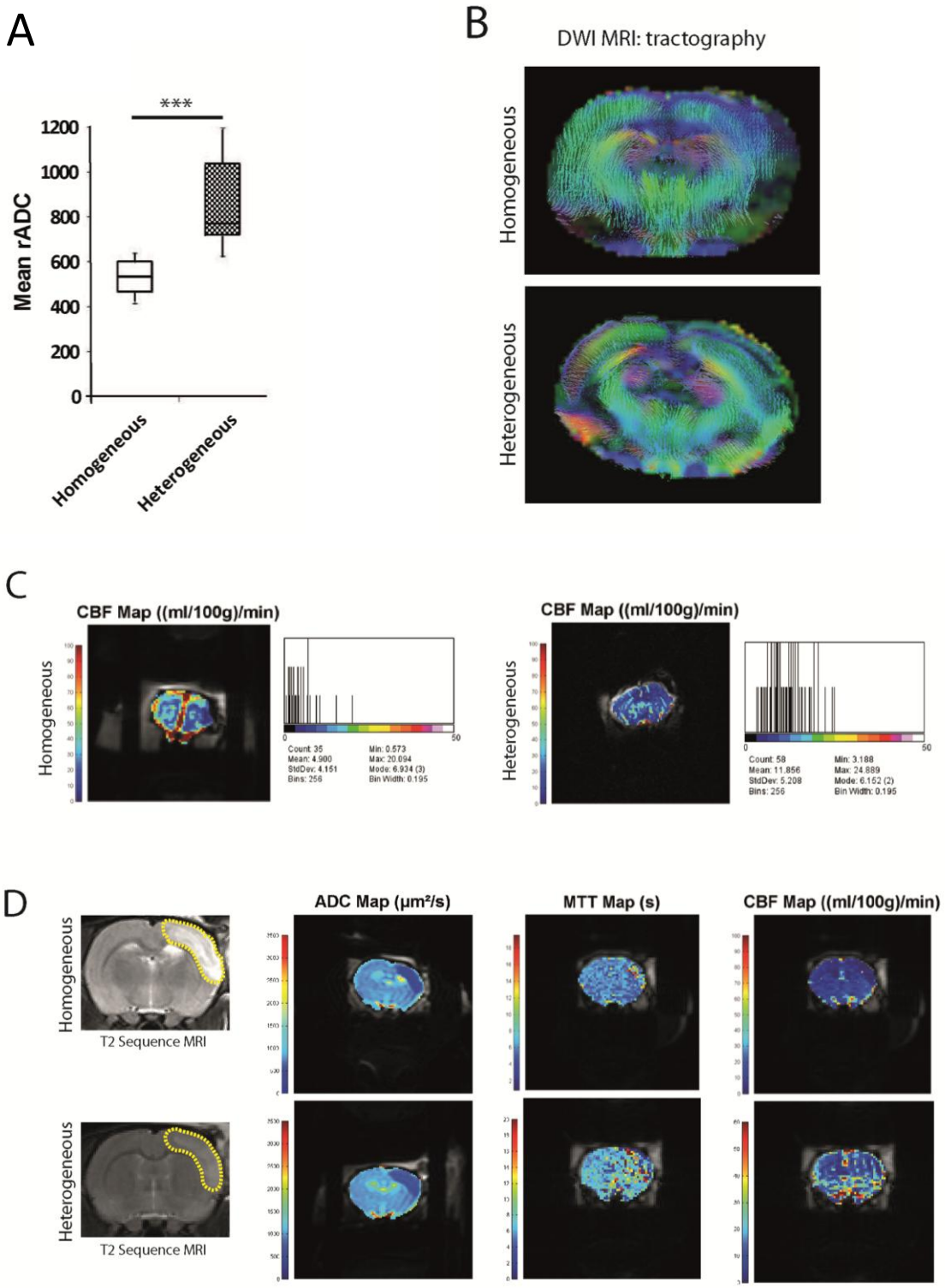
A
***
Mean rADC
1200
1000
800
600
400
200
0
Homogeneous
Heterogeneous
B
DWI MRI: tractography
Homogeneous
Heterogeneous
C
CBF Map ((ml/100g)/min)
Homogeneous
Count: 35
Mean: 4.900
StdDev: 4.151
Bins: 256
Min: 0.573
Max: 20.094
Mode: 6.934 (3)
Bin Width: 0.195
CBF Map ((ml/100g)/min)
Heterogeneous
Count: 58
Mean: 11.856
StdDev: 5.208
Bins: 256
Min: 3.188
Max: 24.889
Mode: 6.152 (2)
Bin Width: 0.195
D
Homogeneous
T2 Sequence MRI
ADC Map (μm²/s)
MTT Map (s)
CBF Map ((ml/100g)/min)
Heterogeneous
T2 Sequence MRI

Figure 4.3. *DWI AND PWI MRI OF HOMOGENEOUS AND HETEROGENEOUS PATTERN.*

A. Mean relative apparent diffusion coefficients of homogeneous and heterogeneous patterns. Heterogeneous patterns show significantly increased mean ADC values (left graph) and clustering of rADC in two different patterns (Box and whisker plots of mean rADC, right graph).

B. Tractography. Homogeneous pattern of intralesional ADC maps (upper image) showing more fiber disruption in MCA territory than heterogeneous pattern (lower image).

C. Perfusion MRI after pMCAO: Homogeneous and heterogeneous patterns. Homogeneous pattern showed less intralesional CBF (left image and graph) than heterogeneous pattern (right image and graph).

D. PWI/DWI mismatch. Homogeneous ADC patterns (upper images) show less mismatch area when compared to heterogeneous type (lower images).

REFERENCES

Albers, G.W., Thijs, V.N., Wechsler, L., Kemp, S., Schlaug, G., Skalabrin, E., Bammer, R., Kakuda, W., Lansberg, M.G., Shuaib, A., Coplin, W., Hamilton, S., Moseley, M., Marks, M.P., 2006. Magnetic resonance imaging profiles predict clinical response to early reperfusion: the diffusion and perfusion imaging evaluation for understanding stroke evolution (DEFUSE) study. Ann. Neurol. 60, 508–17.

Barber, P.A., 2013. Magnetic resonance imaging of ischemia viability thresholds and the neurovascular unit. Sensors (Basel). 13, 6981–7003.

Barlinn, K., Seibt, J., Engellandt, K., Gerber, J., Puetz, V., Kepplinger, J., Wunderlich, O., Pallesen, L.-P., Bodechtel, U., Koch, R., von Kummer, R., Dzialowski, I., 2014. Multimodal Computed Tomography Based Definition of Cerebral Imaging Profiles for Acute Stroke Reperfusion Therapy (CT-DEFINE): Results of a Prospective Observational Study. Clin. Neuroradiol.

Borich, M.R., Wadden, K.P., Boyd, L.A., 2012. Establishing the reproducibility of two approaches to quantify white matter tract integrity in stroke. Neuroimage 59, 2393–400.

Del Zoppo, G.J., Sharp, F.R., Heiss, W.-D., Albers, G.W., 2011. Heterogeneity in the penumbra. J. Cereb. Blood Flow Metab. 31, 1836–51.

Foley, L.M., Hitchens, T.K., Barbe, B., Zhang, F., Ho, C., Rao, G.R., Nemoto, E.M., 2010. Quantitative temporal profiles of penumbra and infarction during permanent middle cerebral artery occlusion in rats. Transl. Stroke Res. 1, 220–9.

Gutiérrez-Fernández, M., Rodríguez-Frutos, B., Alvarez-Grech, J., Vallejo-Cremades, M.T., Expósito-Alcaide, M., Merino, J., Roda, J.M., Díez-Tejedor, E., 2011. Functional recovery after hematic administration of allogenic mesenchymal stem cells in acute ischemic stroke in rats. Neuroscience 175, 394–405.

Gutiérrez-Fernández, M., Rodríguez-Frutos, B., Fuentes, B., Vallejo-Cremades, M.T., Alvarez-Grech, J., Expósito-Alcaide, M., Díez-Tejedor, E., 2012. CDP-choline treatment induces brain plasticity markers expression in experimental animal stroke. Neurochem. Int. 60, 310–7.

Honarmand, A., Beck, R., Soltanolkotabi, M., Ansari, S., Shaibani, A., Daruwalla, V., Hurley, M., 2014. E-005 Short-term Outcomes of Acute Ischemic Stroke Patients with MCA/ICA Occlusion Excluded for Intra-arterial Reperfusion Therapy. J. Neurointerv. Surg. 6 Suppl 1, A39–40.

Kakuda, W., Lansberg, M.G., Thijs, V.N., Kemp, S.M., Bammer, R., Wechsler, L.R., Moseley, M.E., Marks, M.P., Parks, M.P., Albers, G.W., 2008. Optimal definition for PWI/DWI mismatch in acute ischemic stroke patients. J. Cereb. Blood Flow Metab. 28, 887–91.

Kleinschnitz, C., Grund, H., Wingler, K., Armitage, M.E., Jones, E., Mittal, M., Barit, D., Schwarz, T., Geis, C., Kraft, P., Barthel, K., Schuhmann, M.K., Herrmann, A.M., Meuth, S.G., Stoll, G., Meurer, S., Schrewe, A., Becker, L., Gailus-Durner, V., Fuchs, H., Klopstock, T., de Angelis, M.H., Jandeleit-Dahm, K., Shah, A.M., Weissmann, N., Schmidt, H.H.H.W., 2010. Post-stroke inhibition of induced NADPH oxidase type 4 prevents oxidative stress and neurodegeneration. PLoS Biol. 8.

Koyama, T., Marumoto, K., Miyake, H., Domen, K., 2014. Relationship between Diffusion Tensor Fractional Anisotropy and Long-term Motor Outcome in Patients with Hemiparesis after Middle Cerebral Artery Infarction. J. Stroke Cerebrovasc. Dis. 23, 2397–404.

Lima, F.O., Furie, K.L., Silva, G.S., Lev, M.H., Camargo, E.C.S., Singhal, A.B., Harris, G.J., Halpern, E.F., Koroshetz, W.J., Smith, W.S., Nogueira, R.G., 2014. Prognosis of untreated strokes due to anterior circulation proximal intracranial arterial occlusions detected by use of computed tomography angiography. JAMA Neurol. 71, 151–7.

Malik, N., Hou, Q., Vagal, A., Patrie, J., Xin, W., Michel, P., Eskandari, A., Jovin, T., Wintermark, M., 2014. Demographic and clinical predictors of leptomeningeal collaterals in stroke patients. J. Stroke Cerebrovasc. Dis. 23, 2018–22.

Mishra, N.K., Albers, G.W., Davis, S.M., Donnan, G.A., Furlan, A.J., Hacke, W., Lees, K.R., 2010. Mismatch-based delayed thrombolysis: a meta-analysis. Stroke. 41, e25–33.

Moskowitz, M.A., Lo, E.H., Iadecola, C., 2010. The science of stroke: mechanisms in search of treatments. Neuron 67, 181–98.

Murakami, K., Kondo, T., Kawase, M., Li, Y., Sato, S., Chen, S.F., Chan, P.H., 1998. Mitochondrial susceptibility to oxidative stress exacerbates cerebral infarction that follows permanent focal cerebral ischemia in mutant mice with manganese superoxide dismutase deficiency. J. Neurosci. 18, 205–13.

Nagakane, Y., Christensen, S., Brekenfeld, C., Ma, H., Churilov, L., Parsons, M.W., Levi, C.R., Butcher, K.S., Peeters, A., Barber, P.A., Bladin, C.F., De Silva, D.A., Fink, J., Kimber, T.E., Schultz, D.W., Muir, K.W., Tress, B.M., Desmond, P.M., Davis, S.M., Donnan, G.A., 2011. EPITHET: Positive Result After Reanalysis Using Baseline Diffusion-Weighted Imaging/Perfusion-Weighted Imaging Co-Registration. Stroke. 42, 59–64.

Neumann-Haefelin, T., Wittsack, H.-J., Wenserski, F., Siebler, M., Seitz, R.J., Modder, U., Freund, H.-J., 1999. Diffusion- and Perfusion-Weighted MRI: The DWI/PWI Mismatch Region in Acute Stroke. Stroke 30, 1591–1597.

Ogata, T., Nagakane, Y., Christensen, S., Ma, H., Campbell, B.C. V, Churilov, L., Olivot, J.-M., Desmond, P.M., Albers, G.W., Davis, S.M., Donnan, G.A., 2011. A topographic study of the evolution of the MR DWI/PWI mismatch pattern and its clinical impact: a study by the EPITHET and DEFUSE Investigators. Stroke. 42, 1596–601.

Park, C.-H., Kou, N., Boudrias, M.-H., Playford, E.D., Ward, N.S., 2013. Assessing a standardised approach to measuring corticospinal integrity after stroke with DTI. NeuroImage. Clin. 2, 521–33.

Ramos-Cejudo, J., Gutiérrez-Fernández, M., Rodríguez-Frutos, B., Expósito Alcaide, M., Sánchez-Cabo, F., Dopazo, A., Díez-Tejedor, E., 2012. Spatial and temporal gene expression differences in core and periinfarct areas in experimental stroke: a microarray analysis. PLoS One 7, e52121.

Rivers, C.S., Wardlaw, J.M., Armitage, P.A., Bastin, M.E., Carpenter, T.K., Cvoro, V., Hand, P.J., Dennis, M.S., 2006. Persistent infarct hyperintensity on diffusion-weighted imaging late after stroke indicates heterogeneous, delayed, infarct evolution. Stroke. 37, 1418–23.

Sobesky, J., 2012. Refining the mismatch concept in acute stroke: lessons learned from PET and MRI. J. Cereb. Blood Flow Metab. 32, 1416–25.

Suma, T., Koshinaga, M., Fukushima, M., Kano, T., Katayama, Y., 2008. Effects of in situ administration of excitatory amino acid antagonists on rapid microglial and astroglial reactions in rat hippocampus following traumatic brain injury. Neurol. Res. 30, 420–9.

Swanson, R.A., Morton, M.T., Tsao-Wu, G., Savalos, R.A., Davidson, C., Sharp, F.R., 1990. A semiautomated method for measuring brain infarct volume. J. Cereb. Blood Flow Metab. 10, 290–3.

Thompson, J.W., Dave, K.R., Young, J.I., Perez-Pinzon, M.A., 2013. Ischemic preconditioning alters the epigenetic profile of the brain from ischemic intolerance to ischemic tolerance. Neurotherapeutics 10, 789–97.

Tsang, A., Stobbe, R.W., Asdaghi, N., Hussain, M.S., Bhagat, Y.A., Beaulieu, C., Emery, D., Butcher, K.S., 2011. Relationship between sodium intensity and perfusion deficits in acute ischemic stroke. J. Magn. Reson. Imaging 33, 41–7.

Van der Worp, H.B., Claus, S.P., Bär, P.R., Ramos, L.M., Algra, A., van Gijn, J., Kappelle, L.J., 2001. Reproducibility of measurements of cerebral infarct volume on CT scans. Stroke. 32, 424–30.

Yoo, A.J., Zaidat, O.O., Chaudhry, Z.A., Berkhemer, O.A., González, R.G., Goyal, M., Demchuk, A.M., Menon, B.K., Mualem, E., Ueda, D., Buell, H., Sit, S.P., Bose, A., 2014. Impact of pretreatment noncontrast CT Alberta Stroke Program Early CT Score on clinical outcome after intra-arterial stroke therapy. Stroke. 45, 746–51.

DISCUSSION

DISCUSSION

Summary

In the present study, we explored the effect of short-term exposure to H_2S after acute ischemia in an animal model of pMCAO. We hypothesized that hydrogen sulfide exposure after acute ischemic stroke modulates ischemic lesion either by an early protective effect or by promoting post-ischemic repair. To address our hypothesis we exposed rats to H2S after pMCAO and measured functional outcome and infarct size *in vivo* and *post-mortem*. We identified underlying markers of cytoprotection and repair. Finally, we compared brain imaging with immunohistochemical data to look for premature imaging features of ischemic tissue damage that may relate to functional outcome.

H_2S exposure after pMCAO improved functional outcome and decreased infarct size and cell death. H_2S may act very early in the ischemic process, since there were lower levels of acute injury-related markers at 24h without enhancement of repair-associated markers for vasculogenesis, angiogenesis or synaptogenesis at day 14. Significant benefit is likely to occur before major tissue damage ensues and includes modulation of NOX-4, a major generator of reactive oxygen species (ROS) and endothelial dysfunction, as well as vasomodulation of intralesional microcirculation since intralesional CBF assessed by PWI MRI improved in rats exposed to H_2S. Since H_2S limits brain damage after ischemic stroke, hydrogen sulfide donors may play a role as new drugs in the context of acute ischemic stroke.

A main goal in acute stroke treatment is reestablishing previous functional status or, if not possible, improve functional outcome. Therefore, endpoints in clinical and experimental stroke must provide prove of functional benefit. In the present study, we observed a better functional outcome in animals exposed to H_2S, both at 24h and day 14. This observation was in agreement with immunohistochemical data and in vivo imaging that showed improved intralesional tissue preservation and smaller lesion size in rats exposed to H_2S.

One of the reasons for failure in proving clinical benefit in previous research regarding neuroprotectors in the setting of acute ischemia is linked to the exclusive focus on neuron protection. We still nominate brain protection as neuroprotection but recent focus of translational stroke research centers on the complexity of interactions in the the neurovascular unit and the relevance of collateral circulation and regulation of microcirculation broadening the multiplicity of mechanisms involved in regaining homeostasis after acute ischemia (Kulik et al., 2008; Terasaki et al., 2013). Also several previously identified potential neuroprotectors only interfere with isolated paths of the complex ischemic pathophysiology and do not achieve clinical efficacy (Ferro and Dávalos, 2006; Moskowitz et al., 2010). H_2S possesses several mechanisms of action that intervene in the ischemic cascade. The role of H_2S in the regulation of microvascular tone is well established. It also acts as a sensor of oxygen in normal and ischemic brain environment and interferes directly with mitochondrial energy mechanism and ROS production. It influences the cascades of apoptosis and necrosis through pleotropic mechanisms at different time points and pathways of the ischemic cascade (Fu et al., 2012; Luo et al., 2013; Majid et al., 2013; Olson, 2013). This diversity of mechanisms contributes to the higher potential of H2S as a candidate with substantial efficacy in improving outcome after experimental and clinical stroke.

Another advantage of H_2S derives from being a gas and thus be able to interfere with intracellular mechanism without the need of active membrane transportation (Bannenberg and Vieira, 2009). Moreover, in the labile cellular energetic balance, quick adjustment between energy production and needs may contribute to very early protection before major tissue damage occurs(Szabó, 2007; Szabó et al., 2011).

In experimental research, the use of *in vivo* imaging to measure infarct size has the advantage of repetitive measurements over time whereas histological techniques only can be carried out once in each animal. However, immunohistochemical techniques are more precise in identifying distinctive parameters of cell death. Consequently, brain imaging in acute stroke benefits from being correlated with histological markers and parameters for cell death (Zille et al., 2012).

Since ischemia ultimately provokes cell death, the reduction of infarct size and a diminished cell death burden after a potential therapeutic intervention possibly indicates protection (Ferrer and Planas, 2003). In the present study, the group exposed to H_2S showed significantly less TUNEL-positive cells in the peri-infarct zone after pMCAO, indicative of less cell death, both at 24h and at day 14. As such, our results suggest strongly that H_2S modulates cell death after acute ischemic injury. This finding is additionally supported by a diminished infarct size at day 14 in our *post mortem* data.

The possibility of measuring *in vivo* the area of cell death defined as area of definitive necrosis was also approached. MRI DWI ADC maps, by measuring coefficients of attenuation, reflect preserved or destroyed tissue anatomy and may be used as a surrogate of maintenance of tissue structure *in vivo* (Rojas et al., 2006; Rosso et al., 2009; Zille et al., 2012). We found a better anatomical preservation of ischemic tissue in MRI DWI ADC maps in rats exposed to H_2S and an improved functional outcome was observed in functional motor scale and score. It is known from clinical studies that patient selection according to acute MRI profiles can differentiate subgroups of patients that benefit from early reperfusion from those that do not or those for whom reperfusion therapy can even be harmful (so called *futile* reperfusion) (Farr and Wegener, 2010). We measured perfusion through MRI PWI inside the ischemic lesion and found that CBF was higher in the treated group revealing improved tissue perfusion. Higher intralesional CBF was related to both better functional outcome and smaller infarct size in the treated group.

We further observed a pattern of intralesional ADC that consistently discriminated between better and worse functional outcome (heterogeneous *versus* homogeneous), probably by differentiating ischemic tissue fate and its potential for rescue. Since images were obtained by DWI permitting faster image acquisition and processing if compared to PWI, our results regarding ADC patterns represent a translational potential for acute stroke treatment in the clinical context through timely identification of patients with potential for tissue recovery. Observed heterogeneities in ADC coefficients inside the ischemic territory possibly represent previously

described areas of "mini-cores and mini-penumbras", a concept that refers to a central zone of hypoperfused territory at risk of infarction that shows a variable pattern of penumbra evolution with a heterogeneity in molecular and microvascular response (del Zoppo et al., 2011). Characteristic ADC patterns with heterogeneous and homogeneous lesions in ADC maps may consequently represent areas with a different potential for recovery, independently of its localization in the center or in the periphery of the ischemic lesion.

We compared further ADC hetero- and homogeneities with mismatch extension and found a correlation between larger mismatch size and presence of heterogeneous patterns in ADC map as suggested in previous studies (Mishra et al., 2010; Ogata et al., 2011; Sobesky, 2012).

The presence of a heterogeneous coefficient in ADC maps in the treated group related to better outcome highlights the possibility that these heterogeneities could be used as a surrogate imaging marker for outcome in the acute pretreatment stroke setting. This image marker of favorable outcome may prove beneficial in clinical decision making since homogeneous low acute diffusion coefficients inside ischemic lesion showed to be predictive for adverse progression from ischemia to necrosis, a situation where thrombolysis is futile and potentially harmful (Hussein et al., 2010; Oppenheim et al., 2001).

The hypothermic effect of H_2S was described and associated with its beneficial effects in the context of stroke, especially in protocols that included prolonged exposure times (Joseph et al., 2012). Nevertheless, hypothermia, when not externally induced, can be a consequence of decreased metabolism and not its cause (Szabó, 2007). H_2S is known to hold temperature-independent properties including arteriolar vasodilatation by activation of ATP-sensitive K+ channels of the smooth muscle cell membrane. Furthermore, H_2S is also able to contribute to the neutralization of excitocicity mediated by glutamate through increasing of glutathione in neurons by inducing astrocytes to incorporate more glutamate from the extracellular space (Leffler et al., 2011). Notwithstanding, vasodilatation is exactly the opposite of what we would expect if H_2S action would be exclusively related to hypothermia observed after

exposure (since external hypothermia induces vasoconstriction) (Faridar et al., 2011). Furthermore, H_2S also protects neurons from secondary neuronal injury by its anti-oxidant, anti-inflammatory and anti-apoptotic properties (Majid et al., 2013; Szabó et al., 2011).

Despite all benefit and advances that thrombolysis added to the therapy of acute ischemic stroke, it is also known that recovery from ischemia is not only a matter of reestablishing blood flow inside the occluded artery. The contribution of collateral circulation and microcirculation are key determinants of final tissue irrigation and ultimate tissue fate of reestablished homeostasis or definite infarct (Kulik et al., 2008; Shuaib et al., 2011). H_2S does not only interfere with tonus regulation of microcirculation via K^+- ATPase but is also an oxygen sensor both in the ischemic and the healthy brain (Fu et al., 2012; Olson et al., 2013; Zhao et al., 2001). As such, H_2S can potentially be used alone or in association with thrombolytic therapy.

In the present study, we observed less expression of ROS associated enzyme NOX-4 and less cell death together with a better intraregional perfusion and CBF in rats exposed to H_2S. Therefore, our results suggest that the beneficial effect observed after short-term exposure to H_2S might not be explained by the concomitant brief and mild hypothermia but more appropriately by other temperature-independent mechanisms. In our view, the induction of mild hypothermia lasting less than two hours after initial exposure, with a mean decrease in body temperature of merely 1.85ºC may represent an insufficient explanation for the observed benefit in the treated group. Our interpretation is underscored by the fact that we found effects of H_2S action like less expression of cell death and acute markers of necrosis including ROS production enzymes as soon as 24h and as late as day 14. Consequently, hypothermia may be rather the consequence of H_2S action than its cause. Furthermore, a decrease in body temperature of less than 2ºC as observed in the present experimental study would not require management inside highly selective and hardly available intensive care units beds, if our findings could be reproduced in clinical research and human stroke patients.

Previous studies of H_2S in the context of acute stroke used very long exposure times which represents a largely inconvenient aspect if it comes to acute stroke management in patients (Joseph et al., 2012). On the contrary, we observed in the present study that a much shorter exposure time was effective in reducing infarct size and enhancing recovery.

For many years, pretreatment predictors of good outcome have been looked for since they may be useful in clinical decision making together with current NIHSS and time elapsed since symptom onset. DWI MRI with ADC maps represents a technique that is able to differentiate tissue preservation or destruction *in vivo* by identifying distinctive apparent diffusion coefficients in the ischemic zone that depend on preservation of anatomical structure. We studied the hypothesis that different ADC patterns inside lesions in the same location, of the same size and with the same chronological evolution will reflect different fates regarding tissue ischemia and recovery. Our results showed that, although much less common in non-treated group, heterogeneities in ADC maps could still differentiate between more and less favorable outcome after experimental induction of acute ischemia. In summary, the presence of heterogeneities inside an ischemic lesion observed in MRI ADC maps predicts a better functional outcome in a pMCAO model of acute ischemic stroke.

Study limitations

We designed this study to fulfill the most recent recommendations for research in translational stroke.

Because of its high reproducibility, we chose a model of permanent focal brain ischemia including craniotomy and permanent artery ligation combined with temporary common carotid artery occlusion during one hour. As all rodent models for acute ischemic stroke manifest failures regarding volume of infarct area, besides other pitfalls (Gerriets et al., 2004), we minimized bias by using MRI as confirmation tool of complete ischemic induction in the MCA territory and absence of hemorrhagic

transformation. We considered this confirmation crucial since we intended to compare lesion size between treated animals and controls.

We randomized animals to groups and all procedures except surgery were performed in a blinded manner by using codes not known to observers to avoid bias regarding functional outcome, MRI image evaluation, and all other bench procedures. We gave detailed data on procedures to facilitate reproducibility. However, as the time window for administration of H_2S was limited to 3h after induction of ischemic stroke, no conclusions regarding effects outside this interval can be drawn. Exposure dosage of H_2S in the present study was the same for all animals and different dosages might produce distinct effects regarding outcome. Due to a limitation of study design and budget and due to the preliminary nature of our study, we were not able to include female and older animals or animals with co-morbidities in this study.

In the setting of an experimental study using rodents, we only can assess clinical outcome by evaluation of motor skills, not permitting evaluation concerning other signs and symptoms of ischemic stroke. As we used MRI at 24h as a confirmation tool of successful pMCAO, no bias can be attributable to surgical failure. We do not report long-term results of H_2S exposure as study design included comparison of *in vivo* and *post mortem* data in the acute setting at 24h and after day 14.

Implications and future research

Regarding future research, we already proposed a prospective observational clinical study to test if ADC heterogeneities inside the ischemic lesion in pre-treatment MRI represent a candidate for an imagiological pre-treatment marker of a favorable prognosis in acute stroke. After confirmation of the reproducibility of our data, we further propose a clinical trial with H_2S donors that are already available in clinical medicine for other purposes like memantine or diclofenac. Primary outcome measure should include poststroke functional dependency and death.

REFERENCES

Bannenberg, G.L., Vieira, H.L. a, 2009. Therapeutic applications of the gaseous mediators carbon monoxide and hydrogen sulfide. Expert Opin. Ther. Pat. 19, 663–82.

Del Zoppo, G.J., Sharp, F.R., Heiss, W.-D., Albers, G.W., 2011. Heterogeneity in the penumbra. J. Cereb. Blood Flow Metab. 31, 1836–51.

Faridar, A., Bershad, E.M., Emiru, T., Iaizzo, P.A., Suarez, J.I., Divani, A.A., 2011. Therapeutic Hypothermia in Stroke and Traumatic Brain Injury. Front. Neurol.

Farr, T.D., Wegener, S., 2010. Use of magnetic resonance imaging to predict outcome after stroke: a review of experimental and Despite promising results in preclinical evidence. J. Cereb. Blood Flow Metab. 30, 703–17.

Ferrer, I., Planas, A.M., 2003. Signaling of cell death and cell survival following focal cerebral ischemia: life and death struggle in the penumbra. J. Neuropathol. Exp. Neurol. 62, 329–39.

Ferro, J.M., Dávalos, A., 2006. Other neuroprotective therapies on trial in acute stroke. Cerebrovasc. Dis. 21 Suppl 2, 127–30.

Fu, M., Zhang, W., Wu, L., Yang, G., Li, H., Wang, R., 2012. Hydrogen sulfide (H2S) metabolism in mitochondria and its regulatory role in energy production. Proc. Natl. Acad. Sci. U. S. A. 109, 2943–8.

Gerriets, T., Stolz, E., Walberer, M., Müller, C., Rottger, C., Kluge, A., Kaps, M., Fisher, M., Bachmann, G., 2004. Complications and pitfalls in rat stroke models for middle cerebral artery occlusion: a comparison between the suture and the macrosphere model using magnetic resonance angiography. Stroke. 35, 2372–7.

Hussein, H.M., Georgiadis, A.L., Vazquez, G., Miley, J.T., Memon, M.Z., Mohammad, Y.M., Christoforidis, G.A., Tariq, N., Qureshi, A.I., 2010. Occurrence and predictors of futile recanalization following endovascular treatment among patients with acute ischemic stroke: a multicenter study. AJNR. Am. J. Neuroradiol. 31, 454–8.

Joseph, C., Buga, A.-M., Vintilescu, R., Balseanu, A.T., Moldovan, M., Junker, H., Walker, L., Lotze, M., Popa-Wagner, A., 2012. Prolonged gaseous hypothermia prevents the upregulation of phagocytosis-specific protein annexin 1 and causes low-amplitude EEG activity in the aged rat brain after cerebral ischemia. J. Cereb. Blood Flow Metab. 32, 1632–42.

Kulik, T., Kusano, Y., Aronhime, S., Sandler, A.L., Winn, H.R., 2008. Regulation of cerebral vasculature in normal and ischemic brain. Neuropharmacology 55, 281–8.

Leffler, C.W., Parfenova, H., Basuroy, S., Jaggar, J.H., Umstot, E.S., Fedinec, A.L., 2011. Hydrogen sulfide and cerebral microvascular tone in newborn pigs. Am. J. Physiol. Heart Circ. Physiol. 300, H440–7.

Luo, Y., Yang, X., Zhao, S., Wei, C., Yin, Y., Liu, T., Jiang, S., Xie, J., Wan, X., Mao, M., Wu, J., 2013. Hydrogen Sulfide Prevents OGD/R-induced Apoptosis via Improving Mitochondrial Dysfunction and Suppressing an ROS-mediated Caspase-3 Pathway in Cortical Neurons. Neurochem. Int.

Majid, A.S.A., Majid, A.M.S.A., Yin, Z.Q., Ji, D., 2013. Slow Regulated Release of H2S Inhibits Oxidative Stress Induced Cell Death by Influencing Certain Key Signaling Molecules. Neurochem. Res. 38, 1375–93.

Mishra, N.K., Albers, G.W., Davis, S.M., Donnan, G.A., Furlan, A.J., Hacke, W., Lees, K.R., 2010. Mismatch-based delayed thrombolysis: a meta-analysis. Stroke. 41, e25–33.

Moskowitz, M.A., Lo, E.H., Iadecola, C., 2010. The science of stroke: mechanisms in search of treatments. Neuron 67, 181–98.

Ogata, T., Nagakane, Y., Christensen, S., Ma, H., Campbell, B.C. V, Churilov, L., Olivot, J.-M., Desmond, P.M., Albers, G.W., Davis, S.M., Donnan, G.A., 2011. A topographic study of the evolution of the MR DWI/PWI mismatch pattern and its clinical impact: a study by the EPITHET and DEFUSE Investigators. Stroke. 42, 1596–601.

Olson, K.R., 2013. Hydrogen sulfide as an oxygen sensor. Clin. Chem. Lab. Med. 51, 623–32.

Olson, K.R., Deleon, E.R., Gao, Y., Hurley, K., Sadauskas, V., Batz, C., Stoy, G.F., 2013. Thiosulfate: a Readily Accessible Source of Hydrogen Sulfide in Oxygen Sensing. Am. J. Physiol. Regul. Integr. Comp. Physiol.

Oppenheim, C., Grandin, C., Samson, Y., Smith, A., Duprez, T., Marsault, C., Cosnard, G., 2001. Is there an apparent diffusion coefficient threshold in predicting tissue viability in hyperacute stroke? Stroke. 32, 2486–91.

Rojas, S., Martín, A., Justicia, C., Falcón, C., Bargalló, N., Chamorro, A., Planas, A.M., 2006. Modest MRI signal intensity changes precede delayed cortical necrosis after transient focal ischemia in the rat. Stroke. 37, 1525–32.

Rosso, C., Hevia-Montiel, N., Deltour, S., Bardinet, E., Dormont, D., Crozier, S., Baillet, S., Samson, Y., 2009. Prediction of infarct growth based on apparent diffusion coefficients: penumbral assessment without intravenous contrast material. Radiology 250, 184–92.

Shuaib, A., Butcher, K., Mohammad, A.A., Saqqur, M., Liebeskind, D.S., 2011. Collateral blood vessels in acute ischaemic stroke: a potential therapeutic target. Lancet Neurol. 10, 909–21.

Sobesky, J., 2012. Refining the mismatch concept in acute stroke: lessons learned from PET and MRI. J. Cereb. Blood Flow Metab. 32, 1416–25.

Szabó, C., 2007. Hydrogen sulphide and its therapeutic potential. Nat. Rev. Drug Discov. 6, 917–35.

Szabó, G., Veres, G., Radovits, T., Gero, D., Módis, K., Miesel-Gröschel, C., Horkay, F., Karck, M., Szabó, C., 2011. Cardioprotective effects of hydrogen sulfide. Nitric Oxide 25, 201–10.

Terasaki, Y., Liu, Y., Hayakawa, K., Pham, L.-D., Lo, E.H., Ji, X., Arai, K., 2013. Mechanisms of Neurovascular Dysfunction in Acute Ischemic Brain. Curr. Med. Chem.

Zhao, W., Zhang, J., Lu, Y., Wang, R., 2001. The vasorelaxant effect of H(2)S as a novel endogenous gaseous K(ATP) channel opener. EMBO J. 20, 6008–16.

Zille, M., Farr, T.D., Przesdzing, I., Müller, J., Sommer, C., Dirnagl, U., Wunder, A., 2012. Visualizing cell death in experimental focal cerebral ischemia: promises, problems, and perspectives. J. Cereb. Blood Flow Metab. 32, 213–31.

CONCLUSION

CONCLUSION

In our pMCAO model of ischemic stroke, early exposure to hydrogen sulfide after focal brain ischemia improved functional outcome and decreased infarct size and cell death through processes that involve modulation of NOX-4, a major enzyme generator of reactive oxygen species. Regarding brain imaging, perfusion MRI in rats exposed to H_2S revealed improved cerebral blood flow, while diffusion MRI showed spots of heterogeneity inside ischemic lesions in ADC maps, including central regions. H_2S probably acts very early after administration, since lower levels of acute injury-related markers were present at 24h, without increase of repair-associated markers for vasculogenesis, angiogenesis or synaptogenesis at day 14. Significant benefit is likely to occur before major tissue damage has taken place. Since H_2S donors exist already for other clinical purposes, clinical trials in a translational context deserve consideration.

Original Paper

Cerebrovascular Diseases

Cerebrovasc Dis 2015;39:293–301
DOI: 10.1159/000381727

Received: December 30, 2014
Accepted: March 16, 2015
Published online: April 21, 2015

Intralesional Patterns of MRI ADC Maps Predict Outcome in Experimental Stroke

Isabel Lestro Henriques[a–c] María Gutiérrez-Fernández[a] Berta Rodríguez-Frutos[a] Jaime Ramos-Cejudo[a] Laura Otero-Ortega[a] Teresa Navarro Hernanz[d] Sebastián Cerdán[d] José M. Ferro[e] Exuperio Díez-Tejedor[a]

[a]Department of Neurology and Stroke Centre, Neuroscience and Cerebrovascular Research Laboratory, La Paz University Hospital, Neuroscience Area of IdiPAZ (Health Research Institute), Autónoma University of Madrid, Madrid, Spain; [b]Faculty of Medicine, University of Lisbon, and [c]Champalimaud Neuroscience Programme, Champalimaud Center for the Unknown, INDP2007, Lisbon, Portugal; [d]Laboratory for Imaging and Spectroscopy by Magnetic Resonance LISMAR, Institute of Biomedical Research Alberto Sols, CSIC-UAM, Madrid, Spain; [e]Department of Neurosciences, Hospital de Santa Maria, University of Lisbon, Lisbon, Portugal

Key Words

Magnetic resonance imaging · MRI · ADC maps · Ischemic stroke · Stroke model · Functional outcome · Intralesional heterogeneity

Abstract

Background: After acute ischemia, the tissue that is at risk of infarction can be detected by perfusion-weighted imaging/diffusion-weighted imaging (PWI/DWI) mismatch but the time that is needed to process PWI limits its use. As DWI is highly sensitive to acute ischemic tissue damage, we hypothesized that different ADC patterns represent areas with a different potential for recovery. ***Methods:*** In a model of permanent middle cerebral artery occlusion (pMCAO), Sprague-Dawley rats were randomly distributed to sham surgery and pMCAO. We further separated the pMCAO group according to intralesional ADC pattern (homogeneous or heterogeneous). At 24 h after ischemia induction, we analyzed lesion size, functional outcome, cell death expression, and brain protection markers including ROS enzyme NOX-4. MRI included DWI (ADC maps), DTI (tractography), and PWI (CBF, CBV and MTT). ***Results:*** The lesion size was similar in pMCAO rats. Animals with a heterogeneous pattern in ADC maps showed better functional outcome in Rotarod test (p = 0.032), less expression of cell death (p = 0.014) and NOX-4 (p = 0.0063), higher intralesional CBF (p = 0.0026) and larger PWI/DWI mismatch (p = 0.007). ***Conclusions:*** In a rodent model for ischemic stroke, intralesional heterogeneity in ADC maps was related to better functional outcome in lesions of similar size and interval after pMCAO. DWI ADC maps may assist in the early identification of ischemic tissue with an increased potential for recovery as higher expression of acute protection markers, lower expression of cell death, increased PWI/DWI mismatch, and higher intralesional CBF were present in animals with a heterogeneous ADC pattern.

Introduction

After acute ischemia, the viable tissue that is at risk of infarction can be detected by perfusion-weighted imaging/diffusion-weighted imaging (PWI/DWI) mismatch but

I.L.H. and M.G.-F. contributed equally to this work.

Prof. Exuperio Díez-Tejedor, MD, PhD, FAHA, FESO
Department of Neurology and Stroke Center, Neuroscience and Cerebrovascular Research Laboratory, La Paz University Hospital, IdiPAZ Health Research Institute
Autónoma University of Madrid Paseo de la Castellana 261 ES–28046 Madrid (Spain)
E-Mail exuperio.diez@salud.madrid.org

the time that is needed to process PWI limits its use in the acute clinical setting. However, acute ischemic stroke can produce different types of intralesional patterns in DWI [1]. In ADC maps, those patterns can be either homogeneous or patchy and heterogeneous. Since DWI is highly sensitive to tissue damage, we hypothesized that these two patterns in ADC maps represent ischemic areas with a different potential for recovery after acute ischemia and consequently predict functional outcome after acute ischemia.

In this study, we evaluated the correlation between different intralesional patterns in MRI ADC maps, functional outcome, and immunohistochemical markers of tissue damage to further confirm that different patterns are associated to brain tissue preservation despite the same infarct size and interval after permanent middle cerebral artery occlusion (pMCAO).

Material and Methods

Ethical Committee, Animal Rights

Procedures were carried out at the Cerebrovascular and Neuroscience Research Laboratory at La Paz University Hospital, and at the Animal Imaging Department (SIERMAC®), Universidad Autónoma de Madrid, Spain. Experiments were performed in compliance with the Ethical Committee for the Care and Use of Animals in Research rules following the International Guidelines for the Care and Use of Laboratory Animals (Royal Decree (RD)1201/2005 and European Directive 2010/63/UE). The experiments were designed to use the smallest number of animals possible and to minimize their suffering in accordance with the ethical standards of the Helsinki Declaration of 1975. We included post-surgery analgesia for all groups. All rats (sham and pMCAO) had a right cranial suture of the same dimension. Group allocation codes were used to keep observation blinded to group allocation while collecting functional data and performing molecular and histological procedures.

Subject Selection Criteria and Data Collection Tools

Adult male Sprague-Dawley rats, 10 to 12 weeks old, with an average body weight of 250 to 320 g (Charles River® S.L., Barcelona, Spain), were housed with free access to standard rat chow and water. Room temperature was maintained at 21 ± 2°C, with a relative humidity of 45 ± 15% and a light/dark cycle of 12/12 h (7:00–19:00 h/19:00–7:00 h). Rats were randomly assigned to the following groups: sham surgery (craniotomy) and permanent middle cerebral artery occlusion (pMCAO). After 24 h, T2-weighted MRI was performed in order to confirm complete MCAO and equal infarct size in animals submitted to pMCAO. Rats submitted to pMCAO were then further divided into 2 groups according to the result of the DWI MRI ADC maps: group 1 if heterogeneities were present inside the ischemic lesion in more than 2/3 of the ADC maps (subgroup 'heterogeneous'), and group 2 if DWI showed a homogenous lesion in ADC maps (subgroup 'homogeneous'). The number of rats submitted to surgery was progressively increased until a minimum of 12 animals was reached in both groups. Three rats were excluded from the study because of incomplete ischemia in the MCA territory.

We defined ADC patterns according to qualitative visual criteria: heterogeneous pattern if more than 2/3 of the ischemic area was heterogeneous (patchy) and homogeneous pattern for the remaining. Later on, in order to confirm this point, we designed a quantitative method based on a histogram analysis categorization. Briefly, we delineated the lesion zone on each slice of ADC maps. Then, we adjusted the levels from 0 to 3,000 $\mu m^2/s$ (standard values of ADC maps from rat brain). All images visually considered homogeneous showed differences in ADC values (between minimum to maximum) below 300 $\mu m^2/s$. All heterogeneous images showed differences above 300 $\mu m^2/s$. This value was determinated as cut-off for this study using the pMCAO experimental model. Quantitative assessment using the apparent diffusion coefficient showed that there were no heterogeneous patterns with an ADC value below 630.

Experimental Procedures

A surgical model of pMCAO was used as previously described elsewhere [2] and physiological parameters were recorded throughout the procedure (online suppl. material; for all online suppl. material, see www.karger.com/doi/10.1159/000381727).

Functional Evaluation Scales

Functional evaluation scales were performed before procedures at baseline and at 24 h. All rats were evaluated using a variant of the Rogers scale and the Rotarod performance test™ (accelerating course of 4–40 rpm) as previously described [3].

Magnetic Resonance Imaging

The extension of the ischemic lesions was analyzed using T2-weighted MRI. We used diffusion-weighted imaging (DWI) including apparent diffusion coefficient (ADC) maps and tractography, as well as perfusion-weighted imaging (PWI) with determination of cerebral blood flow (CBF), cerebral blood volume (CBV), and mean transient time (MTT). Relative ADC values were calculated in comparison with the corresponding contralateral region (online suppl. material).

Statistical Analysis

Functional evaluation scores, lesion size, cell death, and protein levels are described as the mean and standard error of the mean (SEM) and presented as box and whisker plots. Data were analyzed using the Student's t-test or the non-parametric Mann-Whitney test if data followed a non-normal distribution in the Shapiro-Wilk test. Values of $p < 0.05$ were considered significant at a 95% confidence level.

Results

Physiological Parameters

Glycemia was assessed immediately after starting the procedure and during surgery and it was found to have similar values in all groups. Rectal temperature was significantly lower after induction of anesthesia in all groups ($p < 0.05$) and maintained at 37 ± 0.5°C. Mean $PaCO_2$ and PaO_2 were not significantly different before and after surgical proceedings.

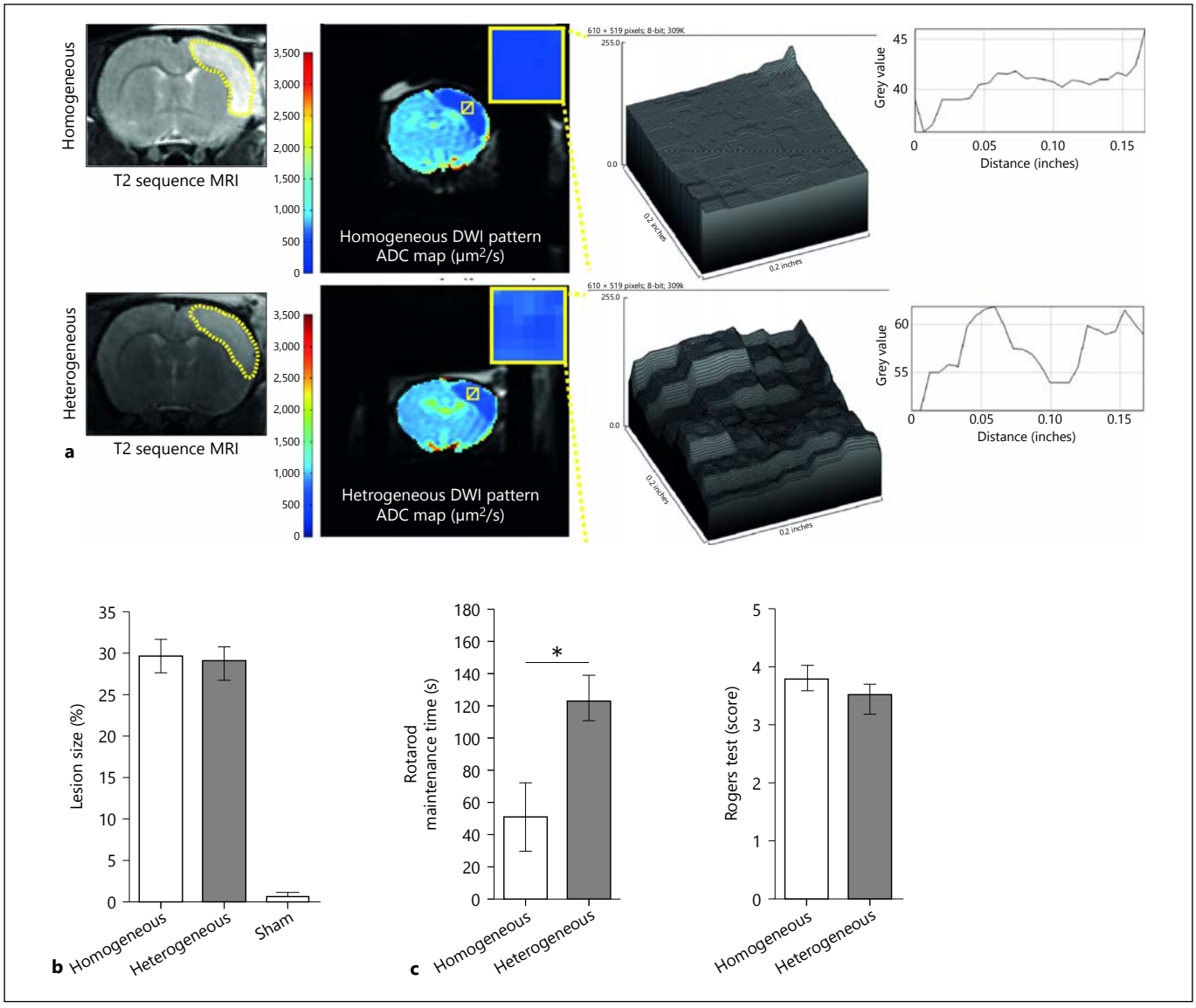

Fig. 1. Lesion size and functional outcome in two different intralesional patterns of MRI ADC maps after permanent MCA occlusion. **a** T2 sequence MRI and DWI ADC maps of intralesional homogeneous (upper images and graphs) and heterogeneous patterns (lower images and graphs). Heterogeneous and homogeneous showed the same infarct size (left images), but heterogeneous pattern showed an increased range of ADC coefficients (right). **b** Lesion size: homogeneous pMCAO, heterogeneous pMCAO and sham groups. For the same interval after stroke induction, lesion size was the same in rats with pMCAO and different ADC patterns. **c** Functional outcome in homogeneous and heterogeneous ADC patterns: maintenance time (s) in Rotarod test is significantly superior in heterogeneous ADC patterns (left graph). No difference observed with Rogers test (right graph).

Same Lesion Size and Time after pMCAO: Homogeneous versus Heterogeneous ADC Infarct Pattern

At 24 h after pMCAO, the lesion size measured by T2-weighted MRI did not differ between groups (heterogeneous vs. homogeneous: 28.99 ± 2.27 vs. 29.55 ± 2.72, p = 0.418). Sham animals showed no ischemic lesion (fig. 1a, b).

Better Functional Outcome in Heterogeneous ADC Pattern

Functional assessment was performed before the procedure and at 24 h. At baseline, Rogers modified scale was zero for all animals and the latency to fall in the Rotarod test was >120 s. Sham-operated animals did not show any functional deficit at 24 h. A better functional outcome was

observed at 24 h in animals with a heterogeneous ADC pattern when compared to animals with a homogeneous pattern regarding the latency to fall in the Rotarod test (110.37 ± 31.43 vs. 51.25 ± 30.87, p = 0.032). No significant differences were observed in the Rogers test (3.43 ± 0.48 vs. 3.57 ± 0.41, p = 0.158) (fig. 1c).

Less Cell Death Expression after pMCAO in Heterogeneous ADC Pattern

Animals with a heterogeneous ADC pattern expressed significantly less TUNEL positive cells at 24 h, when compared to animals showing homogeneous ADC pattern (56.25 ± 13.75 vs. 170.5 ± 61.0, p = 0.014) (fig. 2a). Sham-operated rats did not show TUNEL positive cells.

Brain Protection Associated Markers: Homogeneous versus Heterogeneous ADC Pattern

NOX-4 showed a significantly lower expression in animals with a heterogeneous intralesional ADC pattern when compared to homogeneous pattern (2.1 ± 0.367 vs. 4.693 ± 1.31, p = 0.0063) (fig. 2b, c). The levels of SOD2 at 24 h were significantly higher in animals with a heterogeneous intralesional ADC type when compared to animals with a homogeneous pattern (4.84 ± 1.049 vs. 2.906 ± 0.368, p = 0.0039) (fig. 2b middle, c). At 24 h, the group with a heterogeneous intralesional ADC pattern showed a decreased expression of GFAP when compared to animals with a homogeneous pattern; however, the difference was not significant (2.52 ± 0.53 vs. 4.04 ± 0.71, p = 0.068) (fig. 2b below, c).

Apparent Diffusion Coefficients and Tractographies: Homogeneous versus Heterogeneous ADC Pattern

Apparent diffusion coefficients differed significantly between the two ADC patterns and animals with a heterogeneous pattern showed higher values (844.87 ± 155.402 vs. 537.33 ± 61.15, p = 0.0013). Furthermore, the lowest coefficient was observed in a homogeneous lesion and the highest value in a heterogeneous lesion. No heterogeneous lesion type was observed below 630. Additionally, the SEM of apparently diffusion coefficients was much larger in heterogeneous lesions (155.4 vs. 61.15) (fig. 3a). DWI tractographies showed also a more consistent preservation in the fiber reconstruction model of ischemic areas in the heterogeneous lesion type (fig. 3b).

Higher Intralesional Cerebral Blood Flow in Heterogeneous ADC Pattern

CBF inside ischemic lesions differed between the two patterns. Animals with a heterogeneous pattern showed the higher values for CBF if compared to animals with homogeneous ADC patterns (79.66 ± 32.2 vs. 55.43 ± 16.0, p = 0.0026). The lowest value was observed in a homogeneous lesion (14 ml/100 g/min) and the highest in a heterogeneous lesion (218 ml/100 g/min) (fig. 3c).

Larger PWI/DWI Mismatch in Heterogeneous ADC Pattern

We calculated the PWI/DWI mismatch using the standard volumetric model (mismatch = %PWI – %DWI volume) measured in each slice that showed the lesion and selected the slice that had the largest lesion size. The observed mismatch was higher in the heterogeneous pattern when compared to animals with homogeneous lesions (7.72 ± 1.94 vs. 2.35 ± 1.45, p = 0.007) (fig. 3d).

Discussion

We used a rodent model of pMCAO and identified distinct intralesional patterns in MRI ADC maps that were associated with different functional outcome in lesions of similar size and the same ischemic duration. Animals with heterogeneous patterns in ADC maps showed a better outcome after acute ischemic infarction when compared to animals with the homogeneous type. Intralesional heterogeneity was also related to less expression of cell death and markers of brain tissue protection. When assessing PWI/DWI mismatch, heterogeneous lesions showed a larger mismatch, purportedly related to a higher probability of recovery of ischemic penumbra and without progression to definitive infarction [4–6].

Clinical studies demonstrated inconsistency regarding prognosis in patients with lesions of the same size, arterial territory and time after symptoms onset including complete MCA occlusion [7–9]. Several explanations for this diversity in functional outcome have been brought forward and include individual variability in collateral circulation, preconditioning, and microcirculation response after ischemic insult [10, 11]. However, the relation between heterogeneous patterns in ADC maps and functional outcome has not yet been addressed in the clinical setting. In our experimental model, rats with the same lesion size, territory, and time after ischemic induction, showed also that kind of diversity, with the heterogeneous pattern of ADC maps presenting a better functional outcome. Consequently, patterns of ADC maps indicated different functional prognoses. As MRI DWI sequences better reflect anatomical tissue structure [12], they can be considered a bridge between basic science and

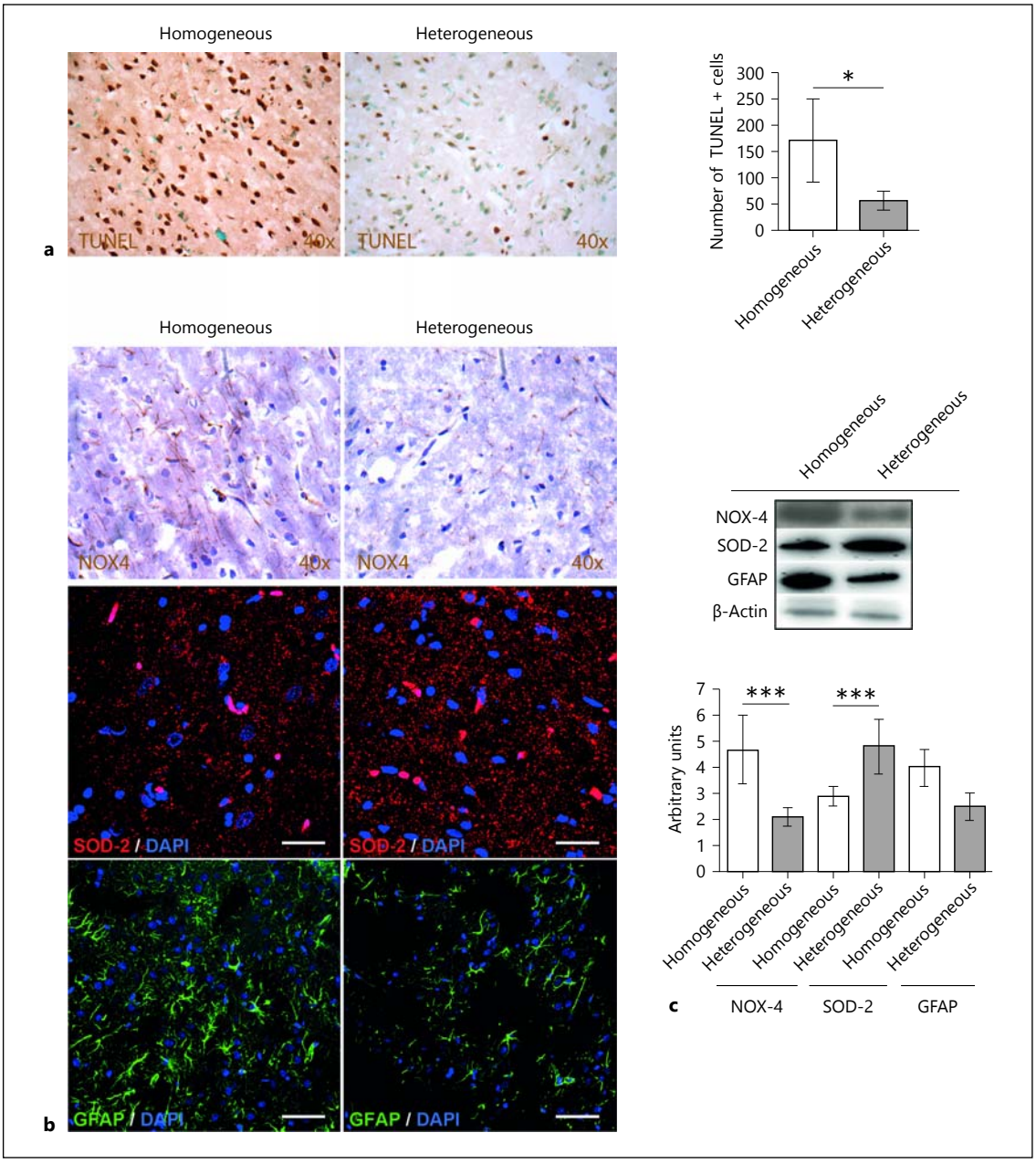

Fig. 2. Cell death and immunohistochemical markers at 24 h after pMCAO in two different intralesional patterns of MRI ADC maps. **a** Cell death evaluation by TUNEL: less cell death was observed in heterogeneous ADC pattern. **b** Immunohistochemical of NOX-4, SOD-2 and GFAP markers at 24 h after pMCAO. Less expression of NOX-4 was observed in the animals showing heterogeneous pattern (upper images). Less expression of SOD-2 was observed in animals showing homogeneous pattern (middle images). Lower levels of GFAP were observed in animals with heterogeneous patterns (lower images). **c** Western blot quantification of NOX-4, SOD-2 and GFAP markers at 24 h after pMCAO.

Fig. 3. DWI and PWI MRI of homogeneous and heterogeneous ADC map patterns. **a** Mean relative apparent diffusion coefficients of homogeneous and heterogeneous lesion type: clustering of rADC values in two different patterns, with no heterogeneous lesion type below 630. Heterogeneous lesions showed significantly increased mean rADC values. **b** Tractography. Homogeneous pattern of intralesional ADC maps (upper image) showing more fiber disruption in MCA territory than heterogeneous pattern (lower image). **c** Perfusion MRI after pMCAO: Homogeneous and heterogeneous patterns. Homogeneous pattern showed less intralesional CBF (left image and graph) than heterogeneous pattern (right image and graph). **d** PWI/DWI mismatch. Homogeneous ADC patterns (upper images) showed less mismatch area when compared to heterogeneous type (lower images).

(*For figure see next page.*)

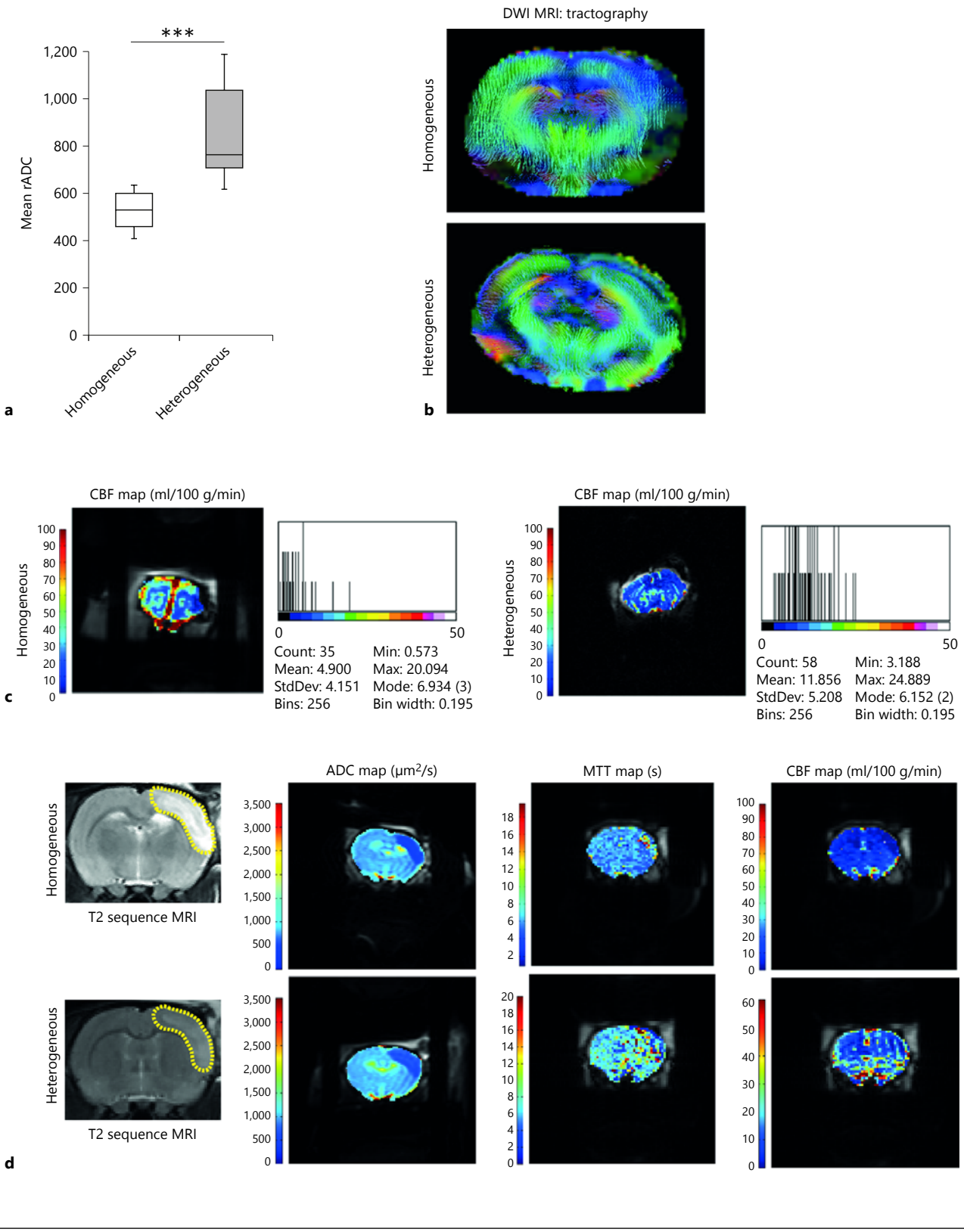

3

Color version available online

clinical assessment through high resolution anatomical delineation of disease at an ionic and molecular level [13]. As our findings support improved preservation of the intralesional region when ADC maps show a heterogeneous pattern in lesions of MCA territory and higher diffusion coefficients that represent a surrogate measure of better anatomical tissue preservation, a reduced risk of definite infarction can be assumed.

The introduction of mismatch measurement as inclusion criteria for reperfusion in clinical trials included significant differences in the definition of mismatch and a rather arbitrary volumetric difference of 20% between PWI and DWI that still lacks validation as a threshold for stratifying patients or as a surrogate measure of penumbra [5, 13]. PWI also requires contrast administration and time-consuming processing, losing valuable time before reperfusion [14, 15]. In this study, we were able to show that the interpretation of distinct intralesional MRI DWI ADC patterns in lesions of the same size might offer similar pretreatment information.

We also observed that animals with heterogeneous intralesional ADC patterns showed higher CBF with larger variations inside the ischemic lesion, along with enhanced functional outcome. Additionally, tractographies showed better fiber preservation in the heterogeneous type. In the clinical setting, tractography has also been used to show structural integrity of the corticospinal tract and was related to recovery [16, 17].

As outlined earlier, DWI is the MRI sequence that more consistently reflects ionic and molecular tissue changes since the effect in the Brownian movement of water molecules is changed in the presence of abnormal anatomical features [18]. In previous studies, our group described gene expression associated with trophic factors and CNS development within the lesion core at 24 h after pMCAO, suggesting the existence of surviving areas inside the ischemic core [19]. Our findings support the argument that the central region of the ischemic territory is not inexorably dead or irreversibly damaged. In this study, we could show differences in the expression of cell death related to different patterns in ADC maps with significantly less expression in the group with a heterogeneous pattern. The present data further emphasize our previous findings and show additionally a relation between ADC patterns and tissue preservation that requires further exploration.

Oxidative stress causes tissue damage after acute brain ischemia with overexpression of ROS above physiological levels [20, 21]. We analyzed the expression of major ROS producing enzyme NOX-4 in both groups of ADC patterns and observed significantly reduced expression of NOX-4 in the heterogeneous pattern. We also found a higher expression of SOD2, a major scavenger of mitochondrial superoxide, in the group with a heterogeneous ADC pattern. SOD2 is synthesized after brain infarction and tissue levels are generally related to lesion size. However, since we compare lesions with equal size, higher expression of SOD2, together with less expression of ROS producing enzyme NOX-4, is indicative of less use of SOD2 for neutralization of mitochondrial superoxide [22] and, consequently, less oxidative stress and definite brain lesion in the heterogeneous type. Additionally, we observed a smaller expression of GFAP in the group with a heterogeneous pattern, albeit not significant. Since after an acute brain lesion, astrocytes occupy the empty space left by phagocytosis in order to maintain tissue structure, reactive gliosis is part of the healing process being massive gliosis related to worse outcome [23]. Consequently, the reduced expression of GFAP in animals with the heterogeneous pattern may indicate a reduced ischemic injury.

Although not addressing early reperfusion directly, we observed a DWI MRI pattern that distinguishes functional outcome. We observed increased PWI/DWI mismatch in ischemic MCA lesions with a heterogeneous pattern indicating a higher potential for reversibility in these animals. On the other hand, in animals with a homogeneous pattern, CBF was reduced and eventually it reached a value as low as 6–15 ml/100 g/min. Despite the variability in CBF thresholds in different brain locations or age groups, levels as low as 6–15 ml/100 g/min correspond to thresholds of biochemical biomarkers of protein synthesis inhibition, preference for aerobic glycolysis, neurotransmitter release, impaired energy metabolism and terminal depolarization with potassium influx. We also observed coherence in our data concerning functional outcome and biochemical markers (with less expression of cell death and less expression of ROS markers) favoring the group with a heterogeneous pattern. Possibly, the homogeneous ADC pattern indicates irreversible brain damage where reperfusion might be futile or even dangerous. However, research in the clinical setting is necessary to confirm our experimental data and validate the usefulness of intralesional ADC patterns to predict outcome and identify patients that may benefit from reperfusion.

Finally, it would be desirable to identify a quantitative threshold that easily distinguishes heterogeneous from homogeneous patterns and consequently subjects with a high potential for recovery from subjects with an increased risk for irreversible infarction. In our study, no heterogeneous samples were observed below 630 and

only a single homogeneous sample showed an ADC value above this threshold (643). If confirmed in the clinical context, the determination of a similar threshold may prove useful in identifying patients with irreversible ischemia without indication for thrombolysis. In this context, the results of this study represent a promising tool in pretreatment decisions in the acute stroke setting.

Study Limitations and Potential Bias

As shown by our experimental data in a pMCAO model of ischemic stroke, the heterogeneity in the coefficients of apparent diffusion inside the ischemic lesion represents areas with a different potential for recovery. Nevertheless, there is significant variability in ADC values depending on MRI apparatus, coil systems, imagers, or employed field strengths that should be taken into account when analyzing data from different MRI equipment. We used relative ADC values because they are more suitable for evaluating diffusion abnormalities than absolute values.

We used a model of permanent MCAO with high reproducibility confirmed by equal lesion size in both the heterogeneous and homogeneous groups and interval after stroke onset was controlled for. However, our experimental model did not include vascular risk factors, older age, or the female gender. Also, variability in preconditioning, individual variability in collateral circulation, or intracranial pressure variations that may interfere with microcirculation are difficult to assess in an experimental model and may have impact on results.

Conclusions

Intralesional patterns of MRI ADC maps in an experimental model of ischemic stroke can be categorized in heterogeneous and homogeneous patterns. Animals with the same infarct size and interval after ischemia but a heterogeneous intralesional ADC pattern showed better functional outcome, higher expression of brain protection markers, and less expression of cell death. Animals with a homogeneous pattern showed a smaller PWI/DWI mismatch, indicating a reduced potential for recovery from ischemic penumbra and an increased risk for progression to definitive infarction. Applied to the clinical setting, early identification of tissue fate after ischemic stroke through DWI ADC map patterns may assist in acute therapeutic decisions.

Acknowledgment and Sources of Funding

We thank Hans Eickhoff for comments and language assistance. This research was supported by the INVICTUS (Spanish Neurovascular Network) research grant (RD 12/0014/0006) from Research Institute Carlos III, Madrid, Spain, and by the Champalimaud Neuroscience Program (INDP2007), Champalimaud Center for the Unknown, Lisbon, Portugal.

Disclosure Statement

The authors declare that they have no conflict of interest.

References

1 Rivers CS, Wardlaw JM, Armitage PA, Bastin ME, Carpenter TK, Cvoro V, Hand PJ, Dennis MS: Persistent infarct hyperintensity on diffusion-weighted imaging late after stroke indicates heterogeneous, delayed, infarct evolution. Stroke 2006;37:1418–1423.

2 Gutiérrez-Fernández M, Rodríguez-Frutos B, Fuentes B, Vallejo-Cremades MT, Alvarez-Grech J, Expósito-Alcaide M, Díez-Tejedor E: CDP-choline treatment induces brain plasticity markers expression in experimental animal stroke. Neurochem Int 2012;60:310–317.

3 Gutiérrez-Fernández M, Rodríguez-Frutos B, Alvarez-Grech J, Vallejo-Cremades MT, Expósito-Alcaide M, Merino J, Roda JM, Díez-Tejedor E: Functional recovery after hematic administration of allogenic mesenchymal stem cells in acute ischemic stroke in rats. Neuroscience 2011;175:394–405.

4 Ogata T, Nagakane Y, Christensen S, Ma H, Campbell BC, Churilov L, Olivot JM, Desmond PM, Albers GW, Davis SM, Donnan GA; EPITHET and DEFUSE Investigators: A topographic study of the evolution of the MR DWI/PWI mismatch pattern and its clinical impact: a study by the EPITHET and DEFUSE investigators. Stroke 2011;42:1596–1601.

5 Sobesky J: Refining the mismatch concept in acute stroke: lessons learned from PET and MRI. J Cereb Blood Flow Metab 2012;32:1416–1425.

6 Kakuda W, Lansberg MG, Thijs VN, Kemp SM, Bammer R, Wechsler LR, Moseley ME, Marks MP, Albers GW; DEFUSE Investigators: Optimal definition for PWI/DWI mismatch in acute ischemic stroke patients. J Cereb Blood Flow Metab 2008;28:887–891.

7 Koyama T, Marumoto K, Miyake H, Domen K: Relationship between diffusion tensor fractional anisotropy and long-term motor outcome in patients with hemiparesis after middle cerebral artery infarction. J Stroke Cerebrovasc Dis 2014;23:2397–2404.

8 Lima FO, Furie KL, Silva GS, Lev MH, Camargo EC, Singhal AB, Harris GJ, Halpern EF, Koroshetz WJ, Smith WS, Nogueira RG: Prognosis of untreated strokes due to anterior circulation proximal intracranial arterial occlusions detected by use of computed tomography angiography. JAMA Neurol 2014;71:151–157.

9 Honarmand A, Beck R, Soltanolkotabi M, Ansari S, Shaibani A, Daruwalla V, Hurley M: E-005 short-term outcomes of acute ischemic stroke patients with MCA/ICA occlusion excluded for intra-arterial reperfusion therapy. J Neurointerv Surg 2014;6(suppl 1):A39–A40.

10 Malik N, Hou Q, Vagal A, Patrie J, Xin W, Michel P, Eskandari A, Jovin T, Wintermark M: Demographic and clinical predictors of leptomeningeal collaterals in stroke patients. J Stroke Cerebrovasc Dis 2014;23:2018–2022.

11 Thompson JW, Dave KR, Young JI, Perez-Pinzon MA: Ischemic preconditioning alters the epigenetic profile of the brain from ischemic intolerance to ischemic tolerance. Neurotherapeutics 2013;10:789–797.
12 del Zoppo GJ, Sharp FR, Heiss WD, Albers GW: Heterogeneity in the penumbra. J Cereb Blood Flow Metab 2011;31:1836–1851.
13 Barber PA: Magnetic resonance imaging of ischemia viability thresholds and the neurovascular unit. Sensors (Basel) 2013;13:6981–7003.
14 Neumann-Haefelin T, Wittsack HJ, Wenserski F, Siebler M, Seitz RJ, Mödder U, Freund HJ: Diffusion- and perfusion-weighted MRI: the DWI/PWI mismatch region in acute stroke. Stroke 1999;30:1591–1597.
15 Mishra NK, Albers GW, Davis SM, Donnan GA, Furlan AJ, Hacke W, Lees KR: Mismatch-based delayed thrombolysis: a meta-analysis. Stroke 2010;41:e25–e33.
16 Park CH, Kou N, Boudrias MH, Playford ED, Ward NS: Assessing a standardised approach to measuring corticospinal integrity after stroke with DTI. Neuroimage Clin 2013;2:521–533.
17 Borich MR, Wadden KP, Boyd LA: Establishing the reproducibility of two approaches to quantify white matter tract integrity in stroke. Neuroimage 2012;59:2393–2400.
18 Tsang A, Stobbe RW, Asdaghi N, Hussain MS, Bhagat YA, Beaulieu C, Emery D, Butcher KS: Relationship between sodium intensity and perfusion deficits in acute ischemic stroke. J Magn Reson Imaging 2011;33:41–47.
19 Ramos-Cejudo J, Gutiérrez-Fernández M, Rodríguez-Frutos B, Expósito Alcaide M, Sánchez-Cabo F, Dopazo A, Díez-Tejedor E: Spatial and temporal gene expression differences in core and periinfarct areas in experimental stroke: a microarray analysis. PLoS One 2012;7:e52121.
20 Kleinschnitz C, Grund H, Wingler K, Armitage ME, Jones E, Mittal M, Barit D, Schwarz T, Geis C, Kraft P, Barthel K, Schuhmann MK, Herrmann AM, Meuth SG, Stoll G, Meurer S, Schrewe A, Becker L, Gailus-Durner V, Fuchs H, Klopstock T, de Angelis MH, Jandeleit-Dahm K, Shah AM, Weissmann N, Schmidt HH: Post-stroke inhibition of induced NADPH oxidase type 4 prevents oxidative stress and neurodegeneration. PLoS Biol 2010;8:e1000479.
21 Moskowitz MA, Lo EH, Iadecola C: The science of stroke: mechanisms in search of treatments. Neuron 2010;67:181–198.
22 Murakami K, Kondo T, Kawase M, Li Y, Sato S, Chen SF, Chan PH: Mitochondrial susceptibility to oxidative stress exacerbates cerebral infarction that follows permanent focal cerebral ischemia in mutant mice with manganese superoxide dismutase deficiency. J Neurosci 1998;18:205–213.
23 Suma T, Koshinaga M, Fukushima M, Kano T, Katayama Y: Effects of in situ administration of excitatory amino acid antagonists on rapid microglial and astroglial reactions in rat hippocampus following traumatic brain injury. Neurol Res 2008;30:420–429.

Cerebrovascular Diseases

Protective effect of hydrogen sulfide exposure after experimental ischemic stroke: smaller infarct size, better functional outcome, and reduced oxidative stress

Journal:	*Cerebrovascular Diseases*
Manuscript ID:	201503034
Manuscript Type:	Translational Research in Stroke
Date Submitted by the Author:	18-Mar-2015
Complete List of Authors:	Henriques, Isabel; La Paz University Hospital, Neuroscience Area of IdiPAZ (Health Research Institute), Autónoma University of Madrid, Department of Neurology and Stroke Centre, Neuroscience and Cerebrovascular Research Laboratory; University of Lisbon, Faculty of Medicine Gutiérrez-Fernández, María; La Paz University Hospital, Neuroscience Area of IdiPAZ (Health Research Institute), Autónoma University of Madrid, Department of Neurology and Stroke Centre, Neuroscience and Cerebrovascular Research Laboratory Rodríguez-Frutos, Berta; La Paz University Hospital, Neuroscience Area of IdiPAZ (Health Research Institute), Autónoma University of Madrid, Department of Neurology and Stroke Centre, Neuroscience and Cerebrovascular Research Laboratory Ramos-Cejudo, Jaime; La Paz University Hospital, Neuroscience Area of IdiPAZ (Health Research Institute), Autónoma University of Madrid, Department of Neurology and Stroke Centre, Neuroscience and Cerebrovascular Research Laboratory Otero-Ortega, Laura; La Paz University Hospital, Neuroscience Area of IdiPAZ (Health Research Institute), Autónoma University of Madrid, Department of Neurology and Stroke Centre, Neuroscience and Cerebrovascular Research Laboratory Navarro Hernanz, Teresa; Institute of Biomedical Research Alberto Sols, CSIC-UAM, Laboratory for Imaging and Spectroscopy by Magnetic Resonance LISMAR Cerdán, Sebastián; Institute of Biomedical Research Alberto Sols, CSIC-UAM, Laboratory for Imaging and Spectroscopy by Magnetic Resonance LISMAR Ferro, Jose M.; Hospital Santa Maria, Servico de Neurologia Díez-Tejedor, Exuperio; La Paz University Hospital, Neuroscience Area of IdiPAZ (Health Research Institute), Autónoma University of Madrid, Department of Neurology and Stroke Centre, Neuroscience and Cerebrovascular Research Laboratory
Keywords:	MRI, experimental stroke, animal models, oxidative stress

Protective effect of hydrogen sulfide exposure after experimental ischemic stroke: smaller infarct size, better functional outcome, and reduced oxidative stress

Isabel Henriques, MD[1, 2, 3], María Gutiérrez-Fernández[1] PhD, Berta Rodríguez-Frutos[1] PhD, Jaime Ramos-Cejudo[1] MSc, Laura Otero-Ortega[1] PhD, Teresa Navarro Hernanz[4] PhD, Sebastián Cerdán[4] PhD, José Ferro[5] MD, PhD & Exuperio Díez-Tejedor[1] MD, PhD

[1]*Department of Neurology and Stroke Centre, Neuroscience and Cerebrovascular Research Laboratory, La Paz University Hospital, Neuroscience Area of IdiPAZ (Health Research Institute), Autónoma University of Madrid, Paseo de la Castellana 261, 28046 Madrid, Spain*

[2]*Faculty of Medicine, University of Lisbon, Av. Professor Egas Moniz, 1649-028 Lisbon, Portugal and Serviço de Neurologia, Centro Hospitalar de Lisboa Zona Central, Avenida Santo António dos Capuchos, 1169-050 Lisboa, Portugal*

[3]*International Neuroscience Doctoral Programme, Champalimaud Neuroscience Programme, Champalimaud Center for the Unknown, Avenida Brasília, 1400-038 Lisbon, Portugal*

[4]*Laboratory for Imaging and Spectroscopy by Magnetic Resonance LISMAR, Institute of Biomedical Research Alberto Sols, CSIC-UAM, Calle Arturo Duperier 4, 28029 Madrid, Spain*

[5]*Department of Neurosciences, Hospital de Santa Maria, University of Lisbon, Av. Professor Egas Moniz, 1649-035 Lisbon, Portugal*

Corresponding authors

Isabel Lestro Henriques, MD, FESO ilh.igc@gmail.com

Serviço de Neurologia, Centro Hospitalar de Lisboa Zona Central, Avenida Santo António dos Capuchos, 1169-050 Lisboa, Portugal

Prof. Exuperio Díez-Tejedor, MD, PhD, FAHA, FESO exuperio.diez@salud.madrid.org

Department of Neurology and Stroke Centre, La Paz University Hospital, Paseo de la Castellana 261, 28046 Madrid, Spain

Keywords: Hydrogen sulfide; H_2S; MRI; NOX-4; stroke; oxidative stress; ROS.

ABSTRACT

Background: Hydrogen sulfide (H_2S) induces hypometabolism through mechanisms that include a dramatic reduction in oxygen consumption, local vasoregulation, and inhibition of cell death. Prolonged exposure to H_2S after experimental ischemic stroke modulates injury through induction of severe hypothermia but the mechanisms and effects of reduced exposure times remain to be further characterized.

Methods: In the present study, we used Sprague-Dawley rats in a model of permanent middle cerebral artery occlusion (pMCAO) and compared functional outcome, *in vivo* and *post-mortem* lesion size, diffusion and perfusion Magnetic Resonance Imaging (MRI), cell death, brain protection and repair-associated markers after short-term exposure to H_2S.

Results: We observed an improved functional outcome (24h and 14d, $P<0.05$), diminished infarct size (14d, $P<0.01$) and cell death (24h and 14d, $P<0.05$) in animals exposed to H_2S. Perfusion MRI revealed higher intralesional cerebral blood flow ($P<0.05$) while diffusion MRI showed intralesional heterogeneity compared to controls ($P<0.05$). In treated animals, expression of NOX-4 was lower at 24h and 14d, HSP-27 was lower at 24h, and SOD-2 and GFAP were lower at 14d ($P<0.05$).

Conclusions: Observed improvements in functional outcome, infarct size and cell death included processes involving modulation of reactive oxygen species and reduction of acute injury-related markers, without enhancement of repair-associated markers for vasculogenesis, angiogenesis, and synaptogenesis. Thus, H_2S possibly acts before the onset of irreversible ischemia and limits brain damage after stroke. In the future, H_2S donors may play a role in the context of acute stroke management in humans.

INTRODUCTION

There are exceptions in nature to the rule that lack of cerebral blood flow during a prolonged period inexorably leads to ischemia and irreversible brain damage. Two examples are cardiac arrest from extreme cold and hibernation. In both cases, survival is possible without permanent neurological damage despite of very little or no cerebral blood flow at all [1,2]. These examples show that severe brain damage may be prevented even in the absence of cerebral blood flow during long periods. The induction of a “hibernation-like” state in mice using the inorganic gas hydrogen sulfide (H_2S) suggested its potential in the context of acute ischemia [3,4].

H_2S is endogenously produced in different organs including the brain [5] and regulates oxygen consumption by competing with O_2 in binding to cytochrome C oxidase at the mitochondrial electron transport chain [3]. Data about the potential benefit of H_2S in the context of acute ischemic stroke is modest and conflicting. First reports showed no functional benefit [6], others demonstrated improvement in functional outcome and lesion size [7]. Data from ischemic heart and kidney experimental models showed protection after acute ischemia [8,9].

We hypothesized that inducing a reversible hypometabolic state after acute cerebral ischemia through administration of H_2S could limit acute ischemic brain damage. We investigated the effects of short-term H_2S exposure after permanent middle cerebral artery occlusion (pMCAO) by analyzing the functional outcome, infarct size, and markers of cytoprotection or repair. We completed the study with *in vivo* brain imaging

by Magnetic Resonance Imaging (MRI) as compared to *post-mortem* immunohistochemical data.

MATERIALS AND METHODS

Experiments were designed to minimize animal suffering in compliance with the ARRIVE criteria and our medical school's Ethical Committee for the Care and Use of Animals in Research (EU directives 86/609/CEE and 2003/65/CE). Researchers were blinded to group allocation after randomization. Male 8 - 12 week old Sprague-Dawley rats (250 to 320g) (Charles River©, Spain) were randomly assigned to 3 groups: sham (craniotomy, n=13), control (craniotomy + pMCAO, n=23) and treated (craniotomy + pMCAO + exposure to 40 ppm H_2S, n=28). Rats were anesthetized with Sevoflurane (CAM 2.5±0.3 volume %). We performed a small craniotomy above the rhinal fissure over the branch of the right middle cerebral artery (MCA), exposing MCA and permanently ligated it with a 9-0 silk suture before its bifurcation. Then, both common carotid arteries were temporarily occluded for 60min with a 6-0 silk suture lace as previously described [10,11]. Scar size and location were equal for all groups, animal cages had no information about group allocation, and codes were used in *post mortem* samples, in order to maintain blinded data collection and analysis. Body temperature and glycemia were measured throughout procedures. Rats were sacrificed at 24h and 14d after surgery.

Gas mixtures

Treated animals were exposed during 24 min to H_2S, 3 hours after acute ischemia, breathing a mixture of atmosphere with H_2S [Gasin medical bottles, 40 ppm H_2S in nitrogen (N_2: 99.9%)] inside a closed box (9.5 x 20 x 10 cm = Volume 1,900 cm^3). Control and sham animals breathed normal atmosphere in the same temperature and humidity conditions. We used rectal temperature before and after exposure as an indirect measure of induction of hypometabolism**.**

Ischemic lesion size

Lesion size was evaluated *in vivo* at 24h and 14d using T2-weighted sequence MRI and *post mortem* hematoxylin/eosin (H&E) stains, as previously described [10,11].

Magnetic Resonance Imaging

The extension of ischemic lesions was analyzed non-invasively after 24h (group sacrificed at 24h) and twice, after 24h and 14d (group sacrificed at 14d), using T2-weighted images. Observers were blinded to allocation groups. After contrast adjustment, the contours of the hemispheres were traced manually on each slice. Data analysis was performed using Image J software from NIH Image, slice-by-slice contouring at lesion site and in the contralateral hemisphere in the same location. Only lesions larger than 2mm x 2mm x 2mm were analyzed to minimize partial volume effects. We used JPG® region of interest (ROI) to measure infarct size. To correct for brain edema effect, lesion size was determined by an indirect method: infarct area = area of the intact contralateral hemisphere – area of the intact ipsilateral hemisphere.

Lesion size was expressed as percentage of total ipsilateral hemisphere. Exclusion criteria were no measurable lesion on MRI, except for the sham group (n=3). T_2-weighted MRI at 24h was used as confirmation tool for successful ischemic lesion induction.

Diffusion-weighted imaging (DWI) was obtained with 3 different directions defined by read, phase, and slice encoding gradients, using a multishot spin-echo echo planar imaging (EPI) sequence. We used the following acquisition conditions: diffusion gradient duration: 3ms, diffusion gradient separation: 18ms, TR: 3000ms, TE: 35ms, FOV: 3.5cm, section thickness of 1.5mm with a 0.1mm gap, 5 axial slices, 3 b values with b as measure of diffusion weighting (100, 400 and 1000 s/mm2), acquisition matrix = 128 × 128 corresponding to an in-plane resolution of 273 × 273 μm^2. The apparent diffusion coefficient (ADC) was computed for each voxel using the exponential model according to the expression: $S_b = S_0 e^{-b*ADC}$, being S_b the signal intensity versus the b factor and S_0 the signal intensity versus b=0.

MRI images were acquired on a 7 Tesla/16 cm Bruker Avance III system (Bruker Medical Gmbh, Ettlingen, Germany) at the MR Imaging Facility (SIERMAC, CSIC/UAM, Madrid). Anesthesia was induced with isoflurane. Rats were monitored during MRI with a Biotrig physiological monitor (Bruker) depicting on-line the respiratory rate.

Hematoxylin/eosin stains

Lesion size was estimated with H&E staining which reveals an ischemic area as a well-defined pale region. Lesion size was expressed as the percentage of brain tissue affected by ischemia in the right hemisphere as evaluated on 10-µm-thick sections.

Brains were sectioned at the optic chiasm and at the infundibular stalk. The resultant brain block from between these two cuts was placed in 4% paraformaldehyde for 24 h and 30% sacarose PBS buffer for 3 days. Optimal cutting temperature (OCT) embedded samples were coronally sectioned in 10-µm-thick slices. A digitized image was made of these slices (Epson Perfection 1260 scanner, Suwa, Nagano, Japan) and used to automatically measure the ischemic area (Image Pro plus 4.0, Media Cybernetics, Rockville, MD, USA) [11].

Functional evaluation scales

Functional evaluation was performed using Rotarod and Rogers modified test, by a blinded observer at baseline, 24h and at 14d after surgery. The latency to fall from a rotator cylinder (accelerating at 4-40 rpm) was recorded. Motor function by Rogers test was scored: 0, no deficit; 1, failure to extend contralateral forepaw fully; 2, decreased grip of the contralateral forelimb while tail gently pulled; 3, spontaneous movement in all directions, contralateral circling only if pulled by the tail; 4, circling or walking to the right; 5, walks only when stimulated; 6, unresponsive to stimulation; and 7, dead [10].

Cell death

Cell death was assessed by TUNEL staining (biotin-dUTP nick end-labeling mediated by terminal deoxynucleotidyl transferase; TdT-FragEL DNA Fragmentation Detection Kit, Oncogene Research Products) following manufacturer's instructions. The number of positive cells was counted using a 40× objective and image analysis software (Image-

Pro Plus 4.1®, Media Cybernetics). We maintained blind access to group allocation and samples were independently counted by two of the authors.

Immunohistochemistry, immunofluorescence and western blot

Immunohistochemistry

NOX-4: Pro-oxidant enzyme, NADPH oxidase 4 (NOX-4) primary polyclonal antibody anti-Nox-4 (1:1000, Abnova, Heidelberg, Germany) was incubated for one hour at room temperature. The slides were then incubated with a secondary antibody (donkey anti-rabbit antibody diluted 1:50) conjugated with horseradish peroxidase (Chemicon International, Temecula, CA, USA) and incubated with 3',3'-diaminobenzidine (Invitrogen).

Immunofluorescence

Serial coronal sections were cut at 10μm in a cryostat (Leica CM1950) and studied by immunofluorescence neural markers. Markers for neuronal nuclei (NeuN) (monoclonal antibody diluted 1:100, Millipore), astrocytes [glial fibrillary acid protein (GFAP) (monoclonal antibody diluted 1:400, Chemicon)], vascular growth [vascular endothelial growth factor (VEGF) marker (polyclonal antibody diluted 1:500, Millipore)], synaptogenesis [synaptophysin (monoclonal antibody diluted 1:200, Sigma - Aldrich)], superoxide dismutase 2 (SOD-2) (polyclonal antibody diluted 1:150, Abcam®), and heat shock protein 27 (HSP-27) (monoclonal antibody diluted 1:200, Abcam®), followed by goat anti-mouse Alexa Fluor 488 and anti-rabbit Alexa Fluor 594 (1: 750, Molecular Probes, Invitrogen) were used.

All sections were mounted with H-1200 VectaShield mounting medium for fluorescence with DAPI (ATOM). Samples were examined using a spectral confocal microscope Leica TCS SPE (Leica Microsystems, Heidelberg, Germany) and the confocal images were analyzed using Leica software LAS AF, version 2.0.1 build 2043. The images were acquired at confocal maximum projection.

Western Blot

Brain proteins levels were measured in the infarct zone of animals (n=4 per group) and its concentration was determined using a BCA protein assay kit (Pierce). Western-Blot for NADPH oxidase 4 (NOX-4) (polyclonal antibody 1:2000, Abnova), SOD-2 (polyclonal antibody diluted 1:5000, Abcam), HSP27 (monoclonal antibody diluted 1:1000, Abcam), GFAP (monoclonal antibody diluted 1:500, Millipore), VEGF (polyclonal antibody diluted 1:500, Millipore) and synaptophysin (monoclonal antibody diluted 1:400, Sigma) were measured in all groups. The units were normalized based on B-actin levels (1:400, Sigma-Aldrich). To reduce methodological bias, at least three Western blots were performed for each animal.

Statistical analysis

Quantitative data is shown as mean ± standard error of the mean (SEM) presented as box and whiskers plot. As data followed a non-normal distribution in the Shapiro-Wilk test, the Mann–Whitney test was used to compare two samples and the Kruskal–Wallis test to compare more than two samples (SPSS 16 for Windows®). Values of $p<0.05$ were considered significant at a 95% confidence level. Power analysis showed that with non-parametric testing randomization of at least 18 animals to each group (exposed or

control) would yield an effect size d of 1.0 with a power of 0.80 (beta-value 0.20) and an alpha-value of 0.05. We used G*Power (Version 3.1.9.2) for power analysis calculations.

RESULTS

Functional outcome after exposure to hydrogen sulfide

We measured functional outcome before procedure, at 24h and 14d. At baseline, Rogers Modified Scale was zero for all animals and the latency to fall in the Rotarod test was >120 seconds. The sham-operated group showed no functional deficit at 24h or 14d. A better functional outcome was observed at 24h in animals exposed to H_2S compared to control group regarding Rogers Modified Scale (1.73 ± 0.23 *vs.* 3.29 ± 0.18, P=0.001) and Rotarod test (65 ± 5.97, *vs.* 37 ± 7.14, P=0.03). At 14d, the functional benefit observed in treated animals was sustained in both tests: Rogers Modified Scale (1.18±0.17 *vs.* 1.82± 0.20, P=0.03), and Rotarod (55.25±5.17 *vs.* 31.5±7.79, P=0.04) (Figure 1A).

Infarct size after exposure to hydrogen sulfide

At 24 hours after pMCAO, lesion size measured by T_2-weighted MRI did not differ significantly between treated and control groups (9.69±1.67 *vs.* 15.45±1.06, P=0.054). However, H&E stains showed a reduced infarct size in the treated group (6.69±1.38 *vs.* 23.20±3.05, P=0.008). At day 14, T_2-weighted MRI and H&E showed smaller infarct size in treated compared to control rats (6.13±0.62 vs. 11.56±0.4, P=0.0004 and 4.94±0.92

vs. 11.63±1.99, P=0.002, respectively). Sham operated rats showed no cerebral lesion. The largest lesion was observed in the control group (Figure 1B).

MRI heterogeneities in ischemic territory after exposure to hydrogen sulfide

In treated rats (rats exposed to H_2S), we observed heterogeneities inside the ischemic MCA territory on MRI ADC maps at 24h (Figure 2D upper right image and graph). These heterogeneities were observed inside the ischemic territory, including central and peripheral areas, presenting some central areas a higher diffusion coefficient than peripheral ones. In animals treated with H_2S, the relative ADC (rADC) coefficients were similar in central and peripheral areas (Figure 2D lower left images and graph). Finally, using perfusion MRI, the differential CBF between the lesion side and contralateral hemisphere was lower in treated rats ($P<0.05$) (Figure 2D, lower right image and right graph).

Cell death after exposure to hydrogen sulfide

Treated rats showed significantly less TUNEL positive cells, both at 24h (367.5 ± 78.03 *vs.* 901.25 ± 217.45 P=0.047) and 14d (42.7 ± 7.76 *vs.* 53.71 ± 6.75 P=0.04) (Figure 2A, Figure 3A) in comparison to controls. No sham operated rats showed TUNEL positive cells.

Exposure to hydrogen sulfide does not increase brain repair but enhances markers associated with brain protection

At day 14, the group treated with H_2S showed no increase in expression of VEGF (0.75 ± 0.22 *vs.* 0.79 ± 0.18 P=0.88) or synaptophysin (1.40 ± 0.39 *vs.*1.29 ± 0.30 p=0.50) compared to control group (Figure 3B and C). GFAP showed significantly lower levels at day 14 in treated animals compared to control (0.36 ± 0.16 *vs. 0.77* ± 0.43, P=0.027). The levels of SOD2 at day 14 were lower than in the control group (0.66 ± 0.06 *vs. 1.07* ± 0.14, P=0.05) (Figure 3B and C), but not at 24h (0.788±0.13 *vs*. 0.90±0.3 P=0.11) (Figure 2B and C). The levels of NOX-4 were lower in treated rats compared to the control group at 24h (0.50 ± 0.12 *vs.* 1.11 ± 0.28 P=0.03) (Figure 2A and C) and day 14 (0.47 ± 0.21 *vs.* 1.40 ± 0.46 P=0.049) (Figure 3A and C). HSP-27 levels were lower at 24h in treated rats compared to control animals (0.41 ± 0.12 *vs.* 0.81 ± 0.11 P=0.49) but not at day 14 (0.84 ± 0, 51 *vs*. 1,056 ±0, 55 P= 0.24) (Figure 2B and C, Figure 3B and C).

Physiological parameters

Glycemia was assessed immediately after starting the surgical procedure and during surgery in all animals and was similar in all groups. Body temperature was significantly lower after induction of anesthesia in all groups (P<0.001). After an exposure time to H_2S of 24 minutes, body temperature decreased by 1.85 ºC (mean) but quickly recovered after animals started to breathe normal atmosphere again; no difference in body temperature was observed at 2 hours after exposure (Figure 4).

DISCUSSION

We report on the role of short-term exposure to H_2S in acute ischemic brain damage. Our results show that exposure to hydrogen sulfide after pMCAO improves functional outcome and decreases infarct size and cell death. The longitudinal study suggests that H_2S may act very early in the ischemic process, since there were lower levels of acute injury-related markers at 24h without enhancement of repair-associated markers for vasculogenesis, angiogenesis or synaptogenesis at day 14. Significant benefit is likely to occur before major tissue damage develops, including modulation of NOX-4, a major generator of reactive oxygen species (ROS) and mediator of endothelial dysfunction.

A main goal of acute stroke treatment is the improvement of functional outcome. In the present study, a better functional outcome in animals exposed to H_2S was observed at 24h and day 14. A similar benefit in functional outcome has been reported in studies that used H_2S in an ischemia-reperfusion model [12] and global brain [13], cardiac or kidney ischemia [14,15]. In our model, functional benefit from H_2S exposure was not limited to short term but sustained until day 14. Immunohistochemical and *in vivo* imaging data support this observation showing improved brain tissue preservation and smaller lesion size.

Previous data using a H_2S donor (NaHS) in an ischemic electrocauterization model did not show reduction in lesion size after NaHS [6]. Later, smaller infarct sizes were reported using longer H_2S exposure times, higher doses [7] or reversible MCAO models [12]. Our data show that lower dose and shorter exposure (40 ppm, during 24 min) are able to decrease infarct size after pMCAO. Despite of smaller infarcts at day 14 both *in*

vivo and *post mortem*, at 24h differences between infarct sizes assessed by T2-weighted MRI were not significant, possibly due to acute post ischemic brain edema that increases lesion volume. However, H&E staining at 24h showed smaller lesion size in treated rats.

Interestingly, MRI ADC maps at 24h in treated rats revealed heterogeneity, with spotty areas inside ischemic lesion and higher ADC coefficients, both in central and peripheral areas. We previously described gene expression associated with CNS development and trophic factors within lesion core at 24h after pMCAO, suggesting the presence of surviving areas within the ischemic core [16]. These heterogeneities, revealing different rates of water diffusion and underlying brain tissue integrity, may represent previously described "mini-cores and mini-penumbras" [17]. As heterogeneity in ADC maps corresponded to better functional outcome as well as smaller lesions and better ischemic tissue preservation in treated rats, prognostic relevance of ADC heterogeneities may deserve further research in a translational context.

Hypothermia, when not induced from external sources, is the result of hypometabolism and not the cause of metabolic changes. H_2S modulation in the context of acute stroke has been associated with induction of hypothermia, especially in protocols that included prolonged exposure times [7]. In our study, after an exposure time of 24 minutes, a mean decrease of 1.85ºC in body temperature was observed. Body temperature fully recovered in less than 120 min (Figure 4). Consequently, hypothermia appears to be a limited side effect of hypometabolism induced by H_2S and other mechanisms must be involved since the effects of H_2S administration were observed until day 14. In the

present study, a shorter exposure time than previously reported was effective with a minor effect on body temperature. This observation represents an important finding in a translational context since minor changes in body temperature will not require patient management in high-dependency or intensive care units.

Previous *in vitro* studies have shown that the use of D-cysteine (a biosynthetic pathway for H_2S production) was associated with attenuation of ischemia-reperfusion injury in the kidney [15]. Also in a murine primary cortical neuron preparation ischemic neuronal death was prevented using a H_2S-releasing NMDA receptor antagonist [18]. Additionally, rats pre-treated with diallyl sulfide showed a significant decrease in TUNEL positive cell count [12]. Our study confirmed that markers for cell death depict significantly less expression in treated animals.

HSP27 is a stress-related protein known to be differentially expressed after stroke. We previously showed in a genomic study that several chaperones including HSP27 were upregulated at 24h, both in the core and peri-infarct areas [16]. Others reported that neuronal expression of another HSP (HSP70) was associated with ischemic penumbra and core, using a reporter mice model [19]. Interestingly, a study with reperfusion in cardiac ischemia showed that HSP27 expression was lower in H_2S-treated pigs [20]. In the present study, we observed less expression of HSP27 at 24h after pMCAO in rats exposed to H_2S, associated with tissue preservation, reflecting an additional indication of a possible protective role for H_2S.

It is known that oxidative stress causes tissue damage in the context of acute brain ischemia with ROS expressed above physiological levels [21,22]. ROS downregulation

after exposure to H_2S was reported in ischemia-reperfusion models, after hemorrhagic shock [23], and during lung transplantation [24]. NOX-4 is a major source of oxidative stress in ischemic stroke [21]. In our study, NOX-4 levels were lower at 24h and day 14 in treated rats. Thus, H_2S may modulate early ROS expression. GFAP levels were lower in rats exposed to H_2S, suggesting that early protection may be related to preservation of tissue structure and less glial scar, since we did not find increased levels of repair-associated markers implicated in synaptogenesis, vasculogenesis or angiogenesis at day 14.

Study limitations

We designed this study to fulfill the recommendations for research in translational stroke. Animals were randomized and all procedures except surgery were performed in a blinded manner to avoid observational bias regarding functional outcome, MRI image evaluation, and in-bench procedures, by using codes not known to observers. Detailed data is shown to facilitate reproducibility.

Dosage of H_2S in the present study was the same in all animals and different dosages might produce distinct effects on outcome. Due to budget limitations and the preliminary nature of our study, we did not include female or older animals or animals with co-morbidities in this study. In the setting of an experimental study using rodents, clinical outcome was limited to assessment of motor skills. We used MRI at 24h as a confirmation tool for successful pMCAO to avoid bias in results that could be attributable to surgical failure. No conclusions regarding long-term results of H_2S exposure should

be drawn as the study design focused on comparison of *in vivo* and *post mortem* data in the acute setting at 24h and after 14d.

CONCLUSIONS

In our pMCAO model of ischemic stroke, early exposure to hydrogen sulfide after focal brain ischemia improved functional outcome and decreased infarct size and cell death through processes that involve modulation of NOX-4, a major enzyme generator of reactive oxygen species. Regarding brain imaging, perfusion MRI in rats exposed to H_2S revealed improved cerebral blood flow, while diffusion MRI showed spots of heterogeneity inside ischemic lesions in ADC maps, including central regions. H_2S probably acts very early after administration, since lower levels of acute injury-related markers were present at 24h, without enhancement of repair-associated markers for vasculogenesis, angiogenesis or synaptogenesis at day 14. Significant benefit is likely to occur before major tissue damage has taken place. In the future, H_2S donors may play a role in the context of acute stroke management in humans.

ACKNOWLEDGMENTS AND SOURCES OF FUNDING

We thank Hans Eickhoff, Íris Vilares, and Rui Costa for comments on the manuscript and Carol Warren for language assistance. This study was supported by the INVICTUS (RD 12/0014/0006) Spanish Neurovascular Network research grant from Research Institute Carlos III, Ministry of Science and Innovation, and from the International

Neuroscience Doctoral Program, Champalimaud Neuroscience Program, Champalimaud Center for the Unknown, Lisbon, Portugal.

DISCLOSURE

The authors declare that they have no conflict of interest.

REFERENCES

1. Storey KB, Storey JM. Metabolic rate depression: the biochemistry of mammalian hibernation. Adv. Clin. Chem. 2010;52:77–108.

2. Schwartz C, Hampton M, Andrews MT. Seasonal and regional differences in gene expression in the brain of a hibernating mammal. PLoS One. 2013;8:e58427.

3. Szabó C. Hydrogen sulphide and its therapeutic potential. Nat. Rev. Drug Discov. 2007;6:917–35.

4. Blackstone E, Morrison M, Roth MB. H2S induces a suspended animation-like state in mice. Science. 2005;308:518.

5. Mani S, Li H, Untereiner A, Wu L, Yang G, Austin RC, et al. Decreased Endogenous Production of Hydrogen Sulfide Accelerates Atherosclerosis. Circulation. 2013;127:2523–34.

6. Qu K, Chen CPLH, Halliwell B, Moore PK, Wong PT-H. Hydrogen sulfide is a mediator of cerebral ischemic damage. Stroke. 2006;37:889–93.

7. Joseph C, Buga A-M, Vintilescu R, Balseanu AT, Moldovan M, Junker H, et al. Prolonged gaseous hypothermia prevents the upregulation of phagocytosis-specific protein annexin 1 and causes low-amplitude EEG activity in the aged rat brain after cerebral ischemia. J. Cereb. Blood Flow Metab. 2012;32:1632–42.

8. Hosgood SA, Nicholson ML. Hydrogen sulphide ameliorates ischaemia-reperfusion injury in an experimental model of non-heart-beating donor kidney transplantation. Br. J. Surg. 2010;97:202–9.

9. Snijder PM, de Boer RA, Bos EM, van den Born JC, Ruifrok W-PT, Vreeswijk-Baudoin I, et al. Gaseous hydrogen sulfide protects against myocardial ischemia-reperfusion injury in mice partially independent from hypometabolism. PLoS One. 2013;8:e63291.

10. Gutiérrez-Fernández M, Rodríguez-Frutos B, Alvarez-Grech J, Vallejo-Cremades MT, Expósito-Alcaide M, Merino J, et al. Functional recovery after hematic administration of allogenic mesenchymal stem cells in acute ischemic stroke in rats. Neuroscience. 2011;175:394–405.

11. Gutiérrez-Fernández M, Rodríguez-Frutos B, Ramos-Cejudo J, Teresa Vallejo-Cremades M, Fuentes B, Cerdán S, et al. Effects of intravenous administration of allogenic bone marrow- and adipose tissue-derived mesenchymal stem cells on functional recovery and brain repair markers in experimental ischemic stroke. Stem Cell Res. Ther. 2013;4:11.

12. Lin X, Yu S, Chen Y, Wu J, Zhao J, Zhao Y. Neuroprotective effects of diallyl sulfide against transient focal cerebral ischemia via anti-apoptosis in rats. Neurol. Res. 2012;34:32–7.

13. Yin J, Tu C, Zhao J, Ou D, Chen G, Liu Y, et al. Exogenous hydrogen sulfide protects against global cerebral ischemia/reperfusion injury via its anti-oxidative, anti-inflammatory and anti-apoptotic effects in rats. Brain Res. 2013;1491:188–96.

14. Szabó G, Veres G, Radovits T, Gero D, Módis K, Miesel-Gröschel C, et al. Cardioprotective effects of hydrogen sulfide. Nitric Oxide. 2011;25:201–10.

15. Shibuya N, Koike S, Tanaka M, Ishigami-Yuasa M, Kimura Y, Ogasawara Y, et al. A novel pathway for the production of hydrogen sulfide from D-cysteine in mammalian cells. Nat. Commun. 2013;4:1366.

16. Ramos-Cejudo J, Gutiérrez-Fernández M, Rodríguez-Frutos B, Expósito Alcaide M, Sánchez-Cabo F, Dopazo A, et al. Spatial and temporal gene expression differences in core and periinfarct areas in experimental stroke: a microarray analysis. PLoS One. 2012;7:e52121.

17. Del Zoppo GJ, Sharp FR, Heiss W-D, Albers GW. Heterogeneity in the penumbra. J. Cereb. Blood Flow Metab. 2011;31:1836–51.

18. Marutani E, Kosugi S, Tokuda K, Khatri A, Nguyen R, Atochin DN, et al. A novel hydrogen sulfide-releasing N-methyl-D-aspartate receptor antagonist prevents ischemic neuronal death. J. Biol. Chem. 2012;287:32124–35.

19. De la Rosa X, Santalucía T, Fortin P-Y, Purroy J, Calvo M, Salas-Perdomo A, et al. In vivo imaging of induction of heat-shock protein-70 gene expression with fluorescence

reflectance imaging and intravital confocal microscopy following brain ischaemia in reporter mice. Eur. J. Nucl. Med. Mol. Imaging. 2013;40:426–38.

20. Osipov RM, Robich MP, Feng J, Liu Y, Clements RT, Glazer HP, et al. Effect of hydrogen sulfide in a porcine model of myocardial ischemia-reperfusion: comparison of different administration regimens and characterization of the cellular mechanisms of protection. J. Cardiovasc. Pharmacol. 2009;54:287–97.

21. Kleinschnitz C, Grund H, Wingler K, Armitage ME, Jones E, Mittal M, et al. Post-stroke inhibition of induced NADPH oxidase type 4 prevents oxidative stress and neurodegeneration. PLoS Biol. 2010;8.

22. Moskowitz MA, Lo EH, Iadecola C. The science of stroke: mechanisms in search of treatments. Neuron. 2010;67:181–98.

23. Ganster F, Burban M, de la Bourdonnaye M, Fizanne L, Douay O, Loufrani L, et al. Effects of hydrogen sulfide on hemodynamics, inflammatory response and oxidative stress during resuscitated hemorrhagic shock in rats. Crit. Care. 2010;14:R165.

24. George TJ, Arnaoutakis GJ, Beaty CA, Jandu SK, Santhanam L, Berkowitz DE, et al. Hydrogen sulfide decreases reactive oxygen in a model of lung transplantation. J. Surg. Res. 2012;178:494–501.

Figure 1. Rats exposed to H_2S after stroke show better functional outcome and smaller lesion size. **A. Functional outcome.** Rats exposed to H_2S had significantly lower score in Rogers scale (left) at 24h (***P<0.001) and at 14d (*P<0.05) (left graph) and more latency to fall from the Rotarod at 24h (*P<0.05) and at 14d (*P<0.05) (right graph). **B. Infarct size.** At 14d, rats exposed to H_2S had significantly smaller ischemic lesion size, both in MRI (T2 weighted sequence) (left graph) (***P<0.001) and H&E stain (right graph) (**P<0.01). At 24h, MRI showed a lower but non-significant difference in lesion size, whereas H&E showed a significantly smaller ischemic lesion after H_2S exposure (**P<0.01).

Figure 2. Rats sacrificed at 24h. At 24h rats exposed to H_2S after stroke show lower expression of cell death and ROS producing enzyme NOX-4 with higher intralesional perfusion. **A.** Rats exposed to H_2S show lower levels of cell death (*P<0.05) and NOX-4 (*P<0.05). **B.** Rats exposed to H_2S show lower levels of heat shock protein 27 (HSP 27) (*P<0.05) and no differences in superoxide dismutase-2 (SOD-2) levels. **C**. Western-blot of NOX-4, HSP27 and SOD2 at 24h. **D. MRI with DWI and PWI.** Rats exposed to H_2S showed intralesional heterogeneities in ADC maps (right upper image and graph) whereas control rats showed homogeneous ischemic lesions (left upper image and graph). ADC maps in rats exposed to H_2S showed islands of ADC diffusion coefficient in central lesion area, similar to ADC observed in peripheral areas (left lower images and graph). For quantification, three manually designed Regions of Interest (ROIs) were considered on ADC maps: ROI 1, ischemic central lesion area; ROI 2, peripheral lesion area; ROI 3, contralateral hemisphere. Animals exposed to H_2S showed similar differential ADC coefficients (rADC) in central and peripheral lesion areas and

intralesional CBF was improved. The difference between intralesional and contralateral hemisphere CBF (ΔCBF) was significantly smaller in comparison to controls (*P<0.05) (right lower image and graph).

Figure 3. Rats sacrificed at 14d. At day 14, rats exposed to H_2S expressed less cell death and ROS producing enzyme NOX-4, without detectable enhancement of repair mechanisms including angiogenesis, vasculogenesis or synaptogenesis. **A.** Cell death (*P<0.05) and NOX-4 levels (*P<0.05) were significantly lower in rats exposed to H_2S **B.** Significant lower levels of SOD2 (*P<0.05) and GFAP (*P<0.05) in rats exposed to H_2S with no differences in HSP27, VEGF or synaptophysin. **C**. Western-blot of NOX4, SOD2, GFAP, HSP27, VEGF and synaptophysin.

Figure 4. Body temperature. Rats exposed to H_2S (lower graph) and controls (upper graph). No difference in body temperature was observed 2h after exposure to hydrogen sulfide. Axis legend: Body temperature. Before: rectal temperature in rats before starting surgery; After surgery: rectal temperature after surgery, before entering the box with atmosphere or enriched with 40 ppm H_2S; Out of Box: Rectal temperature after getting out of the box, 24 minutes later; 1h after and 2h after: rectal temperature one and two hours after exposure to H_2S. All rats showed significant differences in rectal temperature before and after surgery (***P<0.001). Rats exposed to H_2S showed a significant decrease in body temperature after exposition (***P<0.001) until one hour (*P<0.05). No difference in rectal temperature was observed 2h after exposure.

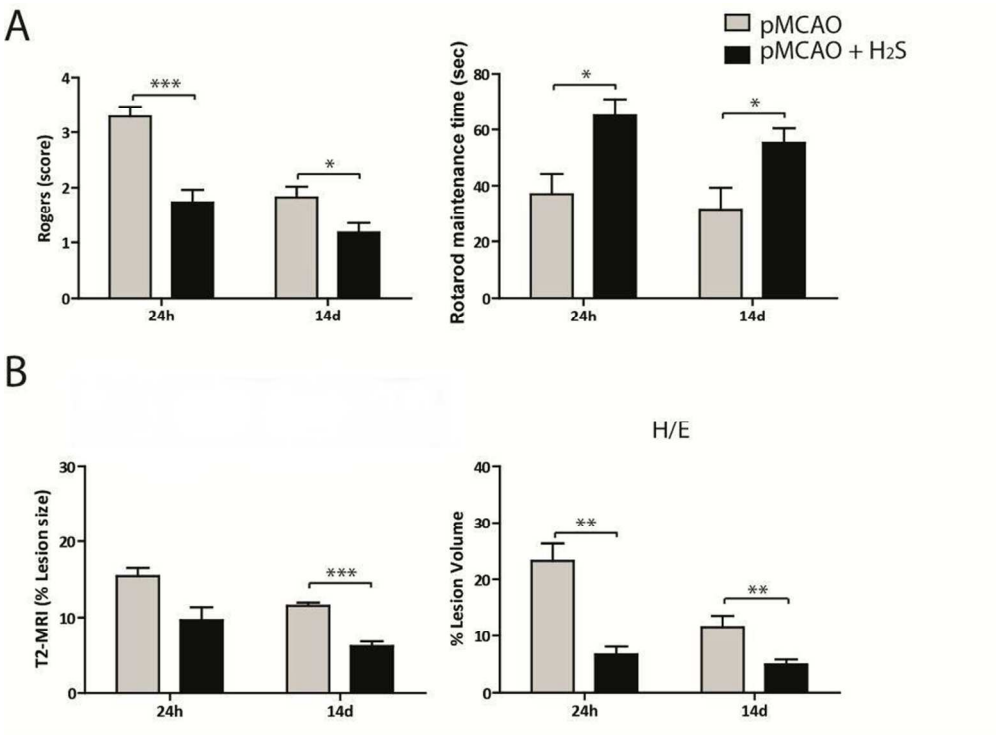

Figure 1
361x264mm (72 x 72 DPI)

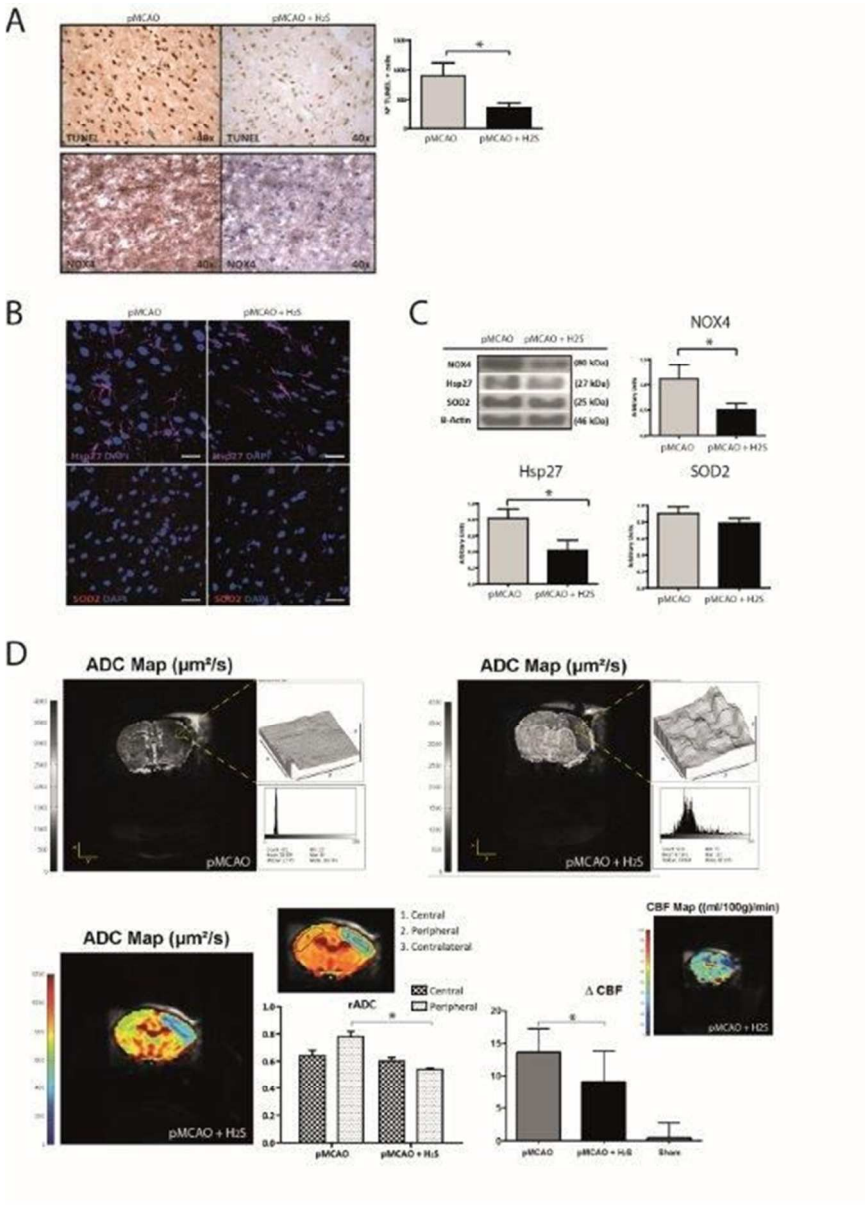

Figure 2
97x135mm (144 x 144 DPI)

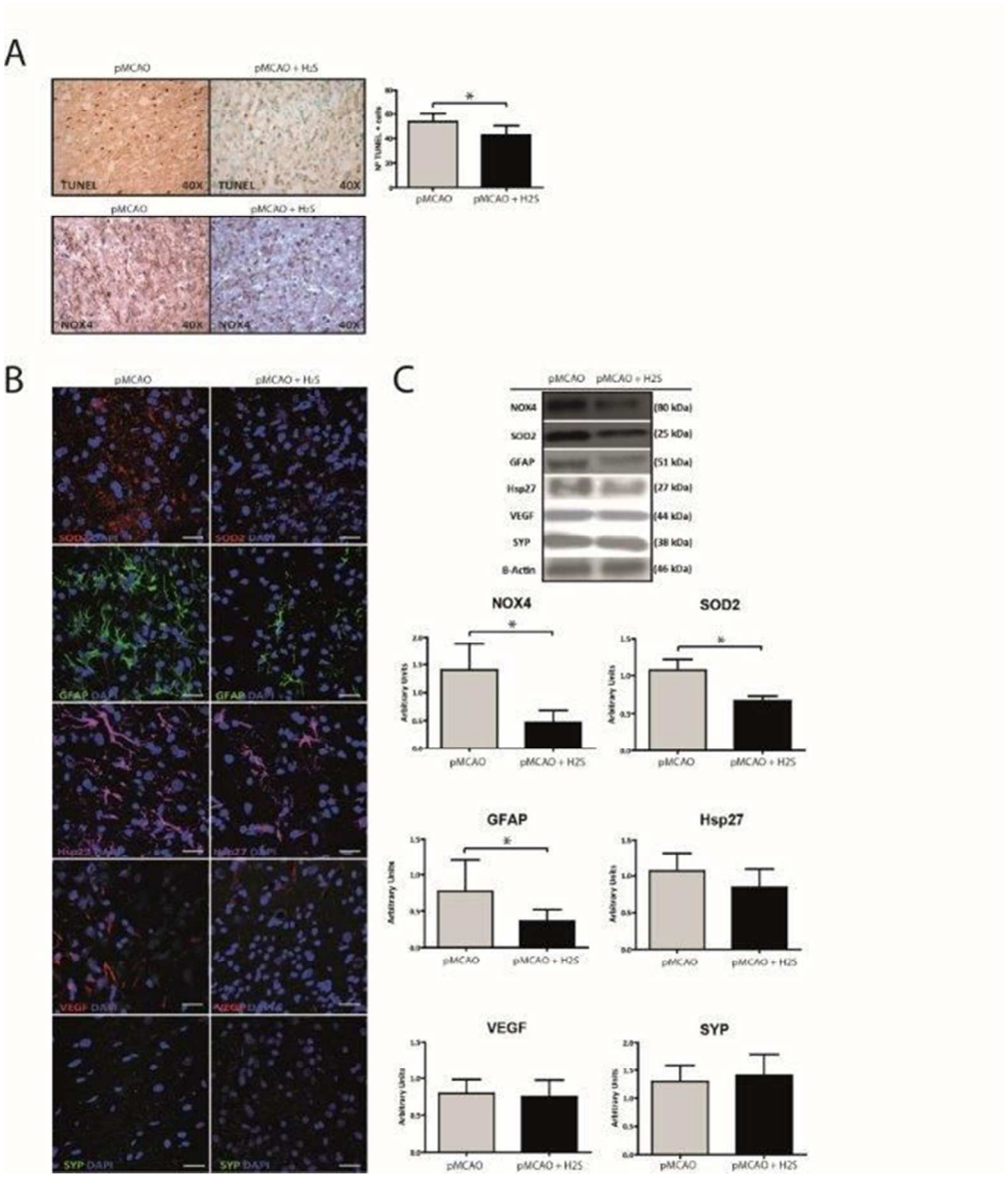

Figure 3
115x135mm (144 x 144 DPI)

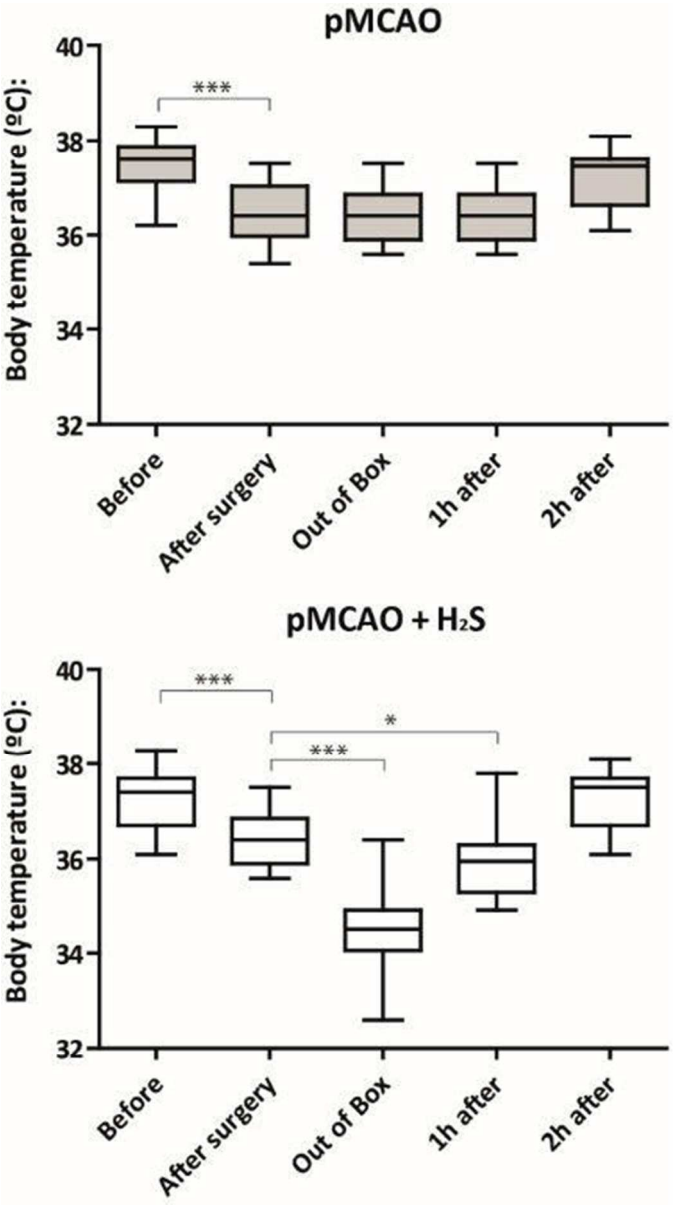

Figure 4
75x135mm (144 x 144 DPI)